THE ASTROPHYSICAL JOURNAL SUPPLEMENT SERIES, 103:109–144, 1996 March


# THE CANADA-FRANCE-HAWAII TELESCOPE IMAGING SURVEY OF BL LACERTAE OBJECTS. I. PROPERTIES OF THE HOST GALAXIES

RON WURTZ[1,2] AND JOHN T. STOCKE[1]
Center for Astrophysics and Space Astronomy, University of Colorado, Boulder, CO 80309
AND
H. K. C. YEE[1]
Department of Astronomy, University of Toronto, Toronto, Ontario M5S 1A7, Canada
*Received 1995 June 16; accepted 1995 September 12*

## ABSTRACT

The results of an extensive imaging survey of 50 BL Lac objects conducted at the Canada-France-Hawaii 3.6 m Telescope (CFHT) are presented. This paper details the results pertinent to the host galaxies of BL Lac objects; a companion paper presents results on the clustering environments of BL Lac objects obtained from the same images. All images were obtained through a Gunn *r*-filter and most during sub-arcsecond seeing conditions. The sample selected for observations includes both X-ray and radio-selected BL Lac objects with known redshifts $<0.65$. Because high-*z* and unknown redshift (i.e., optically very featureless) BL Lac objects are excluded from this study, these results may not be pertinent to all BL Lac objects.

Forty-six of 50 BL Lac objects are resolved by these images, 36 of which were resolved well enough to allow a host galaxy classification based upon their surface brightness profiles. Twenty of these 36 are best-fit unambiguously by elliptical profile host galaxies, 10 are likely ellipticals, three are possible spirals (but with problems with their profiles that make this conclusion tentative), and three host galaxies are best-fit unambiguously by spiral galaxy profiles. One of the three best-fit by a spiral profile (MS 0205+351) is also the only point source which is significantly decentered relative to its "host galaxy" and the lowest luminosity galaxy in the sample. This one BL Lac object and the other two in spiral galaxies (PKS 1413+135 and OQ 530) are the only candidates for gravitationally lensed BL Lac objects to be identified from this study.

Comparisons of host galaxy luminosities and morphology made internal to the sample find no evidence that any BL Lacertae subtype with distinct characteristics (e.g., high vs. low polarization; presence of weak emission lines; X-ray vs. radio-loud) has distinct host galaxy properties. This is particularly important for the X-ray versus radio-selected BL Lac objects which have been suspected of being different types of objects on the basis of their discrepant $\langle V/V_{\max} \rangle$ values, redshift distributions, and emission-line properties. Therefore, the results here support a picture for BL Lac objects in which the X-ray–loud and radio-loud objects are from the same parent population with the X-ray–loud BL Lac objects viewed further from the beaming axis than the radio-loud BL Lac objects.

Comparisons between the CFHT BL Lacertae sample and large, nearby samples of rich cluster brightest cluster galaxies (BCGs) and Fanaroff-Riley (FR) type 1 and 2 radio galaxies find that the host galaxy luminosity distribution is most consistent with the FR 2's, not with the FR 1's as suspected previously using smaller BL Lacertae samples. Paper II in this series shows that the clustering environment of BL Lac objects is also more consistent with that of FR 2's than FR 1's, confirming with a larger sample the suggestion by Prestage & Peacock that BL Lac objects avoid rich clusters. And yet it is well known that the extended radio emission in BL Lac objects is most consistent with FR 1's in luminosity and morphology. The resolution to this apparent contradiction is that the parent population of BL Lac objects is only a subset of FR 1's which excludes at least the BCGs in rich clusters and possibly all radio galaxies in rich clusters as well.

*Subject headings:* BL Lacertae objects: general — galaxies: fundamental parameters — surveys

## 1. INTRODUCTION

It is widely believed that BL Lacertae objects are low-luminosity (Fanaroff & Riley 1974, class 1 [FR 1]) radio galaxies viewed nearly directly down the jet axis (Blandford & Rees 1978; Schwartz & Ku 1983; Wardle, Moore, & Angel 1984; Ulrich 1989; Browne 1989; Padovani & Urry 1990, 1991; Urry, Padovani, & Stickel 1991) primarily because (1) the underlying host galaxies of a few, nearby BL Lac objects are luminous ellipticals similar to FR 1 hosts (Ulrich 1989; Abraham, McHardy, & Crawford 1991, hereafter AMC), (2) their extended radio power and morphologies are consistent with FR 1's (Antonucci & Ulvestad 1985; Perlman & Stocke 1993), and (3) their luminosity functions in the radio and X-ray are consistent with being Doppler-boosted luminosity functions of FR 1's (Padovani & Urry 1991; Urry, Padovani, & Stickel 1991; Morris et al. 1991). However, there are some individual BL Lac objects which cannot be explained easily as "beamed

[1] Guest Observer, Canada-France-Hawaii Telescope, which is operated by NRC of Canada, CNRS of France, and the University of Hawaii.
[2] Current address: Lawrence Livermore National Laboratories, Mail Stop L401, 7000 East Avenue Box 808, Livermore, CA.

FR 1's," primarily high-$z$ objects whose extended radio power levels exceed those of FR 1's (e.g., 1400+162; Kollgaard et al. 1992, Antonucci & Ulvestad 1985), a couple of BL Lac objects with spiral morphology "host" galaxies (PKS 1413+135 and OQ 530; AMC, Stocke et al. 1992) and a few in which the BL Lacertae point source is offset from the nebulosity nearest it, suggesting that the nebulosity is foreground to the high-$z$ BL Lac object (e.g., AO 0235+164, PKS 0537−441, and W1 0846+561; Stickel, Fried, & Kuhr 1988a, b, Yanny, York, & Gallagher 1989). Particularly the latter class stimulated Ostriker & Vietri (1985) to propose that some BL Lac objects could be background normal or optically violent variable (OVV) quasars microlensed by foreground galaxies, creating at least some of the observable BL Lacertae characteristics such as the absence of large equivalent width emission lines, rapid variability and predominance of low redshifts among BL Lac objects (which are attributed to the foreground, lensing galaxy by this model; Ostriker 1989).

Many of the above investigations were carried out using the few BL Lac objects available at the time of these studies. Recently many new BL Lac objects have been discovered, primarily through surveys conducted at X-ray wavelengths (e.g., the *Einstein* Extended Medium-Sensitivity Survey [EMSS; Gioia et al. 1990, Stocke et al. 1991, Maccacaro et al. 1994], the *EXOSAT* high-latitude survey [Giommi et al. 1991]; and the *Einstein* Slew Survey [Schachter et al. 1993; Perlman et al. 1996a]). It has been found that these X-ray-selected BL Lac objects (XBLs) have somewhat different observable properties than the previously known radio-selected BL Lac objects (RBLs) including lower radio luminosities (Stocke et al. 1985), comparable extended radio powers but with smaller mean core dominance (Perlman & Stocke 1993), greater optical starlight fractions (greatly assisting in redshift determination; Morris et al. 1991), lesser optical variability and polarization percentage and, intriguingly, significantly less variation in polarization position angle ($\pm 10°$ in $\sim 85\%$ of XBLs; Jannuzi, Smith, & Elston 1993, 1994) and, possibly, the absence of a hard, inverse-Compton X-ray emission component (Ciliegi, Bassani, & Caroli 1995; Perlman et al. 1996b). To explain these differences within the context of a single population of objects, some investigators have invoked a difference in viewing angle of the beamed jet radiation between RBLs and XBLs (e.g., Stocke et al. 1989), while others (Giommi & Padovani 1994; Padovani & Giommi 1995) have suggested intrinsic differences in electron energy distributions. But by comparing the complete sample properties of the 1 Jy RBL and EMSS XBL samples, Maccacaro et al. (1984), Stickel et al. (1991), Morris et al. (1991), and Perlman et al. (1996b) found significantly different values for $\langle V/V_{\rm max} \rangle = 0.60$ and 0.33, respectively. While this discrepancy argues that these two selection techniques are discovering different types of objects, sample incompleteness is also a possible resolution to this discrepancy (Browne & Marcha 1993; see also Perlman et al. 1996b). Jannuzi et al. (1994) have also argued that some XBLs might not be BL Lac objects because they fail to exhibit variable optical polarization percentages, further complicating comparisons between XBLs and RBLs.

Previous imaging observations of BL Lac objects (see compilation of studies of individual objects by Ulrich 1989; Stickel et al. 1991; AMC; Falomo & Tanzi 1991; Falomo, Pesce, & Treves 1993a, b; Pesce, Falomo, & Treves 1994, 1995) have observed only a few BL Lac objects at quite modest redshifts ($z \leq 0.3$) and few XBLs at all. For example, the most extensive, previous imaging study of BL Lac objects, that by AMC, targeted 23 BL Lac objects and resolved 14, of which only seven had known redshifts, all with $z \leq 0.3$. The only systematic studies of BL Lacertae clustering environments published heretofore are the brief account given by Fried, Stickel, & Kuhr (1993) of optical imaging data obtained on the 1 Jy RBL sample by Stickel, Fried, & Kuhr (1993b) and the very recent comparison between BL Lac objects and FR 1 galaxies made by Smith, O'Dea, & Baum (1995), which used images with relatively bright limiting magnitudes. Therefore, we undertook to obtain deep, sub-arcsecond wide-field images for a large sample of both RBLs and XBLs using the prime focus camera (FOCAM) at the Canada-France-Hawaii 3.6 m Telescope (CFHT). The impetus behind this work was the new availability of redshift information for sizable numbers of XBLs and RBLs that allowed 50 BL Lac objects with $z \leq 0.65$ to be targeted, objects whose host galaxies and clustering environment were within reach of CFHT to study. The goal of this study is to provide a comprehensive view of the host galaxy and clustering environments of BL Lacertae objects.

In this paper we present a portion of the results of the CFHT BL Lacertae imaging survey, those results pertinent to the host galaxies. A companion paper (Wurtz et al. 1996, hereafter Paper II) will examine the clustering environments of this sample. A more detailed treatment of sample properties and data acquisition and analysis than presented here can be found in Wurtz (1994, hereafter W94). Short papers on individual sources of interest can be found in a study of four rich clusters surrounding BL Lac objects in this sample by Wurtz et al. (1993) and a study of the microlensed BL Lacertae candidate MS 0205.7+3509 in Stocke, Wurtz, & Perlman (1995a).

In § 2 we present the CFHT BL Lacertae sample and discuss sample selection and potential biases with respect to BL Lac objects as a whole. In § 3 we describe the observations, data reduction, and host galaxy extraction process and present the basic observational results of this study. In § 4 we interpret the observational results which bear directly upon the nature of BL Lacertae host galaxies including morphology, absolute luminosity, and optical core dominance. In § 5 we summarize our findings and highlight the most important conclusions.

## 2. THE CFHT BL LACERTAE SAMPLE

In order to survey the host galaxy and clustering properties of BL Lac objects, a sample was selected using the following criteria:

1. The object has been classified in one or more publications as a BL Lac object.
2. A declination limit of $\delta \geq -40°$ to facilitate observations at CFHT.
3. A redshift has been measured with $z \leq 0.65$ (a few objects with uncertain redshifts were observed; see below).
4. Roughly equal numbers of XBLs and RBLs were chosen for observation in order to compare those classes. The XBLs observed include 21 of 22 in the complete EMSS sample of Morris et al. (1991) (the 22nd EMSS XBL lies 0.5 from an 11th magnitude star making deep imaging impossible). The

TABLE 1

CFHT SAMPLE OF BL LAC OBJECTS

| Coordinate designation | Name | Survey | z | $\log(f_x/f_r)$ | XBL or RBL? | Radio $f_{core}/f_{ext}$ | Maximum Optical Polarization | Emission line object? |
|---|---|---|---|---|---|---|---|---|
| 0122+090 | MS | EMSS | 0.339 | –4.18 | X | ... | ≤3.50 | ... |
| 0158+003 | MS | EMSS | 0.299 | –4.02 | X | 1.82 | 6.00 | ... |
| 0205+351 | MS | EMSS | 0.318 | –4.74 | X | ... | 3.59 | ... |
| 0219+428 | 3C66A | ... | 0.444 | –6.25 | R | 0.65 | ... | yes |
| 0257+344 | MS | EMSS | 0.247 | –4.81 | X | 22.39 | 6.25 | ... |
| 0317+185 | MS | EMSS | 0.190 | –4.04 | X | 5.50 | 5.21 | ... |
| 0323+022 | ... | ... | 0.147 | –3.77 | X | 10.00 | 10.37 | ... |
| 0414+009 | ... | ... | 0.287 | –4.71 | X | 1.81 | ... | ... |
| 0419+197 | MS | EMSS | 0.512 | –4.40 | X | ... | ≤2.90 | ... |
| 0521–365 | PKS | ... | 0.061 | –6.22 | R | 0.32 | ... | ... |
| 0548–322 | PKS | A-2 | 0.069 | –4.54 | X/R | 0.36 | 3.21 | yes |
| 0607+711 | MS | EMSS | 0.267 | –5.05 | X | 0.87 | 4.82 | ... |
| 0814+425 | ... | 1Jy | 0.258: | –6.02 | R | 23.95 | 12.0 | yes |
| 0823+033 | PKS | 1Jy | 0.506 | ... | R | 323.20 | 22.9 | yes |
| 0828+493 | OJ 448 | 1Jy | 0.548 | –5.81 | R | 549.00 | 7.9 | yes |
| 0851+202 | OJ 287 | 1Jy | 0.306 | –6.48 | R | 87.10 | 37.2 | yes |
| 0922+749 | MS | EMSS | 0.638 | –4.39 | X | ... | ≤3.90 | ... |
| 0950+494 | MS | EMSS | ... | –4.10 | X | ... | 5.19 | ... |
| 0954+658 | ... | 1Jy | 0.367 | –6.47 | R | 151.10 | 33.7 | ... |
| 1101+384 | Mkn 421 | ... | 0.031 | –4.99 | X/R | 2.82 | ... | ... |
| 1207+397 | MS | EMSS | 0.615 | –4.50 | X | ... | ≤4.00 | ... |
| 1218+304 | ... | ... | ... | –4.32 | X | 10.00 | 6.83 | ... |
| 1219+285 | W Com | A-2 | 0.102 | –6.55 | R | 26.90 | ... | yes |
| 1221+248 | MS | EMSS | 0.218 | –5.23 | X | 15.49 | 12.30 | ... |
| 1229+645 | MS | EMSS | 0.164 | –5.00 | X | 10.00 | 2.28 | ... |
| 1235+632 | MS | EMSS | 0.297 | –4.48 | X | >1. | 2.62 | ... |
| 1400+162 | ... | ... | 0.244 | –6.58 | R | 0.38 | ... | yes |
| 1402+042 | MS | EMSS | 0.344: | –5.17 | X | 1.66 | 9.52 | ... |
| 1407+599 | MS | EMSS | 0.495 | –4.82 | X | 0.56 | 8.64 | ... |
| 1413+135 | PKS | ... | 0.247 | –7.68 | R | ≥9600. | ... | ... |
| 1415+259 | ... | ... | 0.237 | –4.56 | X | ... | 7.53 | ... |
| 1418+546 | OQ 530 | 1Jy | 0.152 | –6.74 | R | 55. | 24. | ... |
| 1443+638 | MS | EMSS | 0.299 | –4.76 | X | 0.98 | ... | ... |
| 1458+228 | MS | EMSS | 0.235 | –5.36 | X | 8.71 | 7.03 | ... |
| 1534+018 | MS | EMSS | 0.312 | –5.12 | X | 0.85 | 3.73 | ... |
| 1538+149 | PKS | 1Jy | 0.605 | –6.96 | R | 7.24 | 32.8 | ... |
| 1552+203 | MS | EMSS | 0.222 | –4.84 | X | 1.86 | 5.95 | ... |
| 1652+398 | Mkn 501 | 1Jy/A-2 | 0.033 | –5.21 | X/R | 20.40 | 4.18 | yes |
| 1722+119 | ... | ... | 0.159 | –4.96 | X | ... | 15.54 | ... |
| 1727+502 | ... | ... | 0.055 | –5.12 | X | 3.39 | ... | ... |
| 1749+096 | PKS | 1Jy | 0.322 | –6.43 | R | ≥585. | 32 | yes |
| 1757+705 | MS | EMSS | 0.407 | –4.39 | X | ... | 3.70 | ... |
| 1807+698 | 3C371 | 1Jy | 0.051 | –6.59 | R | 1.35 | 12. | yes |
| 1921–293 | OV–236 | ... | 0.353 | –6.57 | R | ... | ... | yes |
| 2007+777 | ... | 1Jy | 0.342 | –5.76 | R | 28.90 | 15.1 | yes |
| 2143+070 | MS | EMSS | 0.237 | –5.26 | X | 1.32 | 10.83 | ... |
| 2155–304 | PKS | A-2 | 0.116 | –4.59 | X/R | 1.05 | 10.80 | ... |
| 2200+420 | BL Lac | 1Jy | 0.069 | –6.57 | R | 79.40 | 23. | yes |
| 2201+044 | ... | ... | 0.028 | –6.22 | R | 2.50 | ... | ... |
| 2254+074 | PKS | 1Jy | 0.190 | –7.21 | R | 24.50 | 21. | ... |

RBLs observed include all 13 1 Jy BL Lac objects with $z < 0.65$ and $\delta > -20°$ (Stickel et al. 1991; one with an uncertain $z$). While this redshift limit includes virtually all the EMSS BL Lac objects, it includes only half the 1 Jy BL Lac objects accessible from CFHT because the remainder have high or unknown redshifts.

The CFHT BL Lacertae sample is presented in Table 1 with the following basic information by columns: (1) IAU coordinate designation. (2) Other common name. (3) Membership in statistically complete surveys including EMSS, 1 Jy, A-2 (*HEAO-1* A-2; Piccinotti et al. 1982). (4) Redshift. (5) Logarithmic ratio of X-ray to radio flux defined using monochromatic fluxes from the literature in Jy at 1 keV and 5 GHz, respectively. The X-ray fluxes assume a spectral index = −1 to convert from the fixed bandwidths of *Einstein, EXOSAT,* and *ROSAT.* All but one object (1 Jy 0823+033) have both an X-ray and radio flux measurement. (6) Whether the object was discovered in an X-ray or radio source survey (i.e., XBL or RBL). (7) The radio core dominance at 1.4 GHz from the literature where available. (8) The maximum optical polarization percentage from Jannuzi et al. (1994) and Kuhr & Schmidt (1990). (9) Whether weak emission lines have been detected in the object. References for redshifts, radio and X-ray fluxes, and emission-line properties used in Table 1 can be found in W94; most can be found in Burbidge & Hewitt (1987).

While the redshifts were usually accepted as given from the literature, a few objects possessing uncertain or controversial redshifts were kept in this sample. Those redshifts in Table 1 requiring comment are as follows. (1) MS 0205+351, which has a published $z = 0.318$: (Morris et al. 1991) that has not been confirmed either by cross-correlation techniques on the Morris et al. data or by new spectra obtained by one of us

(J. T. S.) subsequently. Thus, this value remains uncertain. (2) 0219+428 (3C 66A), which has $z = 0.444$ based upon a one-time detection of Mg II emission by Miller, French, & Hawley (1978), confirmed by a weak detection of Ly$\alpha$ in the *IUE* spectrum of Lanzetta, Turnshek, & Sandoval (1993), so we list this redshift as firm. (3) 1 Jy 0814+425 has a highly uncertain $z = 0.258$: based upon a one-time detection of Mg II and [O II] emission lines (Wills & Wills 1976). This redshift has not been confirmed despite more recent attempts by one of us (J. T. S.) and by Stickel et al. (1991), so this $z$ remains uncertain. (4) Morris et al. (1991) gave a $z$ for MS 0950+492 of 0.207 based upon a nearby galaxy redshift. However, the object itself has had a featureless spectrum in four separate epochs of observation by one of us (J. T. S.), so we list its $z$ as currently unknown. (5) The previously quoted $z = 0.20$: for MS 1402+04 is based only on the presence of a possible 4000 Å break in the spectrum presented in Morris et al. (1991). However, a cross-correlation analysis of new spectra obtained for this object (Stocke et al. 1995b) yields a possible $z = 0.344$: with no power in the cross-correlation at the lower $z$ value, so we now assume the higher, still uncertain $z$ for this object. (6) The $z = 0.13$ listed extensively in the literature for 1218+304 is, in fact, a photometric redshift based upon the host galaxy luminosity obtained by Weistrop et al. (1981). While our imaging confirms the Weistrop et al. result, the use of a photometrically estimated distance begs the questions asked in the current investigation, and so we list the $z$ as unknown and compute no absolute quantities. (7) The $z = 0.159$ value for 1722+119 is based upon a reevaluation of the published spectrum in Griffiths et al. (1989) by one of us (J. T. S.), for which those authors erroneously reported $z = 0.018$. The photometry presented here is consistent only with the higher value, which we list as firm. (8) While the redshift of PKS 2155−304 remains controversial and is quoted either as $z = 0.116$ or $z = 0.17$, we adopt the former value as a firm redshift based upon the recent work of Falomo et al. (1993b).

A few comments on sample selection are required. While we have not adopted strict BL Lacertae criteria (there is some debate as to which criteria to use; e.g., Stocke et al. 1989 and Stickel et al. 1991 adopt optical spectroscopic criteria, while Jannuzi et al. 1994 adopt optical polarization requirements), most of the objects selected meet all previous criteria suggested for BL Lac objects. The three problematic members of our sample are as follows. (1) 1921−293 (OV 236; Wills & Wills 1981), described by those authors as intermediate between a quasar and a BL Lac object with emission lines of nearly 10 Å equivalent width but high polarization percentage, so we have retained it in this sample. (2) PKS 2201+044 is a luminous X-ray source (Laurent-Meulheisen et al. 1993) for which recent optical spectroscopy (Perlman 1994) shows no signs of a non-thermal continuum blueward of Ca H and K (i.e., it does not meet the spectroscopic criteria of Stocke et al. 1989 or Stickel et al. 1991) and moderately strong ($W_\lambda \sim 20$ Å) H$\alpha$ + [N II] emission lines and so it most resembles an FR 1 radio galaxy, not a BL Lac object. Because the possibility of a time variable continuum is a reasonable one for BL Lac objects, we have retained this object. (3) PKS 0521−365 is another BL Lac object whose recent spectra (e.g., Ulrich et al. 1984) revealed strong Ly$\alpha$ and H$\alpha$ + [N II] emission lines not seen previously and so was rejected as a BL Lac object by Stickel, Fried, & Kuhr (1993a) for the 1 Jy sample but has been retained here. In addition to these three, we also retain the four EMSS XBLs which meet the BL Lacertae spectroscopic criteria of Stocke et al. (1989) but have never been found to be optically polarized and so are questionable BL Lac objects according to Jannuzi et al. (1994). The unusual RBL PKS 1413+ 135 has a point source detected only in the IR and radio owing to high foreground extinction (Stocke et al. 1992). While this object has a featureless near-IR spectrum (H and K bands; Perlman, Stocke, & Elston 1996c) and is highly polarized at *K*-band (Stocke et al. 1992), the polarization has not been observed to vary, and so its classification as a BL Lac object is suspect.

Finally, we have adopted the modern distinction between BL Lac objects and "blazars" (see Impey 1989), objects similar in many ways to BL Lac objects but possessing strong, optical emission lines. So we have not included objects like 3C 279, 3C 446, and PKS 0215+015 in our sample. Most of these "blazars" are at $z > 0.65$ and so would have been rejected by our adopted redshift cutoff anyway.

Introducing a redshift cutoff to the sample was done primarily to increase the likelihood of actually detecting the BL Lacertae host galaxies and surrounding cluster with the telescope, CCD, and seeing combination available and then interpreting the resulting detections; i.e., at $z = 0.65$ the surface brightness profile of a giant elliptical (specifically, 3C 31 at $M_r = -23.1$) has a diameter at the 25th mag isophote of 2.″4 ($H_0 = 50$ km s$^{-1}$ Mpc$^{-1}$ and $q_0 = \frac{1}{2}$ used throughout) compared to 1.″2 for a 21st mag BL Lacertae point source in 1″ seeing. So in the subarcsecond seeing expected at CFHT, a luminous elliptical host galaxy should be detectable in our images out to $z \sim 0.7$ but is problematical at larger distances or for extremely bright point sources. At higher $z$, the observed Gunn $r$-band host galaxy continuum flux is greatly diminished as the 4000 Å break moves through this filter band, making host galaxy detection at $z > 0.65$ in $r$-band images much more difficult.

However, a redshift limit does introduce some possible bias to the sample. Specifically, very featureless and higher power level BL Lac objects are excluded systematically. Since most, but not all, of the BL Lac objects suggested as beamed FR 2 radio galaxies (e.g., PKS 0215+015; Antonucci & Ulvestad 1985) and as gravitationally lensed BL Lac objects (e.g., AO 0235+164 and PKS 0537−441; Narayan & Schneider 1990) are at $z > 0.65$, these types of BL Lac objects are underrepresented in this sample (but 1400+162 and 3C 66A are included, which are possible FR 2 radio galaxies). And if very featureless BL Lac objects (e.g., 0735+175, B2 1147+245) are a distinct class, this survey will not address their properties. For example, these objects could have featureless optical spectra because their host galaxies are underluminous compared to those BL Lac objects with redshifts.

As noted above, there seem to be some distinct observational differences between RBLs and XBLs that are seen in the present sample and so are not attributable to sample selection but rather to intrinsic RBL/XBL differences (Stocke et al. 1985, 1989; Jannuzi et al. 1994). While the XBL and RBL labels reflect the wavelength band in which these objects were discovered, some BL Lac objects (e.g., Mrk 501 and PKS 2155−304) are plausibly both XBL and RBL. Therefore, we have adopted a somewhat different distinction between these two classes as shown in Figure 1, a histogram of X-ray-to-optical flux ($f_X/f_r$)

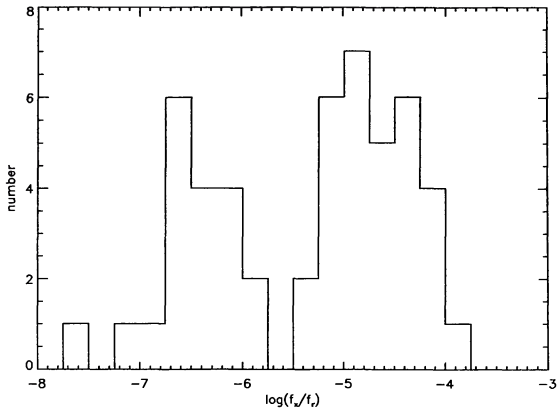


FIG. 1.—A histogram of the X-ray to radio flux ratios for the CFHT BL Lacertae sample. Both flux values are in Jy and the observations are, in general, not simultaneous. On the basis of this histogram, we define those BL Lac objects with $\log (f_X/f_r) \geq -5.5$ to be "X-ray loud" and those with $\log (f_X/f_r) < -5.5$ to be "radio loud."

ratios for our sample (see Table 1). Given the distinct minimum present, we term objects with $\log (f_X/f_r) > -5.5$ X-ray loud and the others radio loud. The EMSS XBL sample is exclusively X-ray loud, and the 1 Jy sample is exclusively radio loud, except for Mrk 501, which is near the dividing line (see Table 1; Ledden & O'Dell 1985; Padovani & Giommi 1995) based upon nonsimultaneous radio and X-ray fluxes from the literature. We stress that this division is somewhat arbitrary, particularly considering that the fluxes used are nonsimultaneous.

The 29 X-ray and 19 radio-loud BL Lac objects in our sample have indistinguishable redshift distributions (Kolmogorov-Smirnov Test [K-S test hereafter] probability = 91%; Fig. 2), facilitating subsample comparisons. Further, by merging the EMSS (21 of 22 objects observed here) and *HEAO-1* A-2 (three of five objects observed here) samples, a nearly complete XBL sample shows a redshift distribution statistically consistent (K-S test probability = 82%) with the 13 1 Jy complete RBL subsample observed at CFHT. But a few other observable properties are not similarly distributed in $\log (f_X/f_r)$ (K-S test probabilities, $P_{KS}$, of being drawn from the same parent population are given in parentheses below),[3] which we believe arise from intrinsic XBL/RBL differences, not from biases in our selection process: (1) The 13 BL Lac objects with weak emission lines are predominantly RBLs compared to the 37 lacking emission lines ($P_{KS} = 0.1\%$), although the emission-line BL Lac objects are similarly distributed in $z$ as the non–emission-line objects ($P_{KS} = 77\%$); (2) the maximum observed polarization percentage of RBLs is distinctly higher than that of XBLs ($P_{KS} = 0.002\%$; see also Jannuzi et al. 1994); and (3) the RBLs are much more highly radio core dominated than the XBLs ($P_{KS} = 0.05\%$; Perlman & Stocke 1993).

## 3. OBSERVATIONS AND DATA REDUCTION

The BL Lac objects in Table 1 were imaged during two observing runs at CFHT in 1991 using the prime focus imaging system (FOCAM) and the CCD detectors whose characteristics are shown in Table 2. Images were obtained for all objects using a Gunn $r$ filter. A journal of CFHT observations used to determine host galaxy parameters is shown in Table 3, which includes the following information by column: (1) object coordinate name; (2) UT date of host galaxy observation (if images obtained on multiple nights, the UT date is given at which the majority of the exposure time was obtained); (3) total integration time used for host galaxy analysis; (4) seeing on the merged image; (5) sky brightness on the merged image; (6) sky rms noise level obtained after flat-fielding and vignetting corrections; and (7) whether the images are photometric or

[3] Strictly speaking, $P_{KS}$ is the probability that the two distributions are *not inconsistent* with being drawn from the same parent population.

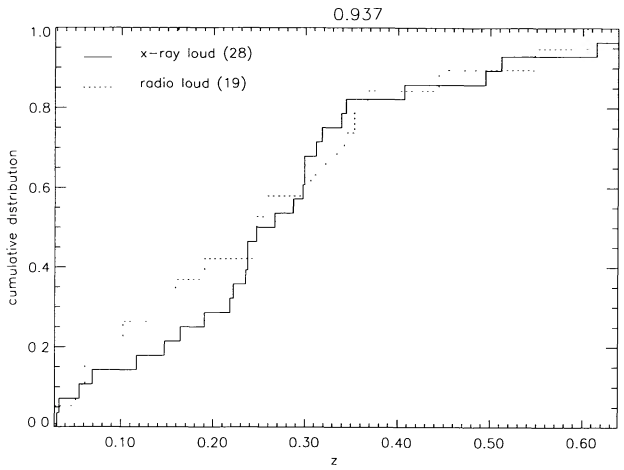


FIG. 2*a*

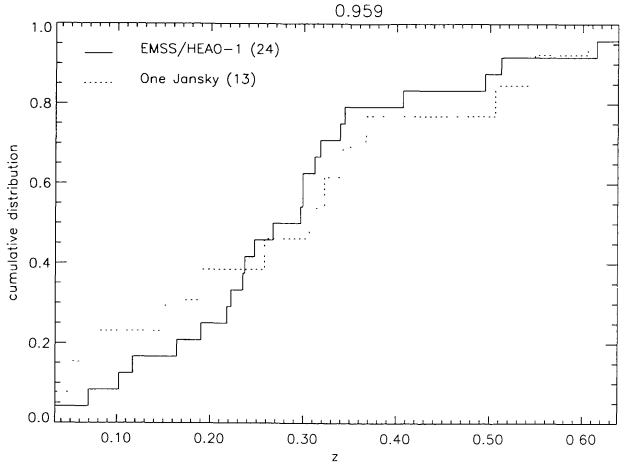


FIG. 2*b*

FIG. 2.—Cumulative redshift distributions for (*a*) the complete CFHT sample divided into radio loud and X-ray loud using the division suggested by Fig. 1 and (*b*) a plausibly complete X-ray–selected sample vs. a plausibly complete radio-selected sample of BL Lac objects observed at CFHT. These distributions are similarly distributed in redshift with K-S test probabilities shown at the top of each plot. Therefore, no redshift bias will be present in comparing results from these subsamples.

TABLE 2

CCD CHARACTERISTICS

| CCD | Dates (UT) | Field Size (pixels) | Field Size | Full Well (ADU) | Pixel Size |
|---|---|---|---|---|---|
| SAIC2 ..... | 1991 Jan 13–16 | 1024 × 1024 | 4.2 × 4.2 | 28,000 | 0.247 |
| Lick2 ..... | 1991 Aug 5–7 | 2048 × 2048 | 7.0 × 7.0 | 10,000 | 0.206 |

not. A "NO" occurs in the last column if even some of the frames used for this analysis were not photometric requiring additional calibration (see below).

During these observing runs, only a few objects suffered from "poor" (>1.2) seeing conditions, so that typical image sampling was 3–5 pixels, allowing excellent point-source modeling and subtraction. Most of the observations were made under photometric sky conditions and calibrated using Gunn standards (Thuan & Gunn 1976; Kent 1985) to a photometric accuracy of 0.02–0.03 mag. Several objects (0607+711, 0823+033, 0851+202, and 1443+638) were imaged in non-photometric conditions and were calibrated using frames obtained during photometric conditions at other times during our CFHT observing runs. These calibrations were checked against photometry obtained at the Palomar 60 inch (1.52 m) telescope and from the literature (Smith, Jannuzi, & Elston

TABLE 3

JOURNAL OF CFHT GUNN *r*-BAND HOST GALAXY OBSERVATIONS

| Name | UT date | Integration (sec) | Seeing (arcsec) | Sky (mag/arcsec$^2$) | Sky rms (mag/arcsec$^2$) | Photometric? |
|---|---|---|---|---|---|---|
| 0122+090 | 8/6/91 | 1200 | 0.9 | 20.28 | 25.37 | |
| 0158+003 | 1/16/91 | 960 | 0.9 | 20.59 | 25.80 | |
| 0205+351 | 1/16/91 | 1200 | 0.8 | 20.67 | 25.97 | |
| 0219+428 | 1/16/91 | 45 | 1.3 | 20.70 | 24.00 | |
| 0257+344 | 1/14/91 | 840 | 0.9 | 20.95 | 25.75 | |
| 0317+185 | 1/14/91 | 720 | 0.9 | 20.89 | 25.63 | |
| 0323+022 | 1/14/91 | 600 | 0.9 | 20.81 | 25.40 | |
| 0414+009 | 1/15/91 | 1079 | 1.1 | 21.03 | 25.99 | |
| 0419+197 | 1/16/91 | 1800 | 0.8 | 20.87 | 26.10 | |
| 0521-365 | 1/16/91 | 360 | 1.2 | 20.59 | 25.15 | |
| 0548-322 | 1/14/91 | 451 | 1.0 | 20.79 | 24.69 | |
| 0607+711 | 1/13/91 | 764 | 1.3 | 20.75 | 25.68 | no |
| 0814+425 | 1/13/91 | 840 | 0.9 | ... | ... | no |
| 0823+033 | 1/13/91 | 1200 | 0.9 | 21.11 | 25.93 | no |
| 0828+493 | 1/16/91 | 1620 | 0.8 | 21.29 | 26.31 | |
| 0851+202 | 1/15/91 | 750 | 1.5 | 20.52 | 25.42 | no |
| 0922+749 | 1/16/91 | 900 | 1.3 | 21.19 | 25.51 | |
| 0950+494 | 1/14/91 | 2735 | 1.0 | 21.17 | 26.41 | no |
| 0954+658 | 1/15/91 | 1080 | 0.9 | 21.12 | 25.92 | |
| 1101+384 | 1/14/91 | 20 | 0.9 | ... | ... | no |
| 1207+397 | 1/16/91 | 1800 | 1.0 | 21.36 | 26.35 | |
| 1218+304 | 1/15/91 | 480 | 1.2 | 21.16 | 25.47 | |
| 1219+285 | 1/15/91 | 45 | 0.8 | 21.41 | 24.22 | |
| 1221+248 | 1/16/91 | 720 | 0.8 | 21.33 | 25.81 | |
| 1229+645 | 1/13/91 | 600 | 1.2 | 21.13 | 25.57 | |
| 1235+632 | 1/13/91 | 840 | 1.2 | 21.18 | 25.82 | |
| 1400+162 | 1/13/91 | 720 | 1.0 | 21.09 | 25.82 | |
| 1402+042 | 8/7/91 | 1800 | 1.4 | 20.48 | 25.80 | |
| 1407+599 | 1/16/91 | 1440 | 1.0 | 21.22 | 26.27 | |
| 1413+135 | 1/15/91 | 840 | 1.0 | 21.44 | 26.09 | |
| 1415+259 | 1/16/91 | 720 | 1.0 | 21.25 | 25.10 | |
| 1418+546 | 1/16/91 | 360 | 1.0 | 21.45 | 25.12 | |
| 1443+638 | 8/5/91 | 960 | 1.0 | 20.49 | 25.32 | no |
| 1458+228 | 1/15/91 | 720 | 1.3 | 21.58 | 25.69 | |
| 1534+018 | 8/6/91 | 960 | 1.2 | 20.54 | 25.29 | |
| 1538+149 | 8/7/91 | 1800 | 1.1 | 20.93 | 25.82 | |
| 1552+203 | 8/6/91 | 720 | 0.9 | 20.80 | 25.44 | |
| 1652+398 | 8/7/91 | 360 | 1.5 | 20.85 | 24.94 | |
| 1722+119 | 8/7/91 | 100 | 1.2 | 21.00 | 24.80 | |
| 1727+502 | 8/5/91 | 600 | 0.7 | 20.68 | 25.19 | |
| 1749+096 | 8/6/91 | 960 | 1.1 | 20.70 | 25.34 | |
| 1757+705 | 8/6/91 | 1800 | 1.1 | 20.53 | 25.81 | |
| 1807+698 | 8/6/91 | 300 | 1.2 | 20.26 | 24.55 | |
| 1921-293 | 8/6/91 | 1200 | 1.0 | 20.66 | 25.62 | |
| 2007+777 | 8/5/91 | 1200 | 1.1 | 20.10 | 25.35 | |
| 2143+070 | 8/5/91 | 720 | 0.7 | 20.87 | 25.43 | |
| 2155-304 | 8/6/91 | 30 | 1.2 | 20.62 | 23.96 | |
| 2200+420 | 8/5/91 | 120 | 0.8 | 20.50 | 24.51 | |
| 2201+044 | 8/5/91 | 360 | 0.7 | 20.49 | 24.64 | |
| 2254+074 | 8/6/91 | 720 | 0.8 | 20.53 | 25.31 | |

1991). Photometric accuracy of 0.04–0.05 mag was obtained. This was not possible for three objects. All CFHT images of MS 0950+494 were nonphotometric, and so they were calibrated using Palomar 60 inch images to ±0.05 mag. Two fields were not calibrated successfully: Mrk 421, which has been well studied previously (Ulrich 1989), but whose CFHT image suffers greatly owing to the presence of a very bright star in the field of view, and 0814+425, which has a reasonably deep image which resolves the host galaxy but a very uncertain redshift, making host galaxy data difficult to interpret. Both these objects are excluded from any discussion of absolute quantities.

The images were reduced in the standard manner using NOAO's Image Reduction and Analysis System (IRAF). Dome flats were applied to correct pixel-to-pixel gain variations, and each night's images were median-combined to obtain "super sky flats" to correct 10% variations in sky brightness across the chip resulting from dome flat illumination irregularities and vignetting at the edges of the Lick2 chip to <1% variations in the inner 1′ around the BL Lac object itself. Galactic extinction corrections were made using hydrogen column densities from Stark et al. (1992) and the equations in Burstein & Heiles (1978). *K*-corrections used the standard elliptical galaxy models of Sebok (1986), and absolute quantities also apply the standard $(1 + z)^4$ surface brightness dimming.

### 3.1. *Extraction of the BL Lacertae Surface Brightness Profile*

Isophotal profiles of each BL Lac object were extracted based upon a method first described in Jedrzejewski (1987, hereafter J87) in the following manner. First, the sky level is fixed using an annulus around each object with 20″ inner radius and 25″–30″ outer radius (somewhat larger for $z < 0.1$ objects) and determining the statistical mode of the sky counts per pixel by parabolic fit to the distribution of counts. While these values are secure with well-understood statistics for most of our images, in a few cases (e.g., MS 0922+749, 1 Jy 0823+493, MS 0607+711, and MS 1458+228) nearby, very bright stars created significant gradients in the sky brightness at the BL Lacertae location. Despite our attempts to mask out these stars and model their effects on sky brightness in areas that could not be masked, we could not convince ourselves that, even after extensive masking, the sky statistics were unaffected by these stars. Therefore, the low surface brightness isophotes in these few cases are suspect as noted for individual cases below.

In the second step of the extraction process, pixels containing an obvious nearby object (star, companion galaxy, cosmic ray, chip blemish) are masked from the isophotal extraction process. The size of the masked region is determined using comparably bright stars and galaxies in other parts of the image. While this procedure is quite straightforward for stars and cosmic rays, the amount of masking of companion galaxies was performed on an individual case-by-case basis. As an example of the masking process, Figure 3 shows two images of the 1E 1415+259 field, which is notable for its numerous, faint companion galaxies. Figure 3*a* is the original image; Figure 3*b* was created by subtracting a model of the BL Lacertae host galaxy built from the extracted isophotal profiles *after* masking off the companions. Except for noisy residuals caused by subtracting a splined model near the center, the subtraction of the symmetrical profile of the host leaves the companions intact. Those companions include what either has been described as an optical "jet" by Romanishin (1992) or an edge-on galaxy (Abraham 1994) at P.A. ≈ 135° from the BL Lac object itself. However, very faint companions are difficult to identify and mask completely, in some cases creating systematic errors in the extracted profile whose amounts are difficult to quantify. Where major uncertainties in best-fit galaxy type (three cases; see § 3.3) and in uncertain values for host galaxy luminosities arise, these are caused by difficulties with these first two steps. Specific instances are mentioned in the notes on individual objects in § 3.4.

Finally, the isophotal extraction process itself is an iterative procedure which, for each radius value, $a$, of the major axis in 0.″5 intervals, returns a pixel centroid, ellipticity, position angle, and intensity along the isophote as well as the amplitude of the harmonic functions used in the iteration, the rms of the mean intensity of the isophote, and the surface brightness gradient along the major axis. Along isophotes with too few pixels to constrain adequately all parameters (typically at ≤0.″5 of the galaxy center or in areas of much masking) or at too low a signal above sky (typically >26 mag arcsec$^{-2}$), the centroid and ellipticity were held fixed.

Several tests were made to determine if the extraction process produced reasonable isophotes. A visual inspection of the isophotes overplotted on the original image determined if the centroids and ellipticities are a reasonable match to the original data. The harmonic fits to the isophote were plotted as a function of the distance around the isophote to locate those with severe, high-frequency excursions away from the mean intensity; such isophotes were discarded from the profile fits. Finally, an inspection of the decentering of the isophotes as a function of semimajor axis aided in determining where profiles might be contaminated by incomplete masking of nearby stars or galaxies. Except for MS 0205+351, which possesses a clearly decentered point source (see below), only a few sources (e.g., MS 0607+711 is contaminated by a relatively bright star at $a > 12''$) showed a large decentering of the 25th mag isophote when compared to the isophotes of the point-spread function (PSF) star in the same images. Most of these profile problems occurred at surface brightness levels >26 mag arcsec$^{-2}$ and beyond the isophotes used in the detailed profile fits of these objects.

The decentering values listed in Table 4 in arcseconds (columns [6]–[7]) were obtained by comparing the centroid of a faint outer isophote to the centroid of the 0.″5 isophote, the position of the point source. Then the BL Lacertae host galaxy decentering was compared to the decentering value for the PSF field star to remove decentering values arising from telescope illumination asymmetries, slightly defocused images, guiding errors, and telescope wobble. Two independent decentering measurements were made using two different outer isophotes. The 25th mag isophote was used for one of these, since it is typically the last isophote detected at high confidence level above sky in our images (excepting a few very bright, nearby BL Lac objects like PKS 2155−304, for which only short exposures were made in order not to saturate the point source; for these, the 23.5 mag isophote was used). For the second decentering measurement, we used the isophote which provided the maximal detection of the galaxy above the point source based upon the photometric errors within each annulus (see

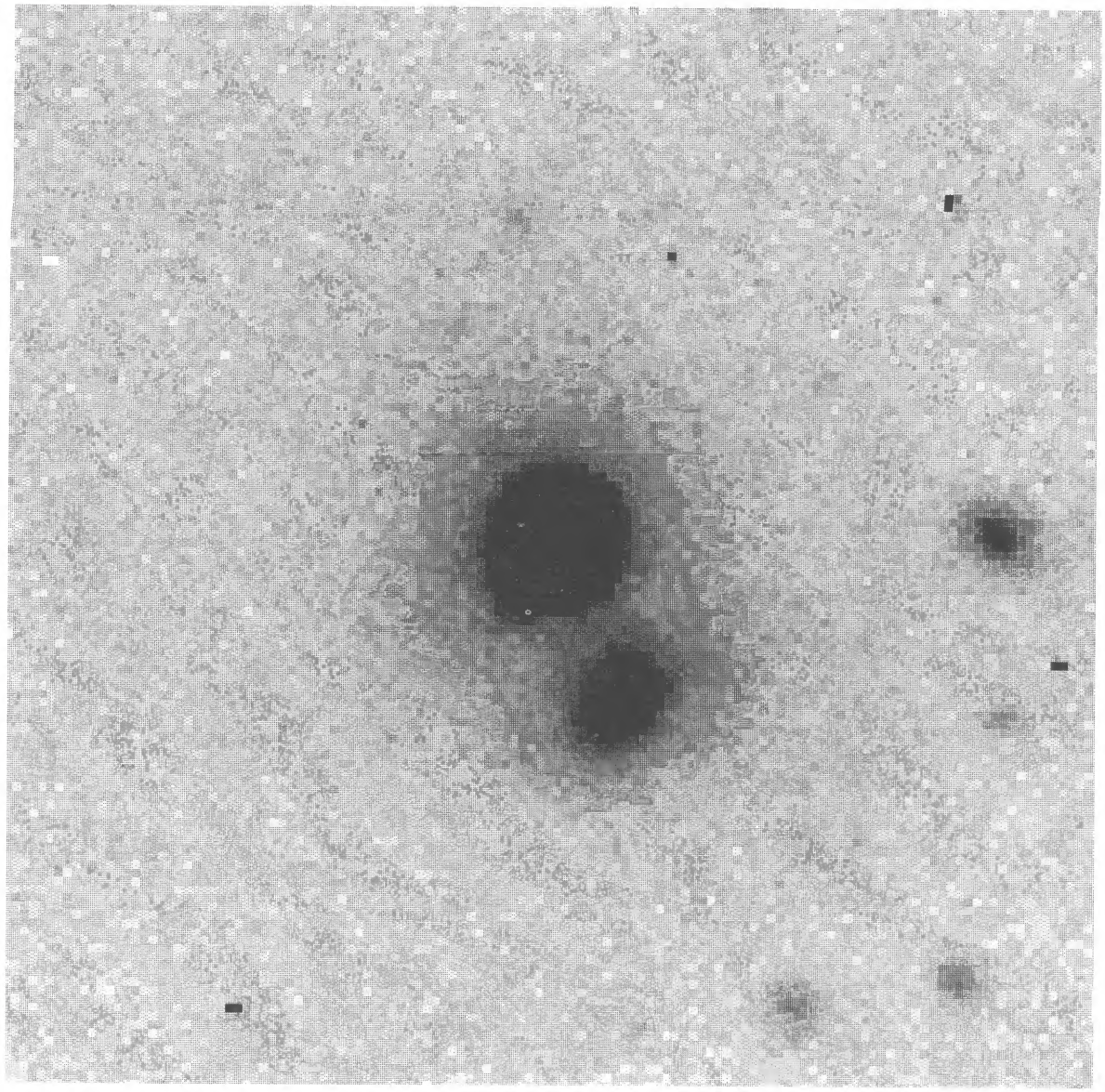

FIG. 3*a*

FIG. 3.—The CFHT Gunn *r*-band image of the BL Lac object 1415+259, which is notable for its numerous close companions. (*a*) The inner portion of the original image; (*b*) the same image after subtracting the best-fit model built from the isophotal profiles of the BL Lacertae host galaxy. For this procedure, the close companions were "masked" so that the resulting image in (*b*) leaves them intact. A small residual core is all that remains of the BL Lac object itself. The full field of view of these images is ~32″ on a side, and the seeing during the observation was 1″, so that the oversampling is ~4:1 (0.″247 pixel$^{-1}$). Note the elongated structure at position angle 135° from the BL Lac object, which Romanishin (1989) claims is an optical jet and which Abraham (1994) claims is an edge-on galaxy.

below); these isophotes (col. [5] in Table 4) are between 21 and 25 mag arcsec$^{-2}$ depending upon the object. While the statistical errors of these measurements are quite small (±0.″03), the actual limits that we can set on any decentering (≤0.″1) are limited by systematic effects. The use of two decentering measurements with different sources of systematic errors checks the validity of a measured decentering value. Spurious 25th mag isophote decentering values can be produced by slight sky variations across the chip on large scales, e.g., the scattering haloes of nearby bright stars. The brighter isophote decentering measurement is affected most by slight errors in the masking of close companion galaxies. Therefore, we required that both methods exhibit decentering values of ≥0.″1 for a BL Lacertae nucleus to be considered decentered. At least one of these tests could be carried out with confidence for 45 of the 50 objects observed. Four of the 50 BL Lac objects were unresolved by our observations, and one object (1749+096) was close enough to the Galactic plane ($b$ = 17.°6) that numerous closely projected stars make both decentering measurements uncertain. Also at the epoch of observation, 18 BL Lac objects had core sources too weak to detect a nonthermal core unambiguously above the level of nuclear emission expected

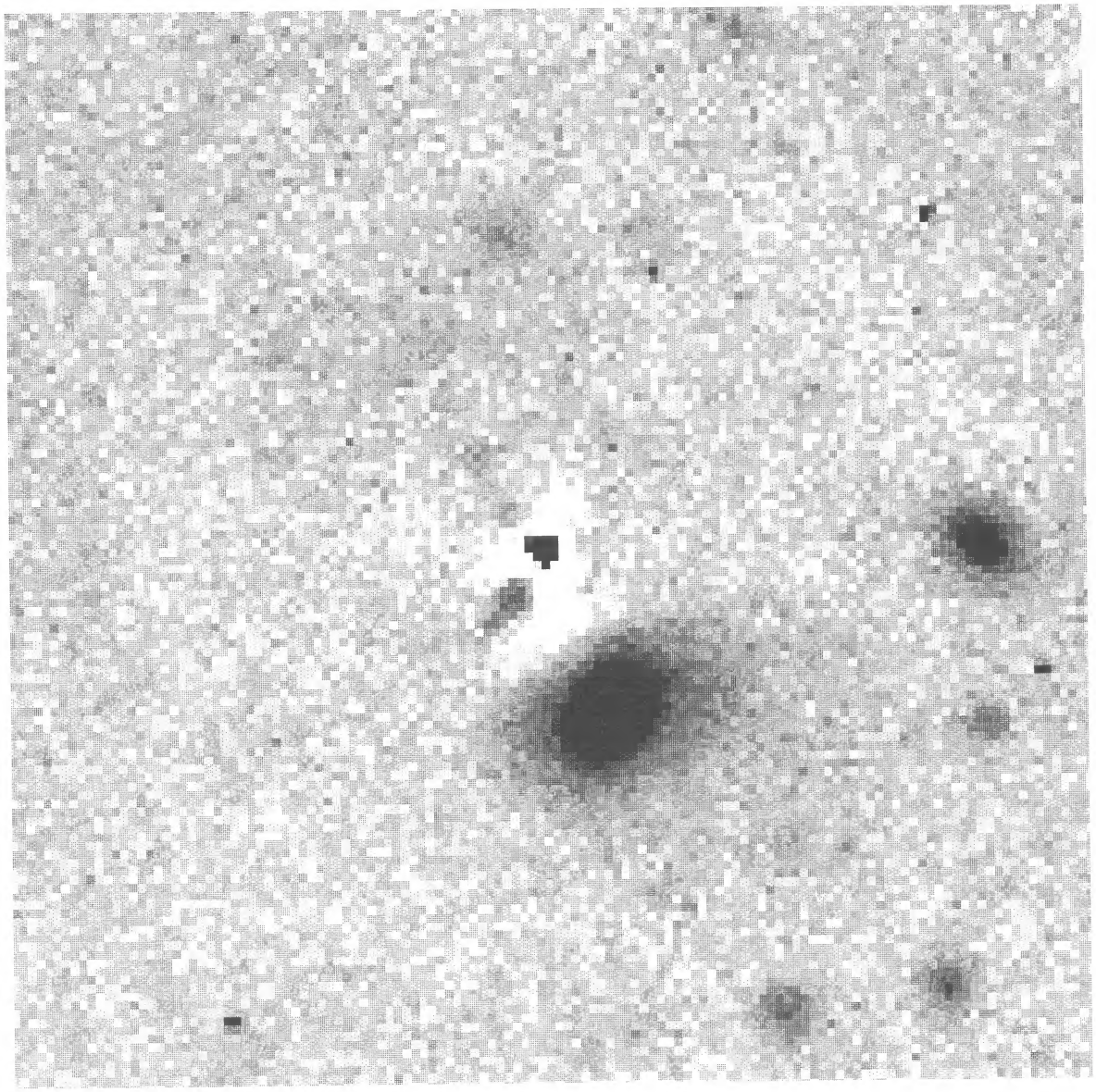

FIG. 3*b*

from the host galaxy; even though we employ a very stringent criterion for the presence of a point source (see below), the interpretation of the decentering measurements in these cases (which are indicated by upper limits in col. [4] of Table 4) must be treated with caution.

Based upon these two decentering measurements, only MS 0205+351 has a definitely decentered "host" galaxy (core offset = 0".3–0".4; see Stocke et al. 1995 for further details), while OJ 287 has a possibly decentered host (core offset = 0".1–0".2). Plots of core offset values relative to outer isophote centroids are shown in Figure 4 for the BL Lac object (*diamonds*) and the PSF star (*plus signs*) for these two sources.

### 3.2. *Functional Fits to the BL Lac Profiles*

A point-spread function (PSF) was determined using a single star close to the BL Lac object in each image with comparable brightness to the BL Lacertae point source. Because most of these fields were at high Galactic latitude, it was usually not possible to find several comparably bright stars for this process, so a single star had to suffice. In the same manner as described above for the BL Lac objects, the J87 one-dimensional profile of the PSF star was extracted and fitted with a three-component, six-parameter analytic profile consisting of a combination of Gaussian core, Moffat profile wings, and an exponential component to provide a smooth transition between these two functions (Stetson 1990).

For the BL Lacertae host galaxy profile analysis, a one-dimensional/two-dimensional hybrid technique was employed similar to that in AMC. The galaxy ellipticity is assumed to be that of the outer few isophotes, the sky level is determined from the mode of the large sky annulus, and these values were assumed to be constants for the fitting process. The one-dimensional PSF is scaled to the central (within one seeing

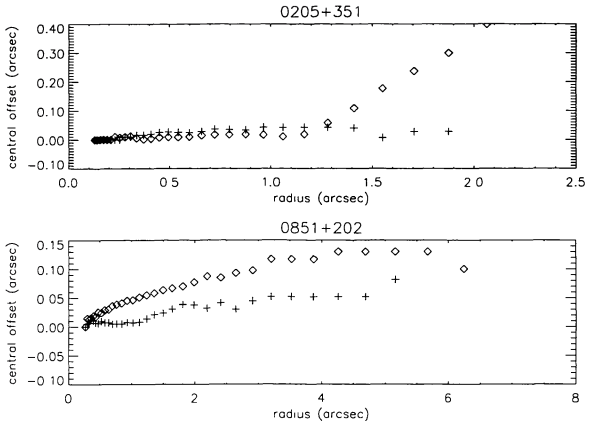


FIG. 4.—Decentering plots for two BL Lac objects. MS 0205+351 has a definitely decentered point source, and OJ 287 (0851+202) has a possibly decentered point source. The central offset values in arcseconds are the difference between the centroid of the 0".5 isophote (the position of the BL Lacertae core) and the isophotal centroid at each semimajor axis radius, shown as a function of radius. Diamonds mark the values for the BL Lac object, while the plus signs are the measured values for the PSF star in each field. Any decentering of the PSF star indicates spurious effects attributable to tracking errors, slight image defocusing, etc.

radius) intensity and subtracted, presumably leaving only galaxy light beyond a few seeing radii. The residual galaxy profile in the range from a few seeing radii to a few percent above sky is then used in a two-parameter linear least-squares fit of surface brightness for either a de Vaucouleurs $r^{1/4}$ law or an exponential profile. Based upon the limited spatial resolution of these observations ($\sim$0".2 kpc$^{-1}$ at a typical $z \sim 0.3$ for these objects) and the presence of a luminous point source at the galaxy center, more sophisticated models (e.g., disk + bulge; asymmetrical) were not attempted. The values of the two structural parameters (scale length and surface brightness at that scale length) obtained by this procedure and the point-source scaling value are then used as the *initial guesses* for the seeing-convolved modeling. The one-dimensional PSF parameterization obtained from a field star is used to create an azimuthally symmetrical two-dimensional PSF. This two-dimensional PSF is convolved with the two-dimensional model object created from the fixed ellipticity and sky level values and the three-parameter, initial-guess galaxy model. The one-dimensional profile of this seeing-convolved model is then extracted and compared with the one-dimensional J87 profile of the data. A $\chi^2$ minimization is then performed using the Levenburg-Marquardt method (Press et al. 1992) on the values of the counts for each extracted isophote. The weightings for this iterative procedure are supplied by the rms noise values in counts per pixel along each elliptical annulus.

This procedure fits the galaxy and the point source simultaneously, instead of the usual procedure of fitting the PSF first, then subtracting it and secondly fitting the residuals to a galaxy profile. In our opinion, the usual procedure bypasses the inherent difficulty in fitting the central pixels as a combination of point source plus sharply peaked galaxy core, which is not always well modeled by an extrapolation of the $r^{1/4}$ or exponential law obtained in the outer regions of the galaxy (see, e.g., de Vaucouleurs & Capaccioli 1979; Schweitzer 1979; Lauer 1985). In fact, it is primarily the uncertain extrapolation of the assumed galaxy profile law into the nucleus that sets the uncertainty in the strength of any point source that is present. This was revealed in several cases in the present procedure when best-fit values for the core flux were found to be negative. In these cases, it is clear that a de Vaucouleurs law or an exponential disk model is not appropriate all the way into the nucleus. Typically, these "negative point source" objects have weak nonthermal cores whose brightnesses are uncertain at the level of the fitted negative value; i.e., the negative values indicate the level of the inaccuracy with which a de Vaucouleurs law or exponential law fits the cores of these galaxies. For these cases, we have used the absolute value of the best-fit core flux as an upper limit to the core flux present at the time of our observations (see cols. [2]–[4] in Table 4). If the usual procedure had been followed, a positive core flux would have been found in all cases, but the subtraction of this core would have created large, negative residuals inside the seeing radius for any galaxy fit attempted thereafter. Since all BL Lac objects have variable optical cores at some level (e.g., Jannuzi et al. 1993), we were less interested in obtaining accurate core fluxes than in accurately determining the host galaxy profile and luminosity—for which the procedure used here is better suited (AMC).

Although it is difficult to quantify the errors associated with the host galaxy magnitudes, we tested the robustness of the fits by changing the isophotal fluxes by an amount determined randomly from a Gaussian distribution which matched the observed flux errors for each isophote. These new surface brightness distributions were then fitted, and total host galaxy magnitudes were determined. Most of these simulations resulted in host galaxy magnitudes within $\pm$0.2 mag of the values in Table 5, although in <5% of the simulations, usually those for which the host galaxy was only marginally resolved, errors of $\pm$1 mag were found.

### 3.3. *BL Lacertae Host Galaxy Profiles*

Figure 5 presents the extracted isophotal profiles for all objects in our sample compared with the best-fit point source (i.e., scaled PSF; *dotted line*), elliptical galaxy ($r^{1/4}$ law) + point source (*solid line*), and spiral galaxy (exponential disk law) + point source (*dashed line*) models. The error bars on the data points are the rms of the object + sky counts within each isophotal annulus and are plotted with each data point until they extend to an infinitely faint magnitude, beyond which only the data points themselves are plotted. Based upon the excellent seeing and transparency conditions experienced at CFHT during this observing, 46 of 50 BL Lac objects in this sample were resolved, 32 of which were resolved well enough to determine the morphology of the underlying host galaxy to these BL Lac objects. These results are distinct improvements upon the previous BL Lacertae imaging surveys (AMC; Stickel et al. 1993a; Falomo & Tanzi 1991; Falomo et al. 1993a, b) both in the total number of objects observed and in the percentage resolved and successfully fit with galaxy profiles.

Tables 4 and 5 present the basic data for the CFHT sample of BL Lac objects derived from these fits. By column number, Table 4 includes (1) BL Lacertae name; (2) core apparent $r$-band mag; where the core was not definitely detected, a lower limit is given (see § 3.2); (3) core absolute $r$-band magnitude

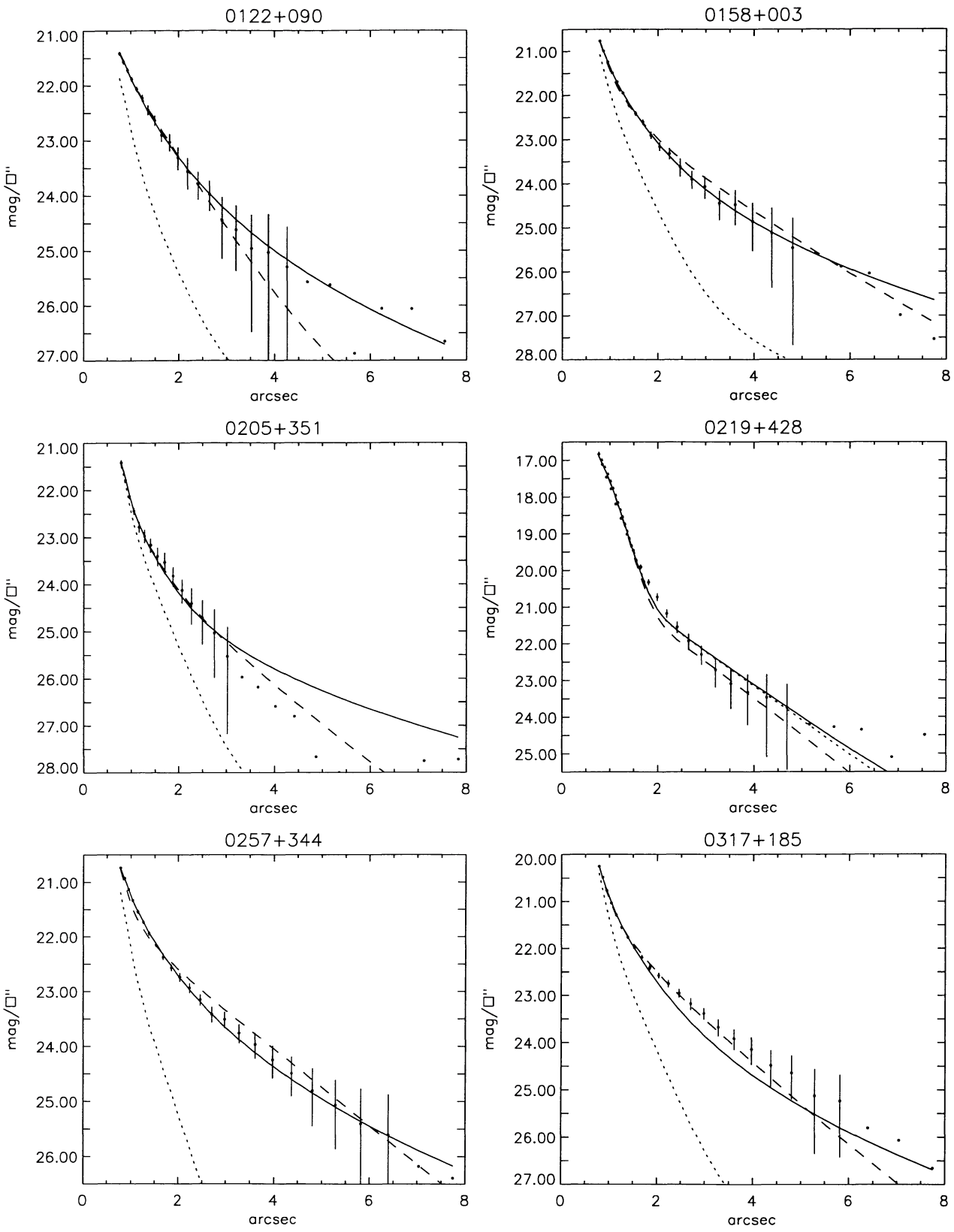


FIG. 5a

FIG. 5.—The extracted isophotal profiles (*points with and without error bars*) for each BL Lac object observed with the best-fit point source only model (*dotted line*), elliptical galaxy + point source model (*solid line*), and spiral galaxy + point source model (*dashed line*). The *r*-band surface brightness values are in observed magnitudes arcsec$^{-2}$ except for 0814+425 and 1101+384, whose frames are uncalibrated and thus are plotted in arbitrary relative magnitudes. The data points are plotted with error bars until the lower error bar reaches arbitrarily faint magnitudes, after which only the data point itself is plotted. If one of the models is not visible in an individual plot, that model lies at the same location as the solid line.

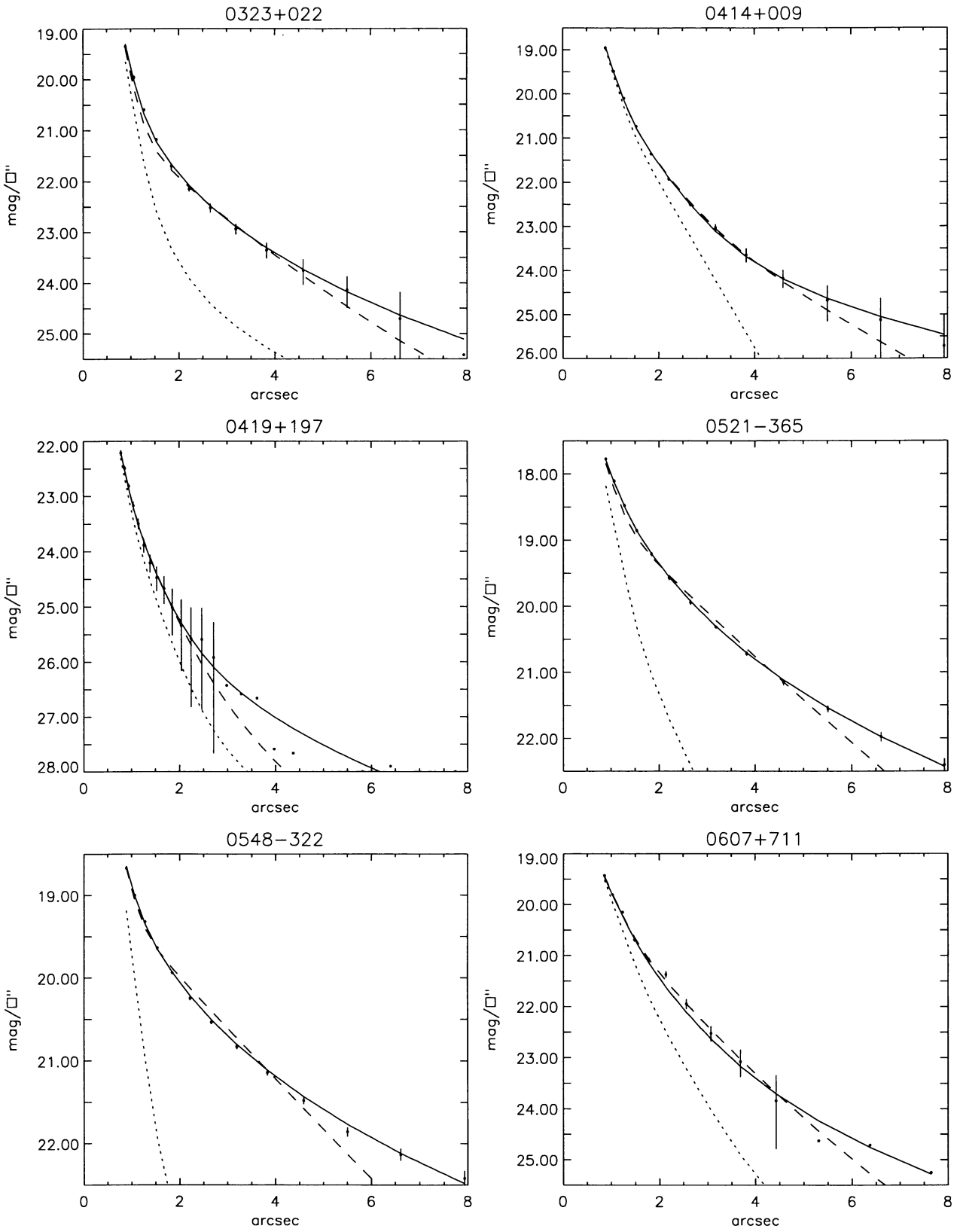


FIG. 5*b*

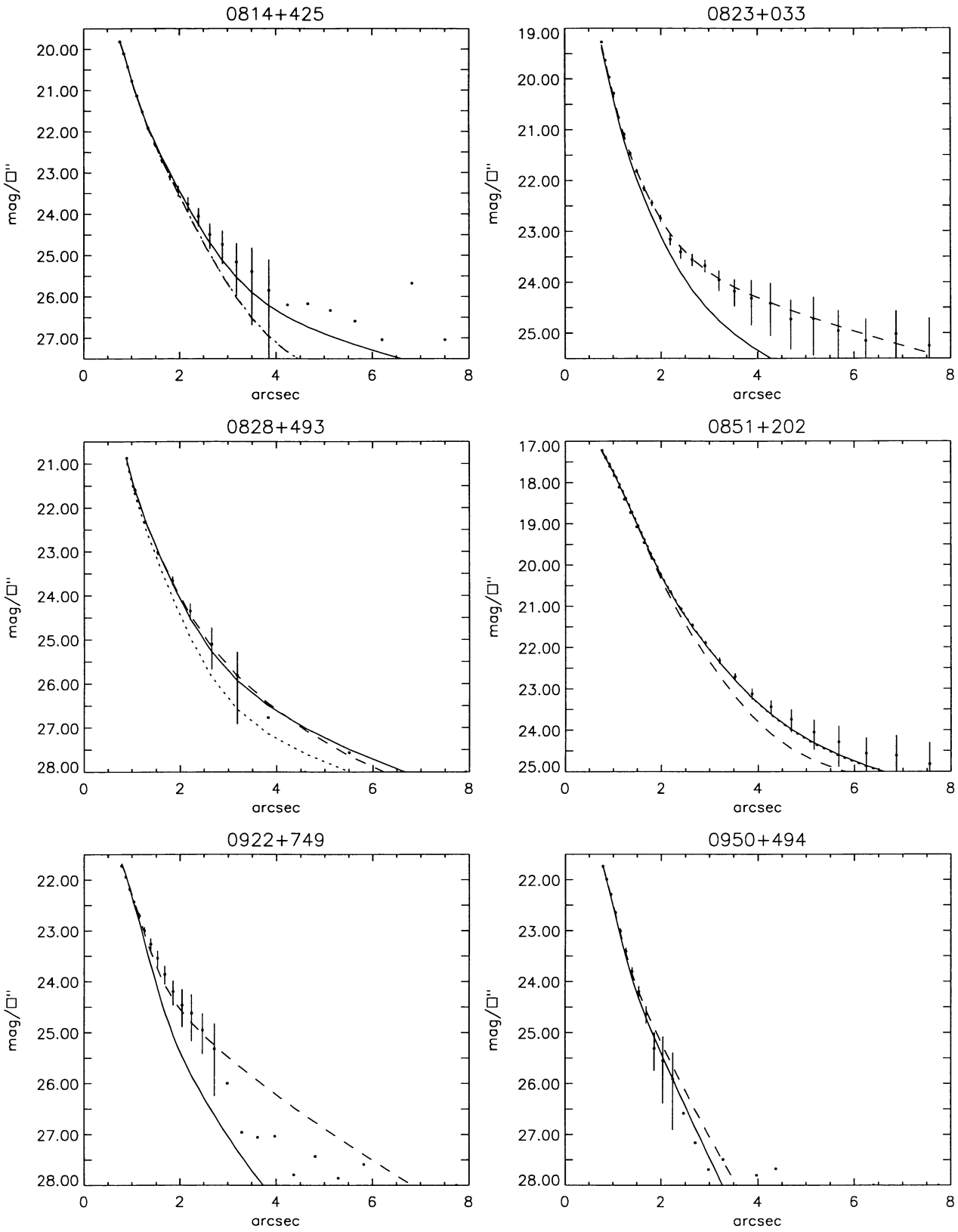


FIG. 5*c*

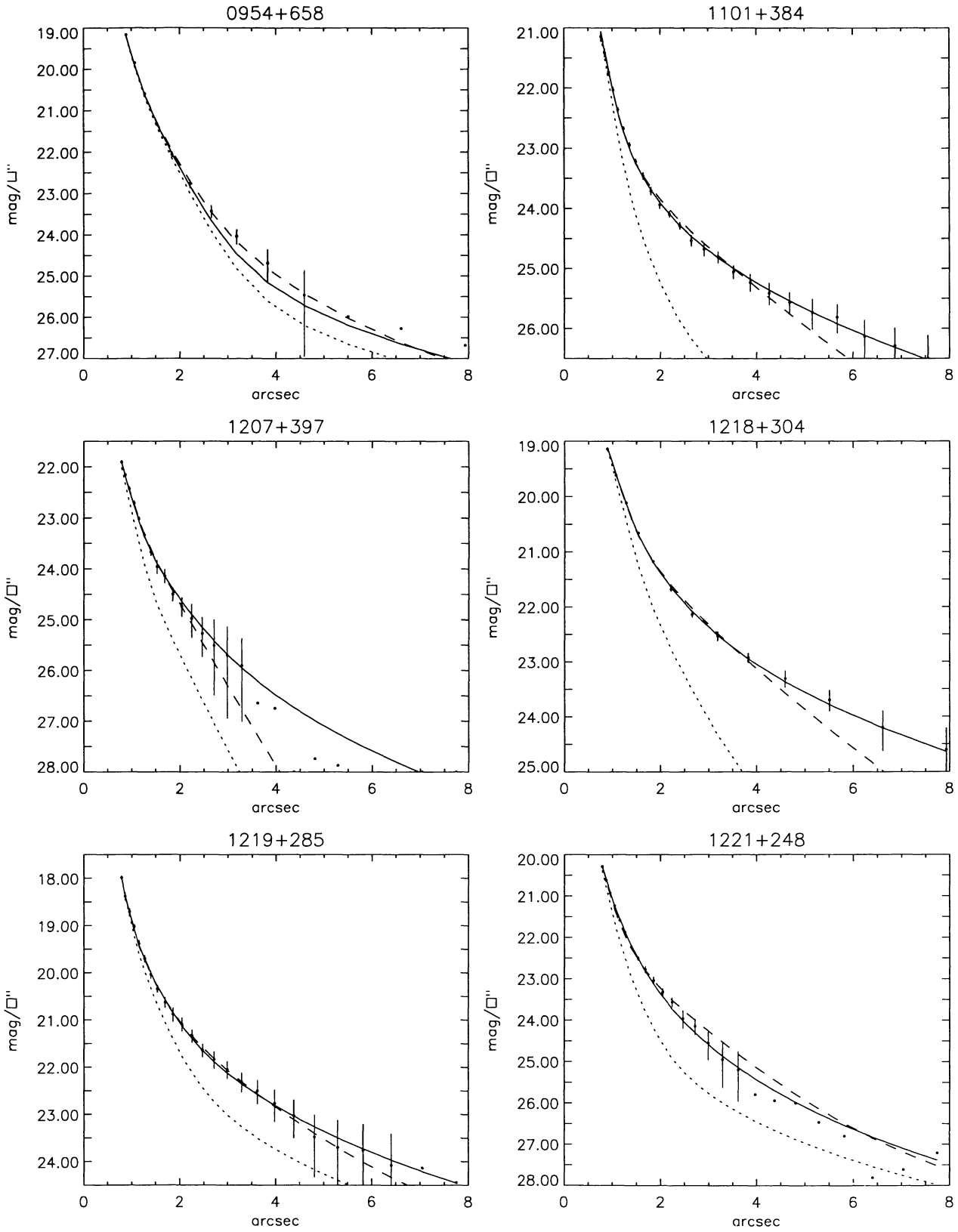


FIG. 5*d*

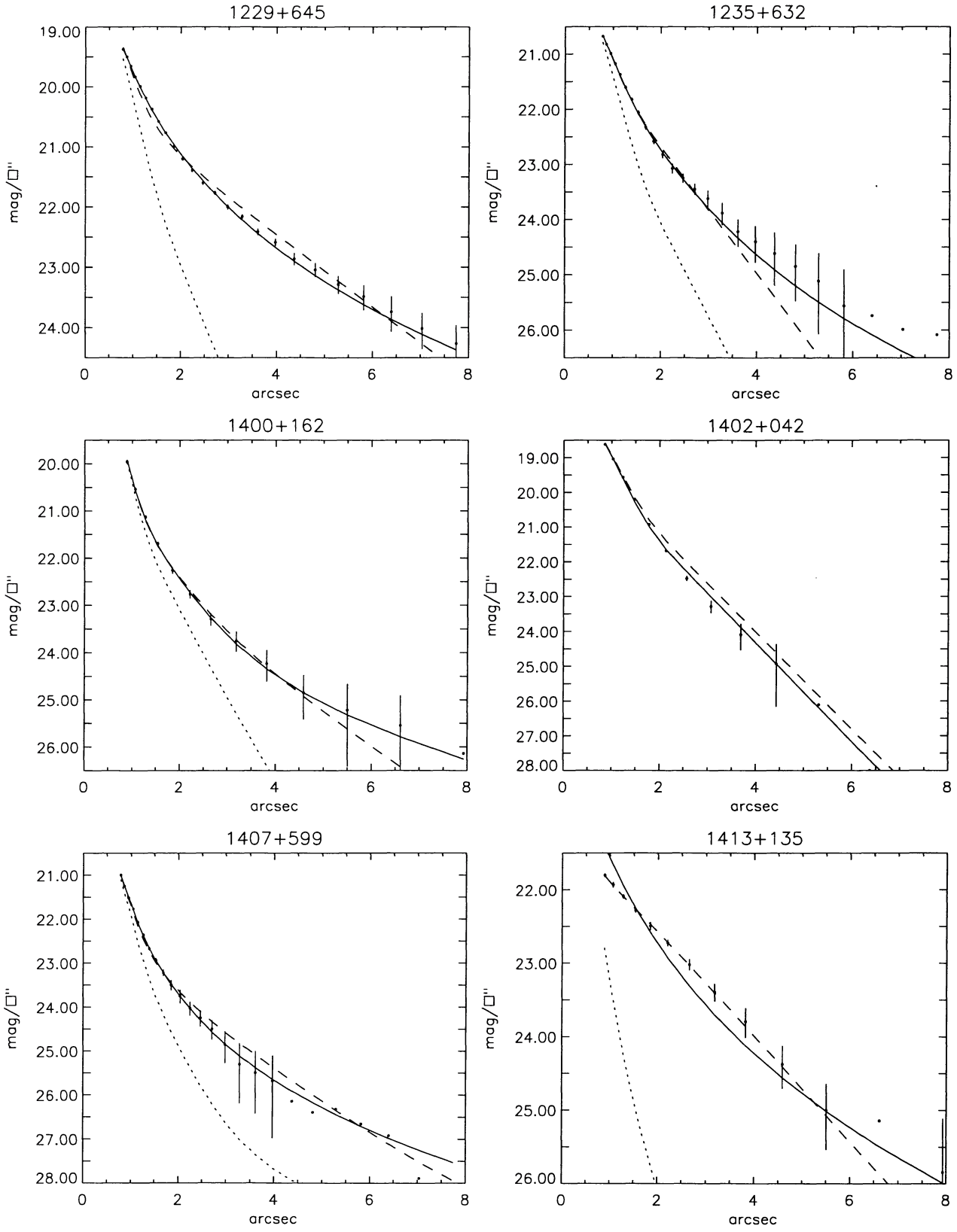


FIG. 5*e*

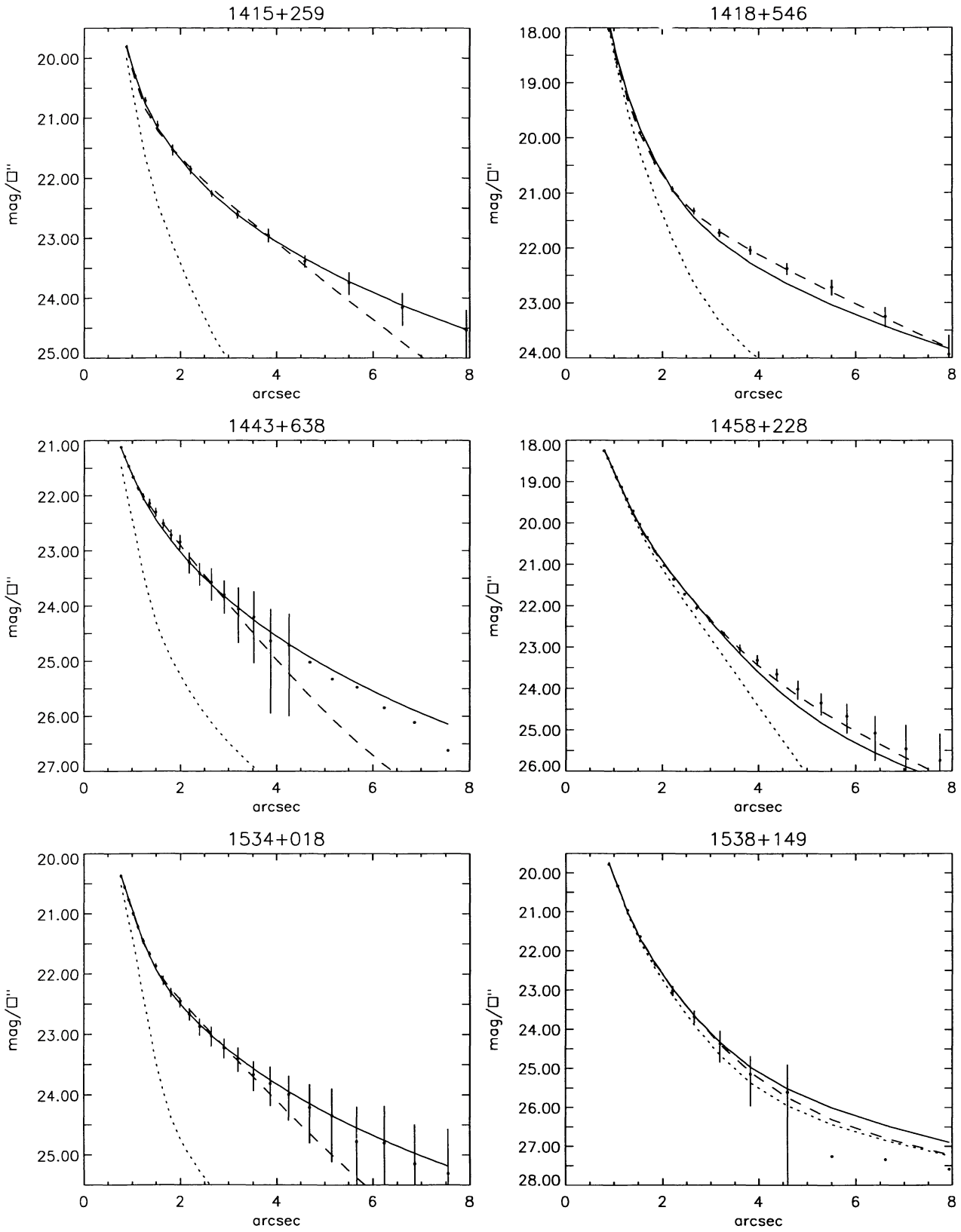


FIG. 5*f*

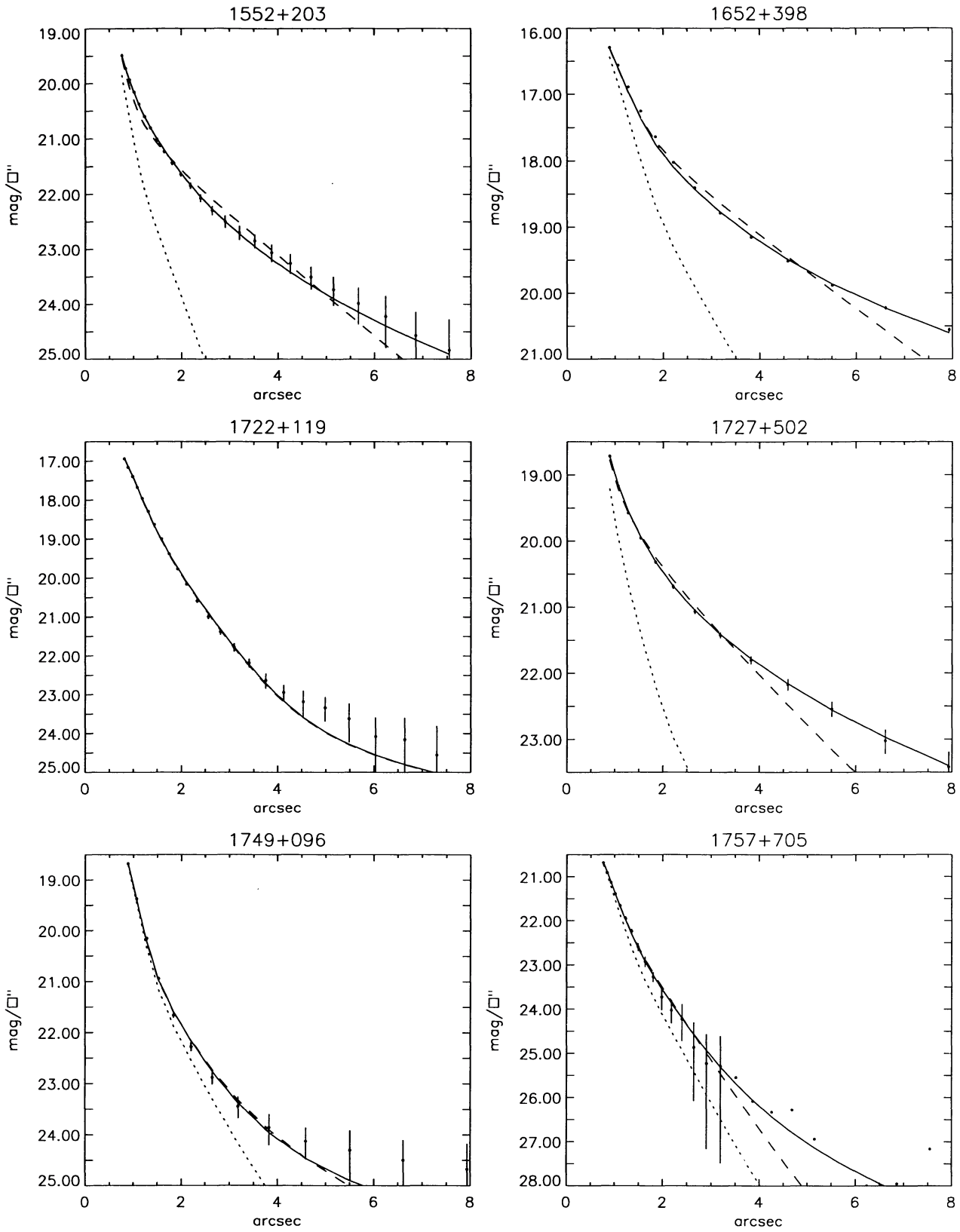


FIG. 5*g*

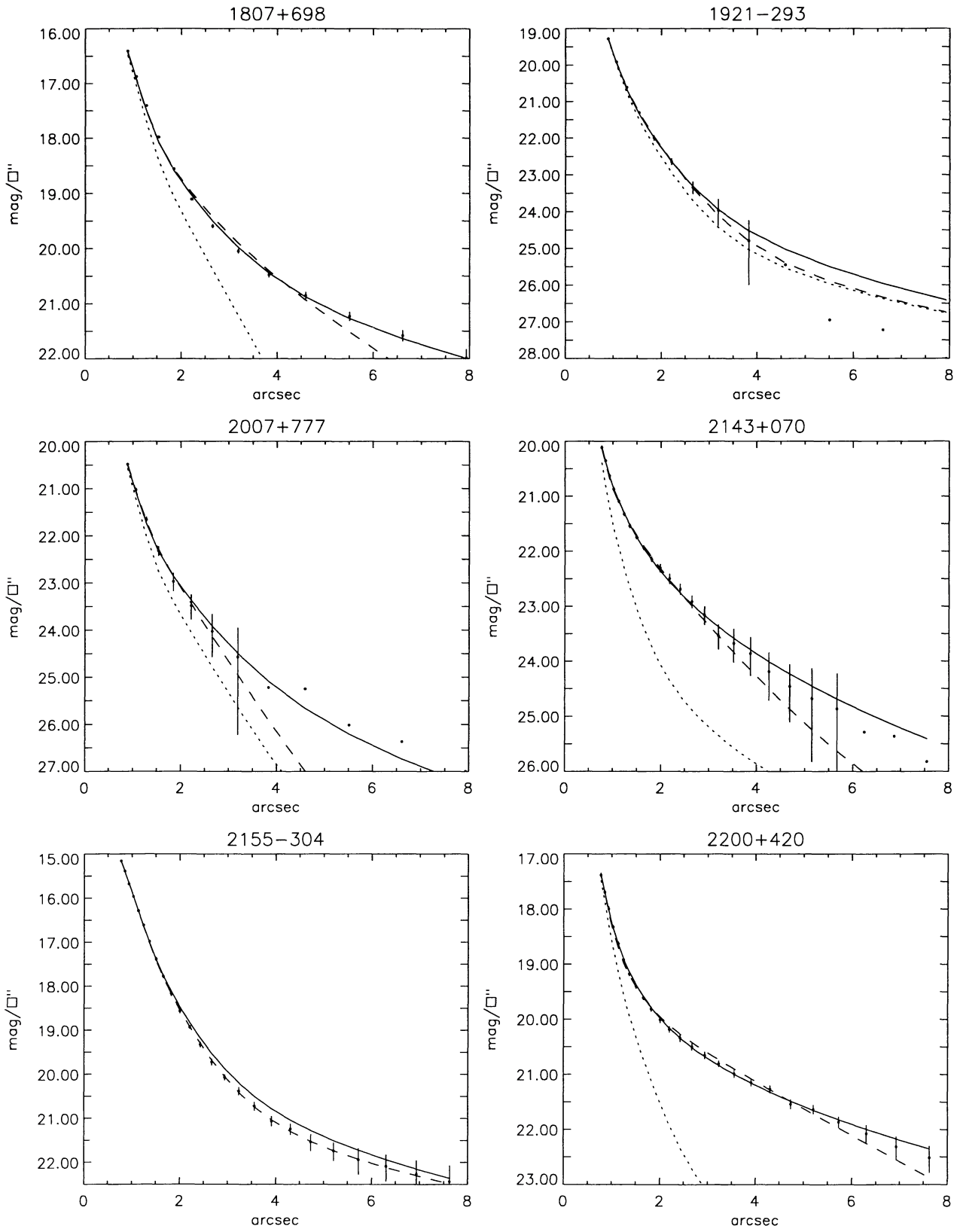


FIG. 5*h*

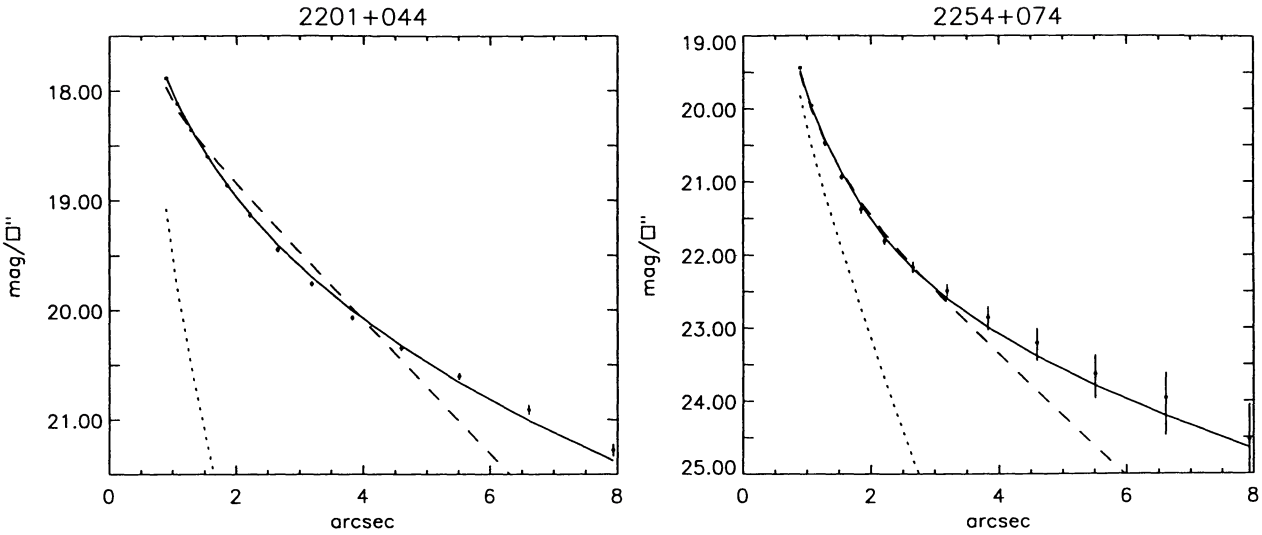


FIG. 5*i*

assuming a *K*-correction of 0, corresponding to an assumed power law with $\alpha = -1$ (dots in this column note the absence of either a redshift or photometry for the object); (4) the *r*-band ratio of integrated total core to host galaxy flux (called optical core dominance in the discussion below) using the values from column (2) in this table and from column (4) in Table 5 (unresolved BL Lac objects have lower limits in this column, and objects with no clearly detected core have upper limits); (5) the maximum contrast isophote in mag arcsec$^{-2}$ is the isophote at which the maximum contrast between galaxy and point source occurs in the best-fit model in units of the 1 $\sigma$ error in counts in that annulus (see Fig. 5); (6) method number 1 core offset (see § 3.1) values in arcseconds, the difference between the core centroid and the centroid of the 25th mag isophote (but see note in col. [8] for a few very bright objects); (7) method number 2 core offset values in arcseconds (see § 3.1), the difference between the centroids of the isophote in column (5) and the core isophote minus the same difference measurement for a PSF star in the same field; (8) reference to footnotes clarifying these measurements in individual cases.

Table 5 contains the following data on the host galaxy fits. Column (1): object name. Column (2): class of best host galaxy fit (E = point source + $r^{1/4}$ law, S = point source + exponential disk law, U = unresolved [cumulative excess above point-source model < 5 $\sigma$], E: and S:, objects have $\chi^2$ values of these fits which favor one Hubble class but not unambiguously [< factor of 2 difference], M = marginally resolved, where source is definitely resolved but the data are insufficient to determine a firm Hubble class [cumulative excess above point-source model between 5 and 20 $\sigma$]. The remaining data in Table 5 for M class objects assumes E best-fit values. Column (3): the ratio of reduced $\chi^2$ values for E fit and S fit models. Column (4): the apparent, total *r*-band magnitude for the host galaxy obtained by integrating the light in the best-fit model to infinity. Column (5): the apparent surface brightness in mag arcsec$^{-2}$ at the best-fit model characteristic radius. Column (6): characteristic radius in arcseconds of the best-fit model. Column (7): Total absolute *r*-band host galaxy magnitude assuming *K*-corrections from Sebok (1986). Column (8): absolute surface brightness at the characteristic model radius [i.e., col. (5) values *K*-corrected and corrected for $(1 + z)^4$ surface brightness dimming]. Column (9): characteristic model radius in kpc.

Thirty-six host galaxies were resolved well enough (cumulative excess above the pure point-source model $\geq 20$ $\sigma$) that an unambiguous morphological class (elliptical or spiral) could have been determined. But this was possible only for 23 of these, including three definite spirals and 20 definite ellipticals. In 10 of the remaining 13 cases, the $\chi^2$ values for the best-fit spiral and elliptical galaxy models differ by less than a factor of 2; in all these cases the point source + E galaxy model is favored, and we have classified these objects as E:. In three cases, the spiral + point-source model is clearly favored by the $\chi^2$ values (0317+185, 0607+711, and 1443+638), but the proximity of nearby bright stars and/or incompletely masked companion galaxies may have adversely affected either setting the background properly or the profile fits themselves (see § 3.1 and 3.3 for notes on individual cases). For consistency, we have classified these objects as S:. Several of the marginal (M class) fits were also adversely affected in this way, notably 0823+033 and 0922+749, as indicated in the notes. It is also possible that some of the E: objects were affected in a similar but much less severe way (e.g., 1757+705).

In general, the presence of close, partially masked companions or the proximity of a bright star, which creates a gradient in the assumed sky background across the BL Lac object, affects the profiles in the same way; a spurious excess is created at intermediate radii. Scrutiny of Figure 5 shows that the addition of spurious counts in a profile at intermediate radii will cause an E galaxy profile to look more like that of a spiral. So the most important sources of systematic errors will bias these profiles toward a spiral best-fit model. For this reason, it is our belief that those objects classified as E: are very likely ellipticals, and the three S: objects could also be ellipticals but require higher resolution imaging to be certain. Those objects classified as unambiguous spirals have been scrutinized carefully by us

TABLE 4

POINT-SOURCE AND ISOPHOTAL DATA

| Name | Core Apparent Gunn r Magnitude | Core Absolute Gunn r Magnitude | Optical $f_{core}/f_{gal}$ | Surface Brightness at maximum host galaxy contrast | Core Offset (arcsec) Method 1 | Core Offset (arcsec) Method 2 | Notes |
|---|---|---|---|---|---|---|---|
| 0122+090 | >23.9 | >-18.2 | <0.01 | 22.5 | <0.1 | <0.1 | |
| 0158+003 | >19.8 | >-21.9 | <0.33 | 22.5 | 0.1 | <0.1 | |
| 0205+351 | 18.4 | -22.8 | 6.08 | 24.5 | 0.4 | 0.4 | 6 |
| 0219+428 | 15.1 | -28.0 | 36.24 | 21.3 | 0.1 | <0.1 | 1 |
| 0257+344 | >22.0 | >-19.5 | <0.03 | 23.5 | <0.1 | <0.1 | |
| 0317+185 | >20.6 | >-20.3 | <0.12 | 23.5 | 0.15 | <0.1 | |
| 0323+022 | 19.2 | -20.8 | 0.18 | 22.0 | 0.15 | <0.1 | |
| 0414+009 | 16.7 | -25.0 | 2.54 | 23.5 | <0.1 | <0.1 | |
| 0419+197 | 20.2 | -24.0 | 2.23 | 24.5 | 0.1 | <0.1 | |
| 0521–365 | >17.4 | >-20.5 | <0.10 | 20.0 | <0.1 | <0.1 | |
| 0548–322 | >20.8 | >-17.4 | <0.01 | 20.5 | 0.2 | <0.1 | |
| 0607+711 | >18.4 | >-23.2 | <0.35 | 21.5 | 0.8 | <0.1 | 2 |
| 0814+425 | ... | ... | 14.4 | ... | <0.1 | <0.1 | 3 |
| 0823+033 | 17.2 | -29.2 | 6.08 | 23.5 | 0.1 | <0.1 | |
| 0828+493 | >19.1 | >-24.8 | <3.87 | 24.0 | <0.1 | <0.1 | |
| 0851+202 | 15.2 | -26.6 | 70.86 | 22.0 | 0.1 | 0.1 | 6 |
| 0922+749 | 19.7 | -27.2 | 9.72 | 24.5 | 0.15 | <0.1 | 2 |
| 0950+494 | 19.7 | ... | >0.83 | 23.0 | <0.1 | <0.1 | no z,4 |
| 0954+658 | 16.7 | -25.6 | 20.38 | 23.5 | 0.1 | <0.1 | |
| 1101+384 | ... | ... | 1.1 | ... | 0.25 | <0.1 | 2,3 |
| 1207+397 | >22.9 | >-21.4 | <0.09 | 24.5 | 0.1 | <0.1 | |
| 1218+304 | 17.7 | ... | 0.55 | 23.0 | <0.1 | <0.1 | no z |
| 1219+285 | 16.1 | -23.0 | 2.36 | 22.5 | 0.15 | <0.1 | 1 |
| 1221+248 | >21.2 | >-19.7 | <0.10 | 23.0 | <0.1 | <0.1 | |
| 1229+645 | >20.1 | >-20.1 | <0.04 | 22.5 | 0.1 | <0.1 | |
| 1235+632 | >21.5 | >-20.2 | <0.06 | 23.5 | 0.15 | <0.1 | |
| 1400+162 | 17.9 | -23.2 | 1.44 | 23.5 | 0.1 | <0.1 | |
| 1402+042 | 16.4 | -25.6 | >8.3 | 23.0 | <0.1 | <0.1 | 4 |
| 1407+599 | >20.1 | >-23.2 | <0.51 | 24.0 | <0.1 | <0.1 | |
| 1413+135 | >22.0 | >-19.0 | <0.04 | 23.0 | <0.1 | <0.1 | |
| 1415+259 | 18.8 | -22.3 | 0.17 | 22.5 | 0.4 | <0.1 | 5 |
| 1418+546 | 15.2 | -24.4 | 0.21 | 22.0 | <0.1 | <0.1 | |
| 1443+638 | >22.6 | >-19.1 | <0.02 | 23.0 | <0.1 | <0.1 | |
| 1458+228 | 16.8 | -24.3 | 2.96 | 23.5 | <0.1 | <0.1 | |
| 1534+018 | 20.8 | -21.1 | 0.06 | 23.0 | <0.1 | <0.1 | |
| 1538+149 | 17.5 | -26.8 | 9.02 | 23.5 | 0.15 | <0.1 | |
| 1552+203 | >18.6 | >-22.4 | <0.22 | 23.0 | <0.1 | <0.1 | |
| 1652+398 | 14.6 | -21.9 | 0.23 | 20.5 | <0.1 | <0.1 | |
| 1722+119 | 14.7 | -25.5 | >13.2 | 23.0 | <0.1 | <0.1 | 4 |
| 1727+502 | 17.6 | -20.0 | 0.16 | 22.0 | <0.1 | <0.1 | |
| 1749+096 | 16.2 | -25.8 | 5.39 | 24.0 | 0.3 | <0.1 | 2 |
| 1757+705 | >19.1 | >-23.5 | <1.83 | 24.5 | 0.1 | <0.1 | |
| 1807+698 | 14.2 | -23.3 | 0.93 | 21.0 | 0.15 | <0.1 | 1 |
| 1921–293 | 17.4 | -24.9 | 4.34 | 22.5 | <0.1 | <0.1 | |
| 2007+777 | 18.8 | -23.5 | 1.45 | 23.0 | 0.2 | <0.1 | |
| 2143+070 | 22.2 | -19.1 | 0.02 | 22.5 | <0.1 | <0.1 | |
| 2155–304 | 13.0 | -26.4 | >19.0 | 23.0 | <0.1 | <0.1 | 1,4 |
| 2200+420 | 15.4 | -23.2 | 0.62 | 21.5 | 0.8 | <0.1 | 2 |
| 2201+044 | >17.8 | >-18.5 | <0.03 | 21.0 | 0.2 | <0.1 | |
| 2254+074 | 17.8 | -22.9 | 0.38 | 23.0 | <0.1 | <0.1 | |

NOTES.—(1) 23.5 mag arcsec$^{-2}$ surface brightness level used for decentering measurement by Method 1. (2) Excess core offset value by method 1 owing to nearby bright star(s) creating background sky gradient in vicinity of BL Lac object. (3) Images not photometrically calibrated; surface brightness levels 1 and 3 mag above sky used for decentering measurements by methods 1 and 2, respectively. (4) For unresolved sources, 23 mag arcsec$^{-2}$ surface brightness chosen arbitrarily for decentering measurement by method 2. (5) Excess core offset value by method 1 owing to incompletely masked nearby companion galaxy. (6) See Fig. 4.

for systematic profile errors; none were found, leading us to classify these objects as spirals.

Therefore, the final morphological tally of BL Lacertae host galaxies in the CFHT survey is 20 definite ellipticals (E), 10 likely ellipticals (E:), three definite spirals (S), three possible spirals (S:) that require better imaging to classify, 10 objects not resolved well enough for galaxy classification (M), and four unresolved objects (U).

### 3.4. *Notes on Individual Objects*

*MS 0205+351.*—This EMSS XBL was the only BL Lac object in our sample found to have a significantly decentered point source. For that reason, unlike the rest of the sample, the point source was fitted with the PSF first then subtracted from the image and the galaxy was fitted independently, with the combined result shown in Figure 5. Other new data on this

TABLE 5

BL LAC HOST GALAXY DATA[a]

| Name | Class of Best Fit | $\chi^2_E/\chi^2_S$ | Apparent Gunn r Magnitude | μ Gunn r (mag/arcsec$^2$) | r (arcsec) | Absolute Gunn r Magnitude | Absolute μ Gunn r (mag/arcsec$^2$) | r (kpc) | Notes |
|---|---|---|---|---|---|---|---|---|---|
| 0122+090 | E: | 1.1 | 18.65 | 23.03 | 1.6 | -23.51 | 21.29 | 9.44 | 1 |
| 0158+003 | E | 0.1 | 18.59 | 23.22 | 1.8 | -23.14 | 21.76 | 9.99 | |
| 0205+351 | S | 2.1 | 20.36 | 22.74 | 1.2 | -21.69 | 21.03 | 6.94 | 2 |
| 0219+428 | M | 0.9 | 19.00 | 22.84 | 1.3 | -24.05 | 20.52 | 9.05 | |
| 0257+344 | E | <0.1 | 18.18 | 22.91 | 2.0 | -23.41 | 21.33 | 9.99 | |
| 0317+185 | S: | 3.1 | 18.28: | 22.02: | 1.2: | -22.64: | 20.71: | 5.09: | 3 |
| 0323+022 | E | 0.2 | 17.37 | 22.35 | 2.2 | -22.67 | 21.52 | 7.56 | |
| 0414+009 | E: | 0.7 | 17.71 | 24.79 | 5.7 | -24.01 | 23.28 | 30.79 | |
| 0419+197 | E: | 1.0 | 21.07 | 26.91 | 3.2 | -23.09 | 23.60 | 22.93 | 1 |
| 0521-365 | E | <0.1 | 14.85 | 20.52 | 3.4 | -23.04 | 20.22 | 5.44 | |
| 0548-322 | E | 0.1 | 14.92 | 22.46 | 7.7 | -23.25 | 22.12 | 13.77 | |
| 0607+711 | S: | 4.3 | 17.25: | 21.78: | 1.7: | -24.44: | 20.21: | 8.89: | 4 |
| 0814+425 | E: | 0.6 | ... | ... | ... | ... | ... | ... | 6 |
| 0823+033 | M | ... | 19.16: | ... | ... | -24.21: | ... | ... | 4,5 |
| 0828+493 | M | 1.0 | 20.57 | 23.08 | 0.7 | -23.13 | 20.29 | 5.16 | |
| 0851+202 | M | ... | 19.83: | 23.50: | 1.2: | -21.97: | 22.00: | 6.59: | 5 |
| 0922+749 | M | ... | 22.17: | ... | ... | -22.16: | ... | ... | 4,5 |
| 0950+494 | U | ... | >19.5 | ... | ... | ... | ... | ... | no z |
| 0954+658 | M | 1.4 | 19.97 | 24.13 | 1.4 | -22.35 | 22.32 | 8.89 | |
| 1101+384 | E | 0.3 | ... | ... | ... | ... | ... | ... | 6 |
| 1207+397 | M | 1.5 | 20.28 | 25.35 | 2.2 | -23.87 | 22.20 | 17.18 | 1 |
| 1218+304 | E | 0.5 | 17.05 | 23.22 | 4.0 | ... | ... | ... | no z |
| 1219+285 | E: | 0.6 | 17.03 | 21.90 | 2.1 | -22.11 | 22.67 | 9.69 | |
| 1221+248 | E | 0.2 | 18.65 | 20.82 | 0.6 | -22.28 | 19.72 | 2.58 | |
| 1229+645 | E | <0.1 | 16.51 | 22.08 | 2.9 | -23.69 | 21.26 | 10.56 | |
| 1235+632 | E | 0.4 | 18.39 | 22.61 | 1.5 | -23.31 | 21.16 | 8.44 | |
| 1400+162 | E | 0.4 | 18.29 | 24.20 | 3.2 | -22.92 | 22.98 | 15.47 | |
| 1402+042 | U | ... | >18.7 | ... | ... | >-23.2 | ... | ... | |
| 1407+599 | E | 0.1 | 19.37 | 23.36 | 1.4 | -23.90 | 20.91 | 9.68 | |
| 1413+135 | S | 56. | 18.59 | 20.87 | 1.4 | -22.41 | 19.52 | 6.94 | |
| 1415+259 | E | 0.1 | 16.86 | 23.55 | 4.9 | -24.28 | 22.36 | 23.22 | |
| 1418+546 | S | 11. | 16.91 | 20.47 | 2.4 | -23.10 | 19.71 | 8.19 | |
| 1443+638 | S: | 2.4 | 18.51: | 23.14: | 2.0: | -23.22: | 21.68: | 11.26: | 3 |
| 1458+228 | E: | 0.9 | 17.98: | 22.41: | 1.7: | -23.17: | 21.20: | 7.91: | 1,4 |
| 1534+018 | E: | 0.6 | 17.66 | 24.08 | 4.3 | -24.27 | 22.47 | 24.38 | 1 |
| 1538+149 | M | 1.1 | 19.89 | 24.15 | 1.5 | -24.21 | 21.05 | 11.85 | |
| 1552+203 | E | <0.1 | 16.97 | 22.25 | 2.5 | -24.07 | 21.08 | 11.23 | |
| 1652+398 | E | 0.5 | 12.99 | 20.89 | 9.0 | -23.53 | 20.72 | 8.14 | |
| 1722+119 | U | ... | >17.5 | ... | ... | >-22.6 | ... | ... | |
| 1727+502 | E | <0.1 | 15.63 | 21.92 | 3.9 | -22.05 | 21.63 | 5.71 | |
| 1749+096 | E: | 0.7 | 18.03: | 25.65: | 7.1: | -24.00: | 23.98: | 40.77: | |
| 1757+705 | E: | 1.0 | 19.76 | 22.96 | 0.9 | -22.94 | 20.89 | 6.13 | 1,4 |
| 1807+698 | E: | 0.6 | 14.12 | 22.59 | 10.5 | -23.44 | 22.26 | 14.23 | |
| 1921-293 | M | 1.6 | 18.99 | 22.56 | 1.1 | -23.33 | 20.71 | 6.64 | |
| 2007+777 | M | 2.0 | 19.20 | 24.11 | 2.1 | -23.14 | 22.20 | 12.32 | |
| 2143+070 | E | 0.3 | 17.89 | 22.95 | 2.4 | -23.35 | 21.66 | 11.60 | |
| 2155-304 | U | ... | >16.2 | ... | ... | >-23.1 | ... | ... | |
| 2200+420 | E | 0.1 | 14.87 | 23.01 | 10.2 | -23.64 | 22.32 | 18.19 | |
| 2201+044 | E | <0.1 | 13.89 | 21.3 | 7.6 | -22.42 | 21.01 | 5.87 | |
| 2254+074 | E | 0.29 | 16.75 | 23.2 | 4.1 | -23.95 | 22.12 | 16.75 | |

NOTES.—(a) Fits favor E galaxy model in outer isophotes. (2) Decentered core; see § 3.3 for method of handling host galaxy data. (3) Contamination of surface brightness profile by very close projected companion galaxy makes fitting results uncertain. (4) Problem with accurate sky subtraction because of nearby bright star(s). (5) One or both model fits did not converge; total galaxy magnitude determined from residual counts after subtraction of core. (6) Not photometric.

[a] Explanation for class of fit: E = elliptical; S = spiral; M = marginal (resolved, but no firm Hubble class, parameters of elliptical fit are given); U = unresolved.

BL Lac object suggesting it as a new microlensed BL Lacertae candidate may be found in Stocke et al. (1995).

*0219+428 (3C 66A).*—This object was observed in both epochs by this survey but was only marginally resolved in our best images owing to the large core dominance and high $z$ (0.444).

*MS 0317+185.*—This EMSS object has a companion within 1″–2″ of the core, making host galaxy profile extraction very difficult. The excess light that is likely present in this companion causes the profile to be better fit by an exponential rather than an $r^{1/4}$ law at intermediate radii. On this basis, we see no compelling evidence that this BL Lac object is in a spiral host despite the lower $\chi^2$ value for the S fit (see Table 5).

*PKS 0521−365.*—Previous studies of this BL Lac object (Cayette & Sol 1987; Macchetto et al. 1991) discovered an optical jet within this galaxy. We detect this feature but have masked it out prior to the extraction and fit of the galaxy profile.

*MS 0607+711.*—This BL Lac object lies within a few arcseconds of a brighter field star, which makes sky level determination suspect and which had to be fitted and subtracted prior

to host galaxy study. Even after subtracting a PSF model for this star, a large region of the BL Lacertae host had to be masked, making the resultant profile much less accurate. Therefore, while the profile fits favor an exponential disk, this fit is not definitive, and a spiral host is not required in this case. This star also contaminates one of our decentering measurements, producing a large core offset value in Table 4 (col. [6]) which is spurious.

*1 Jy 0814+425.*—The host galaxy is clearly resolved in our images, as expected if it is really at $z = 0.258$:. But we lack accurate calibration, and so no absolute quantities can be quoted.

*PKS 0823+033.*—This 1 Jy BL Lac object is within a few arcseconds of a bright star and so was treated in the same way as MS 0607+711 (see above). Owing to this problem plus its high $z$, this object could not be fitted accurately with a galaxy model, although it is resolved in our image. In this case, the host galaxy luminosity was estimated by subtracting a scaled PSF from the image and integrating the residual counts. It is likely that this process underestimates the host galaxy luminosity. The presence of this star also creates a clearly spurious core offset value at the 25th magnitude isophote, so there is no evidence for a real core offset in this source.

*1 Jy 0851+202 (OJ 287).*—This RBL shows a consistent core offset value at the limit of our measurement error. While a close companion galaxy was masked out prior to making the decentering measurements, the consistent offset seen in Figure 3 which grows with radius is unlikely to be attributable to an incompletely masked companion. This possible core offset should be investigated at higher spatial resolution.

*MS 0922+749.*—This EMSS BL Lac object is background to a rich cluster of galaxies (Abell 786 at $z = 0.124$; see Paper II) and also has a very bright star which made background subtraction poor and caused neither of the model fits to converge successfully. The host galaxy luminosity was estimated by subtracting a scaled PSF from the image and integrating the residual light. We suspect, but we cannot prove, that the host galaxy luminosity is significantly brighter than as listed in Table 5.

*MS 0950+494.*—This object is unresolved in 1″ seeing conditions and is also unresolved at 1.4 GHz at the 1″ level (Perlman & Stocke 1993). The lower limit on host galaxy apparent mag of $r > 19.5$ yields an approximate $M_r > -22$ for $z = 0.5$. Given the absolute magnitude distribution for BL Lacertae hosts in this sample (see Fig. 6), these observations suggest $z > 0.5$ for this lineless object.

*1101+384 (Mrk 421).*—This famous BL Lac object lies within 3′ of a very bright star, requiring us to limit exposure times to 20 s only. Further, none of our images were obtained in photometric conditions, so absolute quantities could not be obtained. Ulrich (1989) gives several references for previous studies of this object and its $M_r = -22.7$ elliptical host galaxy. The apparently large core offset of the isophote just above sky level is spurious, owing to the presence of this very bright star.

*1218+304.*—Because there is no measured spectroscopic redshift for this object, we quote no absolute quantities, although the well-resolved host in our data is consistent with the previously suggested $z = 0.13$ (Weistrop et al. 1981) yielding $M_R = -22.5$.

*MS 1402+042.*—This EMSS object has an uncertain $z = 0.344$: but is unresolved in our images and those of Abraham (1994). Our failures to resolve this BL Lac object may owe more to the poor seeing during these attempts than to any unusual nature that the object might possess. The upper limit on host galaxy magnitude ($M_r > -23.2$) is consistent with this BL Lac object being drawn from the same distribution of host galaxy magnitudes as those objects whose hosts we did resolve.

*PKS 1413+135.*—This unusual BL Lac object exhibits no point source in our optical images or those of AMC; both studies find this "host" galaxy to be a spiral (McHardy et al. 1991; Stocke et al. 1992), and recent *Hubble Space Telescope* (*HST*) images show it to be an edge-on spiral (McHardy et al. 1994), confirming our surface brightness modeling. Near-IR images of this unusual BL Lac object place the point source within 0.″25 of the galaxy center (Stocke et al. 1992). Soft X-ray absorption (Stocke et al. 1992), H I 21 cm absorption (Carilli, Perlman, & Stocke 1992), and several species of molecular absorption lines (Wiklind & Combes 1995) have also been detected. This source has a milliarcsecond-scale classical triple VLBI radio continuum structure, unique among BL Lac objects (Perlman et al. 1994). While some authors have suggested that PKS 1413+135 is the first example of a BL Lac object in a spiral galaxy (McHardy et al. 1991), others have suggested that the BL Lac object is background to the spiral at $z = 0.247$ (Stocke et al. 1992).

*1E 1415+259.*—This BL Lac object is surrounded by numerous, close companions (see Fig. 3) which were not excluded in an earlier imaging study by Halpern et al. (1986), causing them to misclassify it as a spiral. Our study and that of AMC agree that it is an elliptical, a result obtained after careful masking of the numerous, close companions. Romanishin (1992) reported the presence of an optical jet (see Fig. 3), which Abraham (1994) suggests is an edge-on galaxy. The apparently large core offset value determined at the 25th mag isophote is spurious, owing to the presence of these close companions.

*1 Jy 1418+546 (OQ 530).*—Previous studies classified this galaxy as an elliptical (Stickel et al. 1993b) and a spiral (AMC). Our profile fit supports the AMC result that the host galaxy is better fit by a spiral surface brightness profile, and we find no reasons to distrust this interpretation (i.e., no close companions, no evidence for sky brightness gradients across our images, etc.). The surface brightness profile resembles an S0 type galaxy. Because the other two BL Lac objects with spiral host galaxies are both quite unusual, this object should be scrutinized further for peculiarities in all wave bands.

*MS 1443+638.*—Close companions cause the galaxy extraction and model fits to be suspect in this case. Owing to the companions, we find no compelling reason why the spiral galaxy fit should be preferred.

*MS 1458+228.*—Bright, nearby stars make sky subtraction difficult and model fits unsatisfactory.

*4U 1722+119.*—While we list this source as unresolved, there is some slight evidence for counts in excess of the scaled PSF at >4″ (see Fig. 5). The upper limit on host galaxy magnitude quoted in Table 5 is consistent with this slight excess and is not inconsistent with a luminous host galaxy for this object similar to others in this sample.

*PKS 1749+096.*—The low Galactic latitude of this BL Lac object ($b = 17.^\circ6$) made the profile extraction suspect beyond 4″ owing to the presence of numerous field stars. Therefore,

this portion of the profile was excluded from the fits, which marginally favor the E galaxy profile. The decentering values found for this source are spurious owing to numerous close field stars creating poor sky subtraction and uncertain masking.

*PKS 2155−304.*—Falomo & Tanzi (1991) reported the detection of extended Gunn *i*-band emission from this host galaxy. Using standard bandpass conversions for a giant elliptical galaxy (Coleman, Wu, & Weedman 1980), their value of $M_i$ (host) = −24.2 implies $M_r = -23.8$, which is 0.7 mag brighter than our limit. We worry that the Falomo et al. host galaxy detection was made using images which were saturated (see their Fig. 1), so we do not consider their detection firm. Because the BL Lacertae point source is so bright in this object, our failure to detect a galaxy is still consistent with the presence of a very bright elliptical, typical of other BL Lac objects in our sample ($M_r > -23.1$).

*1 Jy 2200+420 (BL Lacertae).*—The low Galactic latitude ($b = 10°.4$) of the class prototype made extraction difficult, but an acceptable profile was traced to $a \sim 8''$ (14 kpc). The large decentering of the 25th mag isophote is likely caused by field stars and so is spurious.

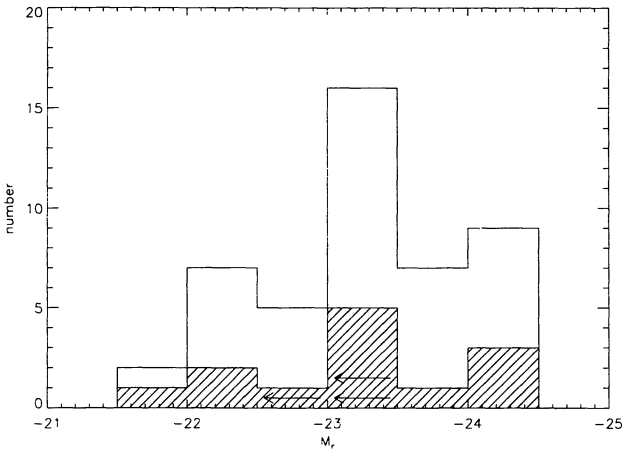


FIG. 6.—A histogram of the host galaxy magnitudes of BL Lac objects uncorrected for the effects of luminosity evolution shown in half-magnitude bins. The shaded areas are the marginal detections, and the shaded areas with arrows indicate the upper limits for the three unresolved sources with redshifts.

## 4. HOST GALAXIES OF BL LAC OBJECTS: BASIC SURVEY RESULTS

Previous work (e.g., AMC; Ulrich 1989; Falomo & Tanzi 1991; Falomo et al. 1993a, b) has shown that a few nearby ($z < 0.2$ typically) BL Lacertae host galaxies are giant ellipticals and have luminosities similar to those found for FR 1 radio galaxy hosts. The galaxy profiles shown in Figure 5 and the host galaxy data shown in Table 5 confirm these earlier results for a substantially larger sample of objects. Besides providing a better sample of BL Lacertae hosts to compare to FR 1 hosts (see § 4.3), in this section we make comparisons of host galaxy properties for various BL Lacertae subsamples. These comparisons allow us to conclude that, from the perspective of the host galaxy, there are no statistically significant differences between BL Lac objects selected using the two different selection techniques (i.e., RBLs and XBLs) or with different properties (e.g., highly polarized objects or objects with weak emission lines).

First, we will address the question of possible biases in the observational results, which will require us to make one minor correction to the host galaxy luminosity data (§ 4.1). Then these data will be subdivided using other BL Lacertae properties to determine whether any type of BL Lac object has distinct host galaxy properties (§ 4.2). Finally, the full sample of BL Lacertae host galaxy data will be compared to similar data for brightest cluster galaxies, FR 1 radio galaxies, and FR 2 host galaxies (§ 4.3).

### 4.1. *Possible Systematic Biases in the CFHT Survey Data*

Figure 6 is the histogram of host galaxy absolute magnitudes for the 50 BL Lac objects in the CFHT sample. While the marginal host galaxy detections (*shaded boxes*) span a similar range of host galaxy magnitudes as those that are well resolved, three of the nine BL Lacertae host galaxies with $M_R < -24$ are marginal detections. This could be attributable to these objects being at high $z$, where evolutionary effects create brighter host galaxies (see below), or it could also be that the marginal fitting of the host galaxies has overestimated somewhat the brightness of the host in these instances. If the latter is the case, the host galaxies of BL Lac objects do not extend much beyond $M_r = -24$. But because the marginal detections are not clearly anomalous compared to the more well-resolved BL Lac objects, both the definite and marginal host galaxy detections will be used in our comparisons. The three BL Lac objects with plausible spiral morphology "host" galaxies will also be used in the comparisons for completeness, even though MS 0205+351 has the least luminous host galaxy in the sample; the other two spiral hosts fall well within the overall distribution. In any case, their presence does not alter the statistics of the full sample by much. And although the unresolved objects will not be used in any comparisons, there is no evidence from this study that they are different from the remainder of the sample in host galaxy properties.

Abraham, Crawford, & McHardy (1992) have outlined a number of ways by which problems could arise in fitting the profiles of active galactic nucleus (AGN) host galaxies, but find no strong bias in estimating the total host galaxy luminosity. We have scrutinized our data for the presence of such biases first by comparing our extracted host galaxy luminosities with those found by others for the same objects and then internally by utilizing the large range of redshifts and of core to host galaxy luminosities (optical core dominance) present in our sample (see Table 4, col. [4]).

Because several of the BL Lac objects in the CFHT sample have been observed previously, a comparison of host galaxy magnitudes determined by this work and previous surveys can be made and is shown in Figure 7. After correcting the Ulrich (1989) compilation data to $r$ band using $(V - r) = 0.2$ (Sebok 1986) and from limiting isophotal magnitudes to total magnitudes where required, the host galaxy mags from Ulrich (1989), AMC, Stickel et al. (1993b), and McHardy et al. (1991, 1992) show no evidence of bias with respect to the magnitudes in Table 5 (mean difference = +0.03 ± 0.4 mag). In

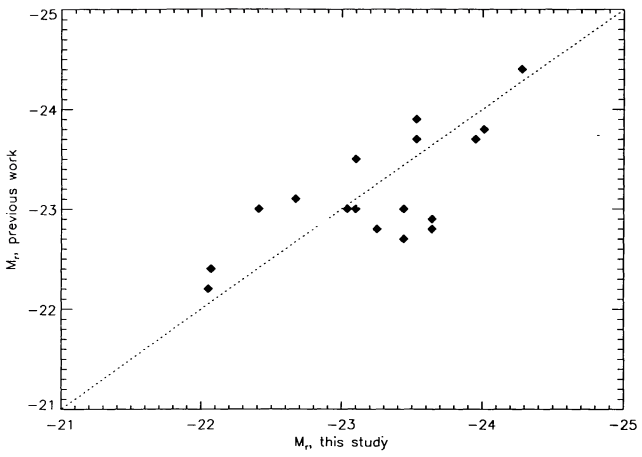


FIG. 7.—A comparison of individual host galaxy magnitudes from this study and from the studies of Ulrich (1989), Abraham et al. (1991), Stickel et al. (1991), and McHardy et al. (1991, 1992). The mean difference between values obtained for the same BL Lac object is $0.03 \pm 0.4$ mag.

addition, we have found no individual case for which our host galaxy luminosities disagree with the results of others by $\geq 1$ mag; almost all agree with our results to within $\frac{1}{2}$ mag. The largest discrepancies we have noted are for BL Lacertae itself, where the host galaxy mag found by us is 0.7–0.8 mag brighter than that listed in Ulrich (1989) and Stickel et al. (1993b), and for PKS 2155−304, where we do not detect a host galaxy (see § 3.4 above).

Because the CFHT sample spans twice the range in redshift of previous samples, the host galaxy luminosities may exhibit some cosmological evolution. In their studies of clusters surrounding quasars, which span a similar redshift range and find similar richness clusters at similar redshifts to this sample (see Paper II), Ellingson, Yee, & Green (1991) found that the luminosity function of cluster galaxies at $z = 0.6$ to present exhibits a mild amount of luminosity evolution of the form $E(z) = z$. Figure 8 shows that the CFHT BL Lacertae sample also shows evidence for similar host galaxy evolution. The cumulative distribution of host galaxy magnitudes divided into equal halves by redshift (Fig. 8*a*) shows a few tenths magnitude shift to brighter host galaxies at higher $z$, consistent with the Ellingson et al. (1991) result. While it would be inappropriate to use our modest-sized sample to construct an independent luminosity evolution model, Figure 8*b* shows that the application of $E(z) = z$ brings the high-$z$ and low-$z$ BL Lacertae subsamples into closer agreement; an even larger correction would be required to match the subsample distributions more precisely. Because many of the luminosity distributions with which we wish to compare the present data (e.g., FR 1 and FR 2 hosts, brightest cluster galaxies) are constructed from $z < 0.2$ samples, this is an important correction to make to the BL Lacertae hosts. Therefore, for all the comparisons in this section, the $E(z) = z$ luminosity evolution model of Ellingson et al. (1991) will be applied.

Because it is more difficult to extract and correctly fit the host galaxy profiles of more highly core-dominated BL Lac objects, the host galaxy extraction of these objects could be biased with respect to the more well-resolved BL Lac objects. However, a comparison of the *observed* (i.e., not corrected for evolution) host galaxy absolute magnitudes for highly core-dominated BL Lac objects (values in Table 4, col. [4] > 1) with less core-dominated BL Lac objects (values <1) finds no statistically significant difference ($P_{KS} = 97\%$). Likewise, there is no correlation between the core dominance and the observed effective surface brightness or effective radius, the actual quantities obtained by our extraction technique. The absence of apparent biases in the actual fitted quantities (effective surface brightness and radius) is comforting, since simulations by Abraham et al. (1992) have shown that such biases are possible. So, while we cannot rule out biased results for individual

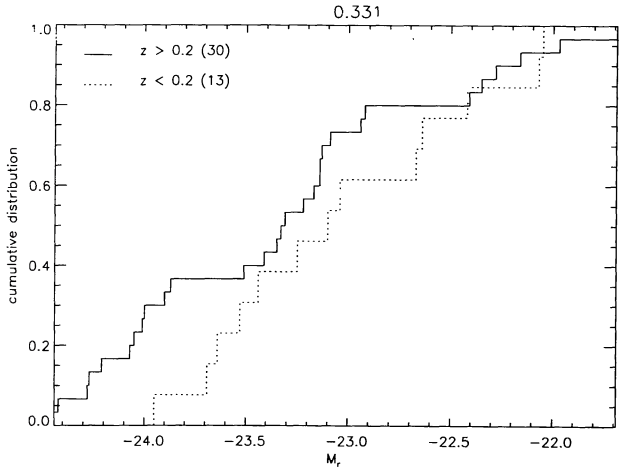


FIG. 8*a*

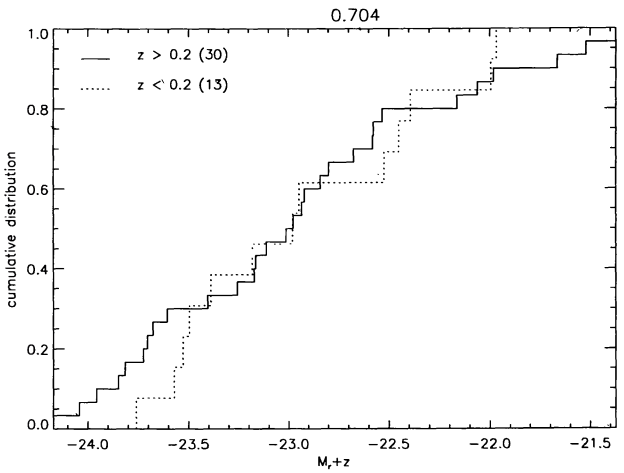


FIG. 8*b*

FIG. 8.—The cumulative host galaxy magnitude distributions for the high- and low-$z$ subsamples. (*a*) Distributions using observed absolute magnitudes; (*b*) Distributions with magnitudes corrected to $z = 0$ for a modest amount of luminosity evolution of the form $E(z) = z$ (Ellingson et al. 1991). K-S test probabilities are shown at the top of each plot. Although this sample is too small and has galaxy magnitudes too inaccurate to confirm this relationship in detail, this figure shows that these BL Lacertae data are consistent with $E(z) = z$ luminosity evolution, so that this correction will be applied before using these data for any statistical tests.

BL Lac objects which are highly core-dominated, there is no evidence for a statistical bias that would contaminate the comparisons we make in the following sections.

Even though we find no obvious correlation between host galaxy magnitudes and measured optical core dominance in the present sample, we cannot rule out the possibility that BL Lac objects without redshifts (and so not included in this study) are found in less luminous host galaxies. If the host galaxies of featureless objects are systematically fainter, this could account for our failure to detect absorption lines in these objects. But until higher resolution images are obtained for very featureless BL Lac objects, this remains a matter of pure speculation.

### 4.2. *Internal Sample Comparisons of BL Lacertae Host Galaxies*

The large number of objects in this homogeneous set of images of BL Lac objects allows us to make internal comparisons between different subclasses of BL Lac objects not possible before. The strength of comparisons internal to the CFHT survey is that a homogeneous set of images were reduced and analyzed in the same fashion, using the same magnitude system and the same corrections from observed to absolute quantities as described in § 3. Also, many of the subsamples have similar redshift distributions so that potential distance-dependent biases will not be important sources of error (see § 2). A summary of internal comparisons is shown in Table 6 and the general result is that, from the perspective of the host galaxy, there is no evidence for differences between BL Lac objects with varying characteristics; all appear to have host galaxy properties consistent with being drawn from the same parent population. And although we use the evolution-corrected magnitudes in all cases, similar results are obtained using the uncorrected magnitudes in Table 5, since as shown in § 2, the redshift distributions of the various subclasses of BL Lacs within the CFHT sample are quite well matched.

The similarity in the distributions of host galaxy magnitudes is particularly important for the X-ray and radio-selected subsamples, which have been suggested for several reasons to be different types of objects; e.g., the large difference in $\langle V/V_{\max} \rangle$ values and difference in redshift distributions and emission-line properties (Stickel et al. 1991; Morris et al. 1991). Both the comparisons between the plausibly complete X-ray and radio-selected samples observed at CFHT and the entire sample divided into radio- and X-ray–loud populations show no statistically significant differences in host galaxy luminosities. But the 1 Jy RBL sample observed at CFHT is too small to provide a definitive comparison in this regard (Fig. 9*a*) and deep optical imaging of the remainder of the 1 Jy sample would be an important but difficult addition to the present work. The more physically meaningful division by X-ray to radio flux ratio shown in Figure 9*b* is much more convincing evidence that RBLs and XBLs have indistinguishable host galaxy properties. We note also that the optically unresolved and thus highly core-dominated objects in our sample neither are exclusively radio or X-ray loud nor are those few BL Lac objects with spiral host galaxies confined to one or the other of these types. Since Perlman & Stocke (1993) have shown recently that the extended radio luminosities and morphologies of XBLs and RBLs are statistically indistinguishable, the similarity in their host galaxy properties and clustering environments (see Smith et al. 1995 and Paper II) means that all the observable "unbeamed" properties of XBLs and RBLs are indistinguishable, arguing strongly that they are drawn from the same parent population. However, it is important to emphasize that this statement is based upon the current sample, which has explicitly excluded $z > 0.65$ BL Lac objects and very featureless BL Lac objects. While these objects constitute a very small percentage of XBL samples (i.e., one or two of 22 in the EMSS), they are a much larger fraction of the RBLs; e.g., the 1 Jy sample has half its 36 members which are excluded by our redshift criterion. Therefore, the most comprehensive statement that can be made currently is that the $z < 0.65$ XBLs and RBLs have similar "unbeamed" properties and are likely drawn from the same parent population. High-resolution *I*-band imaging of the remainder of the RBLs in the 1 Jy sample and perhaps *HST* images will be required to determine whether the higher redshift RBLs are similar objects to those RBLs observed at CFHT.

Not only do the high- and low-polarization objects have similar host galaxy properties, but the host galaxies for four of the five optically unpolarized XBLs (see Tables 1 and 5) from the EMSS have host galaxy luminosities typical of the full sample. Since their extended radio properties are also similar to the rest, there is no clear evidence from their "unbeamed" emission that they are not BL Lac objects. The exception is MS 0205+351, the BL Lac object with an offset, low-luminosity spiral "host" galaxy whose optical polarization is <1.9% as limited by interstellar polarization in that direction (Jannuzi et al. 1994). Thus, absence of optical polarization may be another of this object's anomalous properties.

TABLE 6

SUMMARY OF K-S TEST PROBABILITIES THAT BL LACERTAE SUBSAMPLES ARE DRAWN FROM THE SAME PARENT POPULATION

| Subsamples being Compared | Dividing Line Value | Number of Objects in Subsamples | K-S Test Probabilities |
|---|---|---|---|
| Emission Line/Non-Emission Line | $W_\lambda \sim 1$ Å | 13/33 | 75% |
| Complete XBL/complete RBL | EMSS+*HEAO 1* A-2/1 Jy Samples | 22/12 | 43% |
| X-ray–loud/radio-loud | $\log (f_X/f_r) = -5.5$ | 26/17 | 64% |
| High polarization/low polarization | $P = 10\%$ | 20/19 | 99% |
| Polarization P.A. "preferred"/no preferred P.A. | $\delta$ (P.A.) = 20° | 11/13 | 39% |
| Core dominated/not core dominated in optical | OCD = 1 | 25/17 | 86% |
| Core dominated/not core dominated in radio | RCD = 10 | 16/19 | 53% |

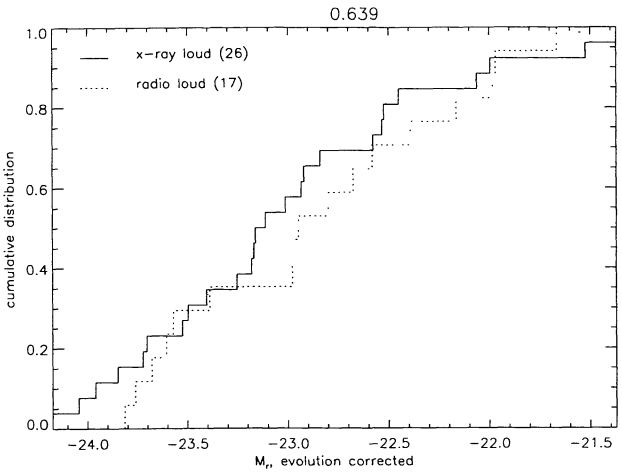


FIG. 9a

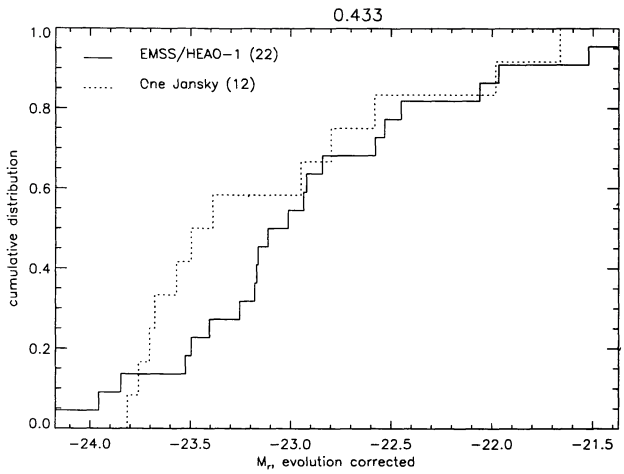


FIG. 9b

FIG. 9.—Host galaxy magnitude distributions for X-ray and radio-loud BL Lac objects. The full sample divided into radio- and X-ray–loud objects is shown in (*a*), while the members of the complete 1 Jy and EMSS + *HEAO 1* A-2 samples are shown in (*b*). The K-S test probabilities shown at the top of each plot indicate no obvious statistical differences in host galaxy luminosities for these subsamples.

Table 6 also shows that the important XBL property of preferred position angles of optical polarization is not clearly attributable to BL Lac objects with an unusual distribution of host galaxy luminosities. Although this subsample division shows the largest statistical difference in host galaxy luminosities of any test we conducted, this is primarily attributable to the modest sample sizes available. For this test, we have used only those BL Lac objects for which extensive optical polarimetry has been performed (Jannuzi et al. 1993; Kuhr & Schmidt 1990) and for which the behavior of the polarization position angle is well established. Unfortunately, only using BL Lac objects which are well observed polarimetrically leaves two subsamples which are too small from which to draw firm conclusions. The preferred position angle trait (seen in ~85% of XBLs and almost never in RBLs; Jannuzi et al. 1994, Smith et al. 1992) is a crucial discriminator favoring the hypothesis that XBLs are intrinsically identical to RBLs, just viewed further off the beaming axis (Elston, Jannuzi, & Smith 1989; Jannuzi et al. 1994; Stocke et al. 1989). So, more extensive polarimetry of a large sample of BL Lac objects is needed to determine more accurately the properties of these two subsamples to determine if the preferred position angle objects are a special type of BL Lac object.

Although there is no correlation between maximum polarization percentage and host galaxy luminosity, Figure 10 shows the existence of a strong correlation between optical core dominance and polarization (Spearman rank-order correlation coefficient = 0.4, implying that the two variables are correlated at the 99% probability level). Jannuzi et al. (1994) argue that the smaller polarization percentages of XBLs cannot be attributable exclusively to starlight dilution from the host galaxy because even the polarization of the XBL nonthermal continuum blueward of the Ca H and K break is small compared to that of RBLs. But it is likely that the larger host galaxy contribution creates at least some of the correlation seen in Figure 10. The existence of several highly core-dominated BL Lac objects (e.g., 1402+042 and 0950+494) with modest maximum polarization percentages (9.5% and 5.2%, respectively) argues that starlight dilution cannot be the sole cause of this correlation, as Jannuzi et al. (1994) suggest on the basis of detailed modeling. The preferred position angle objects do not occupy a unique locus in this figure, arguing further that they are no different from other BL Lac objects. The four unpolarized XBLs (indicated by downward arrows in Fig. 10) have a significant spread of optical core dominance values.

Although neither optical nor radio core dominance appears related to host galaxy properties (Table 6), Figure 11 shows that the radio and optical core dominance values for BL Lac objects are correlated weakly (correlation coefficient = 0.198, implying a correlation present at 62% probability) based upon

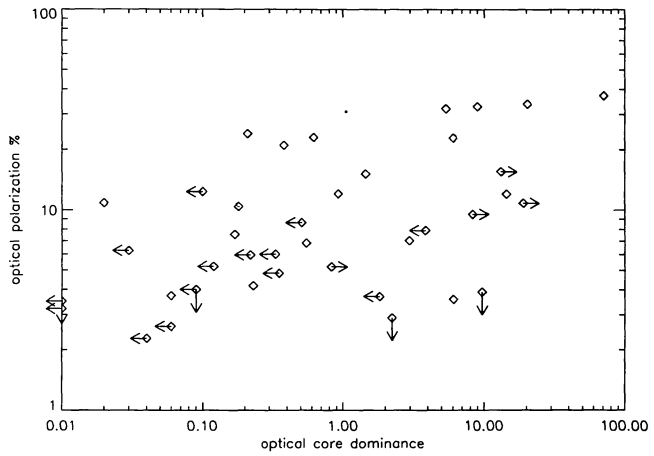


FIG. 10.—The integrated Gunn *r*-band optical core dominance (core luminosity divided by host galaxy luminosity) obtained by this study compared with the maximum percentage of optical polarization from the literature. A correlation is present between these two variables at the 99% level using a nonparametric rank correlation test. The best-fit linear regression to the data points in this logarithmic plot yields a slope of 0.174, a *y*-value = 12.5 at $x = 1$, and a correlation coefficient of 0.565.

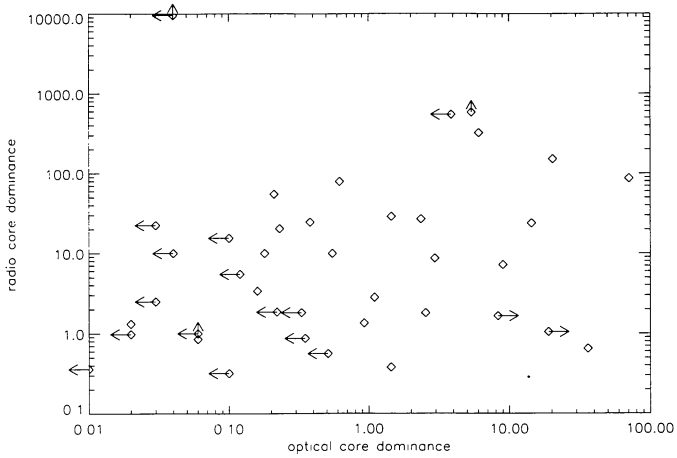


FIG. 11.—The radio core dominance at 1.4 GHz vs. the optical $r$-band core dominance obtained from this study. The highly discrepant point at upper left is PKS 1413+135, a very unusual BL Lac object which may be a gravitationally lensed system. The lower limit at coordinates (6,1000) is MS 0205+351, another gravitational lens candidate. A weak correlation is present between these two variables at the 62% probability level.

nonsimultaneous observations. Note the highly discrepant point at top left attributable to PKS 1413+135, which may be a background quasar whose BL Lacertae characteristics are created by gravitational microlensing (Stocke et al. 1992). Another plausible microlensed BL Lac object (MS 0205+351) also has only a lower limit to its radio core dominance (Stocke et al. 1995) and, given more sensitive radio observations, it could be as discrepant as PKS 1413+135 in Figure 11 [the lower limit for MS 0205+351 is at (6, 1000) in Fig. 11]. Thus, Figure 11 could supply a useful discriminator for such objects.

In summary, there is no evidence from host galaxy properties for any obvious differences between BL Lac objects with differing observable properties as might be expected if they were different types of AGNs. We conclude that these observable differences are either aspect dependent or delineate the range of inherent properties of these objects but do not require different populations of objects to be present. Thus, the only host galaxy properties that require some BL Lac objects to be different from others are the decentered host galaxy for MS 0205+351 and the spiral host galaxies for MS 0205+351, PKS 1413+135, and 1 Jy 1418+546 (OQ 530).

### 4.3. *Optical Core Dominance and Linelessness in BL Lac Objects*

Despite the ubiquity of the beamed FR 1 model for BL Lac objects in the literature over the last several years (Padovani & Urry 1990, 1991; Urry, Padovani, & Stickel 1991; Morris et al. 1991; Stickel et al. 1991; Perlman & Stocke 1993), there remains a possibility that at least some BL Lac objects are beamed or gravitationally lensed quasars. Unlike the FR 1 galaxies, whose optical spectra possess intrinsically weak emission lines (Longair & Seldner 1979; Stocke & Perrenod 1981), the large equivalent width emission lines in normal quasars are difficult to hide. A very luminous optical continuum would need to be present in order to decrease the $W_\lambda \geq 100$ Å emission lines in quasars to the $W_\lambda < 5$ Å levels seen in BL Lac objects. In this section, we make no assumptions about the process that makes the continuum in BL Lac objects so bright, requiring only its presence to diminish the large equivalent width emission lines in any putative broad and/or narrow-line regions.

An upper limit on the amount by which emission lines are diminished in equivalent width can be obtained using our optical images. Using the best-fit models for BL Lac objects displayed in Figure 5 and Tables 4 and 5, we have computed the ratio of core to galaxy $r$-band light that would be present in a 2″ circular aperture in good seeing (<1″), simulating a spectroscopic observation of these objects. A similar calculation has been done by Browne & Marcha (1993) using simulated data. These "spectroscopic" core dominance values range from 40% larger (for marginally resolved BL Lac objects like 3C 66A) to 16 times larger (for very nearby, well-resolved BL Lac objects like Mrk 501 and BL Lacertae itself) than the total core dominance values listed in column (4) of Table 4 because virtually all of the core but only a fraction of the galaxy light falls within the aperture. Since these "spectroscopic" core dominance values are ratios between the observed core and the underlying host galaxy light, they are the *maximum* amount of brightening that could have occurred to the nonthermal continuum to dilute the emission lines; i.e., for a very weak quasar continuum, the equivalent widths are measured relative to the starlight continuum of the underlying host galaxy, setting the faintest possible level for the continuum. If a normal (i.e., unbeamed or not gravitationally lensed) quasar continuum were present in the object, then the "spectroscopic" core dominance values would overestimate the dilution of the emission-line strengths and underestimate the emission-line equivalent widths seen in the spectrum. Therefore, this simulation is conservative in the sense that the equivalent widths obtained are firm lower limits.

We then computed the expected equivalent width of the H$\alpha$ + [N II] $\lambda\lambda$6548, 6584 emission-line complex and the H$\beta$ + [O III] $\lambda\lambda$4959, 5007 complex assuming undiminished values of $W_\lambda = 200$ Å for H$\alpha$ + [N II] and 100 Å for H$\beta$ + [O III], as seen in low-$z$ quasars. These are the most prominent emission lines that would be observed in normal quasars at the redshifts of our BL Lac objects ($z < 0.65$). The $W_\lambda$ values chosen are the mean observed strengths of these emission lines among quasars in the EMSS X-ray–selected quasar sample (i.e., a sample not selected by or biased by emission lines strengths); seldom do these lines have equivalent widths <50 Å (Morris & Stocke 1991). These canonical emission-line strengths were then diminished by the "spectroscopic" core dominance values for a 2″ aperture to yield the estimated emission-line equivalent widths that would be observed if each object were a normal quasar with the highly brightened continuum found in its CFHT image.

Figure 12 is a histogram of the expected emission-line strengths in the optical spectra of BL Lac objects resulting from this simulation. The optical spectra are assumed to extend only to 7600 Å (i.e., blueward of the atmospheric $A$-band) so that H$\alpha$ + [N II] emission is within the observable region only for $z < 0.16$; at higher redshifts, the H$\beta$ + [O III] lines would be within the spectral region covered. Figure 12 shows that for at least half the sample the expected emission-line strengths are ≥50 Å, large enough so that the object would be classified as a

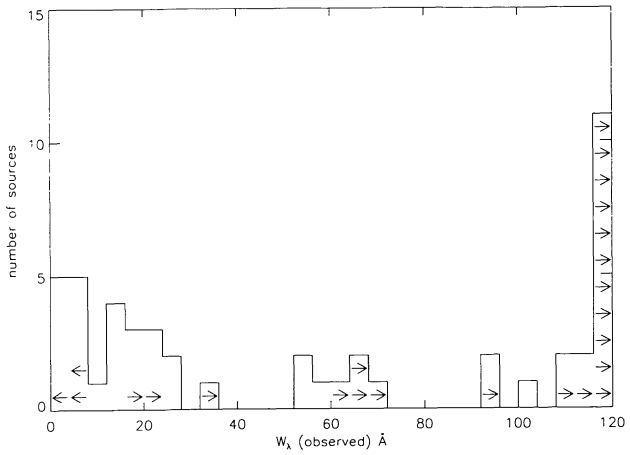


FIG. 12.—A histogram of the simulated emission line equivalent widths for BL Lac objects in the CFHT survey under the hidden quasar hypothesis. This plot assumes that BL Lac objects are quasars whose emission-line strengths are diluted by the presence of a highly Doppler-boosted or gravitationally lensed continuum. The upper and lower limits in this figure result from limits on the "spectroscopic" core dominance, as measured in the images. See the text for the procedure used to determine the maximum amount of dilution of the Hα + [N II] or Hβ + [O III] emission-line complexes from our CFHT images. This procedure causes these simulated values to be firm mimima. As this figure shows, ≥60% of the CFHT BL Lac objects would still possess high equivalent width emission ($W_\lambda$ > 20 Å) lines in their optical spectra even when diluted by the BL Lacertae continuum and so would not be classified as BL Lac objects.

normal quasar, not a BL Lac object. And 80% of the sample would possess observed emission lines at $W_\lambda > 10$ Å, twice the maximum proposed emission-line strength used by Stocke et al. (1989) and Stickel et al. (1991) as a BL Lacertae identification criterion. In addition, the values in Figure 12 are lower limits on the expected emission-line strengths. Thus, most of these BL Lac objects do not lack strong emission lines because of the presence of a very bright optical continuum. This conclusion has been reached previously on the basis of observing weak, stellar absorption lines in the spectra of some BL Lac objects (Morris et al. 1991). Evidently, the broad- and narrow-line regions in BL Lac objects must be either intrinsically very faint, as in the model of Guilbert, Fabian, & McCray (1983; see also Perlman et al. 1996b), or occulted by a dense obscuring medium (Falcke, Gopal-Krishna, & Biermann 1995).

By allowing for some variability of the BL Lacertae core source, approximately 20 of these BL Lac objects (primarily the unresolved and marginally resolved objects) are highly enough core dominated to hide typical quasar broad-line regions. Twelve of these 20 BL Lac objects with simulated $W_\lambda \leq 25$ Å have been observed to have weak emission lines in their optical spectra and so are candidates for possessing quasar-like broad-line regions. We emphasize that this simulation shows that normal quasar strength emission lines *could be* present in these objects and still be effectively hidden by the bright continuum; this simulation does not prove that such emission lines are actually present in many BL Lac objects.

Because many FR 1 radio galaxies possess a stellar continuum and no optical emission lines or only weak Hα + [N II] emission lines ($W_\lambda \sim 35$ Å) and even weaker Hβ + [O III] emission ($W_\lambda \sim 5$ Å; these values are for the prototype wide-angle tail (WAT) 3C 465; De Robertis & Yee 1990), the addition of a featureless BL Lacertae continuum easily can produce the observed optical spectra of BL Lac objects. Indeed, using the same simulation described above and the emission-line equivalent widths of 3C 465, the optical spectra of only eight out of the 50 CFHT BL Lac objects would have observed emission-line equivalent widths ≥10 Å. And five of these eight sources (PKS 0521−365, PKS 0548−322, Mrk 501, PKS 2201+044, and PKS 2254+074) do have weak emission lines in their optical spectra comparable to the strength expected on the basis of being beamed FR 1 galaxies. The remaining three sources (MS 0317+185, H 0323+022, and H 1218+304), whose spectra should show weak Hα + [N II] emission according to the simulation, do not have high signal-to-noise spectra of the Hα region in hand. The very weak Hβ + [O III] emission that is typical of FR 1's could be hidden easily in the spectra of these three objects by their modestly bright, featureless continuum. Therefore, even the quite modest core sources found in many X-ray–selected BL Lac objects are sufficient to hide the emission lines seen in FR 1's and create the lineless character of BL Lacertae optical spectra for every object in this survey. This is especially true when the redshift is high enough to move the Hα + [N II] complex out of the observable band.

### 4.4. *External Sample Comparisons: Host Galaxies of BL Lac Objects Compared to Brightest Cluster Galaxies and Radio Galaxies*

Using the full CFHT BL Lacertae sample, the cumulative distribution of host galaxy luminosities is shown compared with brightest cluster galaxies (BCGs) and FR1 and FR 2 radio galaxies in Figures 13, 14, and 15, respectively with the K-S test results shown in Table 7.

Past work (e.g., Ulrich 1989) has used comparisons between the host galaxies of a small sample of BL Lac objects with FR 1 radio galaxies to argue that FR 1's are the parent population of

TABLE 7

SUMMARY OF K-S TEST PROBABILITIES THAT BL LAC OBJECTS AND OTHER AGNS ARE DRAWN FROM THE SAME PARENT POPULATION

| COMPARISON SAMPLE | NUMBER OF OBJECTS IN COMPARISON SAMPLE | K-S TEST PROBABILITIES | | |
|---|---|---|---|---|
| | | With Evolution | Z < 0.2 only | No Evolution |
| Brightest cluster galaxies | 116 | $10^{-9}$ | $2 \times 10^{-3}$ | $4 \times 10^{-6}$ |
| B2 Sample FR 1 radio galaxies | 44 | 13% | 33% | 59% |
| Owen & Laing FR 1 radio galaxies | 19 | 10% | 17% | 58% |
| Owen & Laing FR 2 radio galaxies | 31 | 32% | 68% | 5% |

BL Lac objects. While these comparisons can support a plausible argument that BL Lac objects are beamed FR 1's, the distribution of host galaxy luminosities (and morphologies) of FR 1's largely overlaps that of FR 2's (e.g., Owen & Laing 1989; Owen & Ledlow 1994), so that these comparisons are not critical in determining whether BL Lac objects are beamed FR 1's or FR 2's. In this regard, the comparison of extended radio properties is a far more clear-cut discriminator, since the radio power levels and morphologies of FR 2's and FR 1's are quite distinct (Fanaroff & Riley 1974; Owen & Laing 1989; Owen & Ledlow 1994; Ledlow & Owen 1995). We showed in § 4.3 above that BL Lac objects also lack the large equivalent width emission lines seen in quasars and FR 2 radio galaxies. The result from these comparisons is quite clear: most BL Lac objects are beamed FR 1's (Wardle et al. 1984; Antonucci & Ulvestad 1985; Ulrich 1989; Perlman & Stocke 1993).

Also, unlike the internal comparisons made in the last two sections, these external comparisons require conversions between various observing strategies (e.g., sample selection, filter, and bandpass) and imaging analysis techniques (e.g., magnitude systems) to carry out and so they are somewhat less secure than the internal comparisons made above. In order to make these comparisons, the absolute magnitudes from these other imaging studies were not only corrected to the ($H_0$, $q_0$) system used here but also color-corrected to Gunn $r$-band using Sebok (1986) and Kent (1985), corrected from isophotal magnitudes to total magnitudes using prescriptions in de Vaucouleurs, de Vaucouleurs, & Corwin (1976) and corrected for a small amount of luminosity evolution using $E(z) = z$ (Ellingson et al. 1991), as used for the BL Lac objects. While the total mean corrections to the BCGs ($\langle \delta m \rangle = -1.1$ mag), the Ulrich FR 1's ($-0.3$ mag), the Owen & Laing FR 1's ($-0.5$ mag), and the Owen & Laing FR 2's ($-0.55$ mag) are substantial, most of these corrections have little error associated with them (cosmology conversions and standard bandpass conversions). However, the conversions from isophotal or metric to total magnitudes ($\delta m = 0.1-0.3$ mag conversions made here) are dependent upon the exact surface brightness distribution of each individual object, and so additional errors of 0.1 mag are possible for individual objects in these comparisons. However, given this expected error in the magnitude for individual objects, the comparisons in this section should be accurate to $\leq \pm 0.2$ mag.

The evolutionary corrections are another source of potential systematic error in these comparisons since only the BL Lacertae sample extends to redshifts at which significant luminosity corrections may be required. While the internal comparison of high- and low-$z$ BL Lacertae host galaxy magnitudes shown in § 4.1 appear to exhibit the characteristics of luminosity evolution consistent with $E(z) = z$, this is not proven. Specifically, the evolution of the BCGs in rich clusters might be significantly different from other cluster galaxies if it is dominated by the "cannibalizing" of other, smaller galaxies (Ostriker & Tremaine 1975; Ostriker & Hausman 1977) or by accretion of matter from "cooling flows" (Sarazin 1988). For that reason, we also show in Table 7 the K-S test probabilities for two other ways of handling the BL Lacertae data: (1) by restricting the BL Lacertae sample to only those 13 objects which are at redshifts comparable to the BCG, FR 1, and FR 2 samples (i.e., $z < 0.2$; the cumulative distribution of host galaxy magnitudes for this subsample is shown in Fig. 8b as a dotted line). Because this minimizes the differences between the redshift distributions of the BL Lac objects and the various comparison samples, the differences in evolutionary corrections are so small as to be inconsequential; and (2) by not making any evolutionary correction to the BL Lacertae host galaxy magnitudes at all. Using the low-$z$ subsample is the most secure comparison strategy, since it minimizes the uncertainties in the evolutionary correction and also uses the best BL Lacertae host galaxy data by largely avoiding those sources which were only marginally resolved. But this does substantially reduce the size of the BL Lacertae sample and thus the statistical significance of these tests. As seen in Table 7, the low-$z$ subsample comparisons validate the trends seen in the full sample, evolution-corrected comparisons, and so the latter will be used in the discussion of results below unless otherwise specified.

#### 4.4.1. *BL Lac Objects versus Brightest Cluster Galaxies (BCGs)*

Hoessel, Gunn, & Thuan (1980) presented $V$-band CCD imaging and Gunn & Oke (1975) metric mags for 116 brightest cluster galaxies (BCGs) in richness class $\geq 1$ Abell clusters at $z < 0.15$ (although some richness class 0 clusters were included in addition). The BCG sample has a mean absolute magnitude (corrected to total evolution-corrected Gunn $r$-band magnitudes and to the $H_0$, $q_0$ values used here) of $\langle M_r \rangle = -23.8 \pm 0.35$. This is 0.5 mag brighter than the BL Lacertae mean, and the BCGs have a much smaller spread in absolute brightnesses so that the K-S test yields a very low probability ($P_{KS} = 1.5 \times 10^{-9}$) that the two samples are drawn from the same parent population. While a significant number of BL Lac objects have absolute magnitudes typical of BCGs, >50% of BL Lac objects have host galaxies too faint to be BCGs in rich clusters ($M_r > -23$). This is a somewhat surprising result since many rich cluster BCGs are FR 1 radio galaxies, either a WAT or, in the instance of a cooling flow cluster, an amorphous, steep-spectrum source with a weak core (Ball, Burns, & Loken 1993).

Figure 13 is consistent with many BL Lac objects being non-BCGs in rich clusters, since the radio morphology of less luminous cluster galaxies is often a narrow-angle tail (NAT) (Owen & Laing 1989; Burns & Owen 1980; O'Dea & Owen 1986). Even though it is difficult to determine the radio source morphology of BL Lac objects because of their large radio core dominance, the eight BL Lac objects with unambiguous (according to Perlman & Stocke 1993) NAT radio morphology (including AP Librae, with optical observations by AMC) have $\langle M_r \rangle = -22.7$, while the five unambiguous WATs have $\langle M_r \rangle = -23.6$. Therefore, the very limited radio morphology information for BL Lac objects and the BCG/BL Lacertae host galaxy comparison in Figure 13 suggest that both beamed WATs and NATs can produce BL Lac objects.

Because poorer clusters have less luminous BCGs, the distributions in Figure 13 are also consistent with many BL Lac objects being BCGs in poorer clusters, since a correlation exists between cluster richness and the BCG absolute magnitude (Morgan, Kayser, & White 1975; Thuan & Romanishin 1981). This correlation is also present for the BL Lacertae host galaxies themselves (Paper II), and the clustering data presented in Prestage & Peacock (1988) and in Paper II are con-

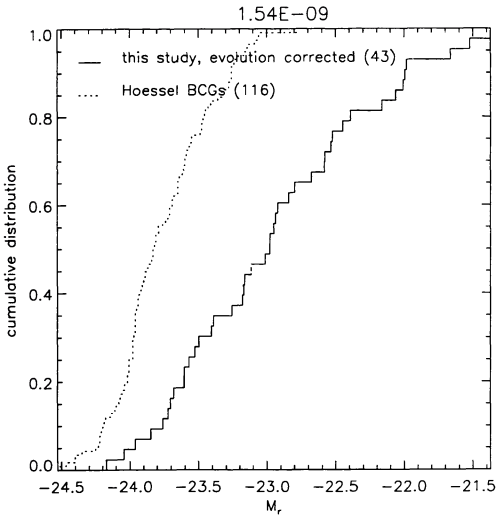


FIG. 13.—The absolute magnitude distributions for BL Lacertae host galaxies and for the brightest cluster galaxies (BCGs) in rich Abell clusters from Hoessel et al. (1980). Notice that no BL Lacertae host galaxy is as bright as the brightest BCGs, and the K-S test probability at the top of the plot shows that the two distributions are incompatible with being drawn from the same parent population.

sistent with many BL Lac objects being members of poor clusters. The absence of BL Lac objects in the richest clusters at low $z$ is further evidence that it is appropriate to make the luminosity evolution corrections to BL Lacertae hosts. If $E(z) = z$ is not applied to the BL Lac objects or BCGs, Table 7 shows that the two distributions are still incompatible, but now the brightest BL Lacertae hosts are nearly as bright as the brightest BCGs.

#### 4.4.2. *BL Lac Objects Compared to FR 1 Galaxies*

In order to test directly the important assertion that BL Lac objects are Doppler-boosted FR 1 radio galaxies, Figure 14 compares the BL Lacertae host galaxy distribution with the FR 1 hosts from two studies, that by Owen & Laing (1989; Fig. 14*a*) and the Ulrich B2 sample compilation (1989; Fig. 14*b*). The FR 1 sample of Owen & Laing (1989) consists of those 14 radio galaxies with $\log P_{1.4} < 25$, a subset of radio galaxies from a large CCD imaging survey of radio galaxies selected primarily from the 3CR and thus dominated by FR 2–type sources. Galaxy magnitudes from Owen & Laing (1989) were converted from 24.5 mag arcsec$^{-2}$ isophotal magnitudes in the Kron-Cousins $R$-band system to total Gunn $r$-magnitudes for this comparison. The Owen & Laing (1989) sample also includes a few so-called "fat doubles", which have some morphological similarities to both FR 1's and 2's. Owen & Laing (1989) found that the "fat doubles" possess some of the most luminous host galaxies of all the radio galaxies they imaged. These borderline FR 1/2 objects are excluded from Figure 14 and Table 7. If these objects were included in the comparison with BL Lac objects, the K-S test results would show a slightly lower probability that the BL Lac objects and FR 1's are drawn from the same parent population.

The Ulrich (1989) comparison between BL Lac objects and FR 1's uses radio galaxies from the B2 survey (Colla et al. 1975a, b) and utilizes Zwicky magnitudes corrected to $V$-band 26th mag arcsec$^{-2}$ isophotal magnitudes, which were in turn converted to our mag system using $(V - r) = 0.2$ (Sebok 1986) and $\delta m = -0.12$ to correct to total magnitudes. The 44 member Ulrich (1989) FR 1 comparison sample includes all the B2 radio galaxies listed in that paper except the two spiral sources omitted by Ulrich and four other B2 sources with FR 2 morphology (0055+26, 1113+29, 1350+31, and 1833+32, one of which, 0055+26, is a "fat double"). Using the K-S test, the

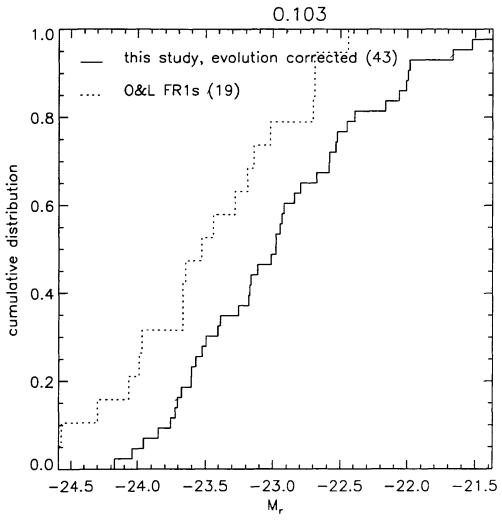


FIG. 14*a*

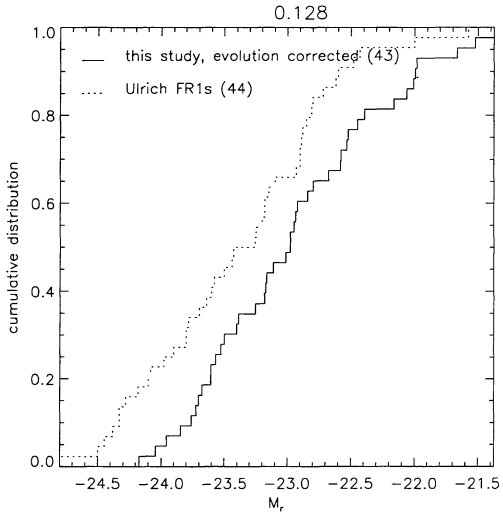


FIG. 14*b*

FIG. 14.—Cumulative distributions of host galaxy magnitudes for BL Lacertae and FR 1 host galaxies. (*a*) The CFHT BL Lacertae sample compared with FR 1 galaxies from Owen & Laing (1989); (*b*) the BL Lac objects compared with the B2 FR 1 sample of Ulrich (1989). The K-S test probabilities at the top show that the luminosity of BL Lacertae hosts are marginally consistent with FR 1 hosts.

cumulative host galaxy absolute magnitude distributions of these two FR 1 samples have $P_{KS} = 82\%$ probability of being drawn from the same parent population. This sets the standard by which BL Lacertae/FR 1 host galaxy distributions can be compared.

In both these cases the BL Lacertae and FR 1 host galaxy distributions are consistent with being drawn from the same parent population at only about the 10% level (see Table 7), a result which marginally supports the earlier claim that BL Lac objects are beamed FR 1's. While Figure 14 show that the BL Lacertae and FR 1 host galaxies span nearly the same range of absolute magnitude, both the FR 1 samples appear to have a definite excess of very luminous galaxies compared to the BL Lacertae hosts. Further, recalling our earlier concern that one third of the $M_r < -24$ BL Lacertae host galaxy magnitudes were obtained from profile fits of marginally resolved objects (§ 3), this excess among the FR 1's compared to BL Lac objects could be even larger than Figure 14 shows. Also an even larger difference would be apparent if the Owen & Laing (1989) comparison sample included the fat doubles, which mostly have $M_r < -24$. Note that the most luminous FR 1's in Figure 14 have approximately the same luminosity as the most luminous BCGs in Figure 13 and that these exceed the BL Lacertae host galaxies by 0.5 mag. It is most unlikely that this difference is attributable to accumulated photometric and conversion errors between the various magnitude systems, since they are all different and yet the two FR 1 samples and the BCG sample yield the same most luminous galaxies to $<\pm 0.2$ mag. A systematic $\delta m = 0.3-0.5$ mag underestimate of BL Lacertae host galaxy luminosities would be required to bring these samples into close agreement. We see no evidence for systematic errors as large as this amount in our data. In § 4.5 we speculate on the importance of the small, but significant, luminosity difference between BL Lacertae and FR 1 host galaxies.

In the last column of Table 7 are listed the K-S test results if no luminosity evolution correction is made to the BL Lacertae host galaxies. Under this assumption, the BL Lac objects and FR 1's are much more likely to have been drawn from the same parent population because the BL Lacertae hosts now extend to $M_r \sim -24.5$. However, these luminous BL Lacertae hosts are entirely at $z > 0.2$, as can be seen by comparing the test results in the last two columns of Table 7. When comparisons are made using only $z < 0.2$ BL Lac objects, so that objects in the same low-redshift range are compared directly, the FR 1 host galaxies remain a less accurate match to the BL Lac objects than the FR 2's.

#### 4.4.3. *BL Lac Objects Compared to FR 2 Galaxies and Quasars*

The comparison between the Owen & Laing (1989) FR 2's ($\log P > 25$ W Hz$^{-1}$) is shown in Figure 15, and the K-S test result for this comparison shows that the BL Lacertae and FR 2 hosts are more likely to be drawn from the same parent population than are the BL Lacertae and FR 1 hosts. But even for the FR 2's, there are some host galaxies with absolute magnitudes brighter than any BL Lacertae host galaxy, which decreases the K-S test probability to the 30% level. It will be shown in Paper II that the clustering environments of BL Lac objects and their changing environment with redshift are also more consistent with FR 2's than with FR 1's so that from the perspective of the unbeamed optical properties, BL Lac objects appear more similar to FR 2's than to FR 1's. This is clearly different from (but not inconsistent with, as we will show) the comparisons using unbeamed radio properties.

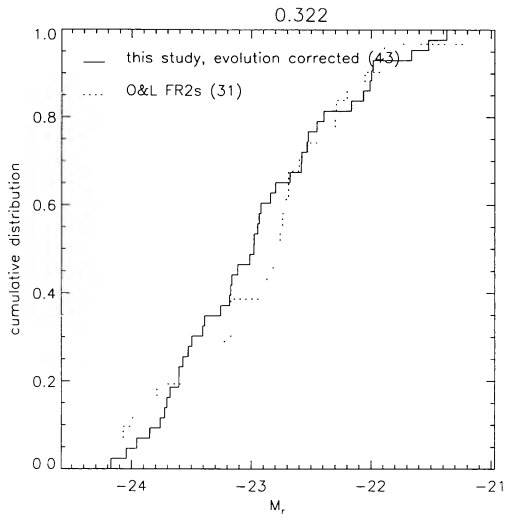


FIG. 15.—Cumulative distributions of host galaxy magnitudes for BL Lacertae and FR 2 host galaxies from Owen & Laing (1989). Although the FR 2 host galaxies are the best statistical match with the BL Lacertae hosts, a very few FR 2 hosts also exceed the most luminous BL Lacertae hosts by a few tenths of a magnitude. The K-S test probability is shown at the top.

Although we do not show the comparison explicitly here, the host galaxies of radio-loud quasars appear to have lower luminosity host galaxies than the BL Lac objects; e.g., $\langle M_r \rangle = -21.4$ (Hutchings 1987) and $\langle M_r \rangle = -22$ (Smith et al. 1986). Recent *HST* imaging (e.g., Bahcall, Kirhakos, & Schneider 1994, 1995) supports this conclusion, although very few radio-loud objects have been well imaged with *HST* as yet. Because so few radio-loud quasars are nearby (i.e., $z < 0.3$), their higher redshifts and lower host galaxy luminosities compared to the CFHT BL Lacertae sample could lead to greater difficulties in host galaxy extraction than those experienced with the current sample (Abraham et al. 1992). This renders detailed comparisons with BL Lac objects problematical at best. Radio-quiet quasi-stellar objects (QSOs) are typically found in even fainter host galaxies than radio-loud ones and also prefer spiral morphology host galaxies (see Lawrence 1987 review, and references therein).

#### 4.4.4. *Radio and Optical Power Levels of BL Lac Objects*

Because extended radio power levels are available for many of the BL Lac objects in the CFHT survey, BL Lac objects can also be compared to both FR 1's and FR 2's in a two-dimensional plot of absolute quantities shown in Figure 16. The FR 1 and 2 data come from the compilation of Ledlow & Owen (1995), who noted (as did Owen & Laing 1989 before them) that the dividing line between FR 1's and FR 2's is a diagonal line across this plot and not at a single value of radio power as originally proposed by Fanaroff & Riley (1974). The Ledlow & Owen (1995) FR 1 radio galaxy sample shown in Figure 16 includes the Owen & Laing (1989) sample used in the cumu-

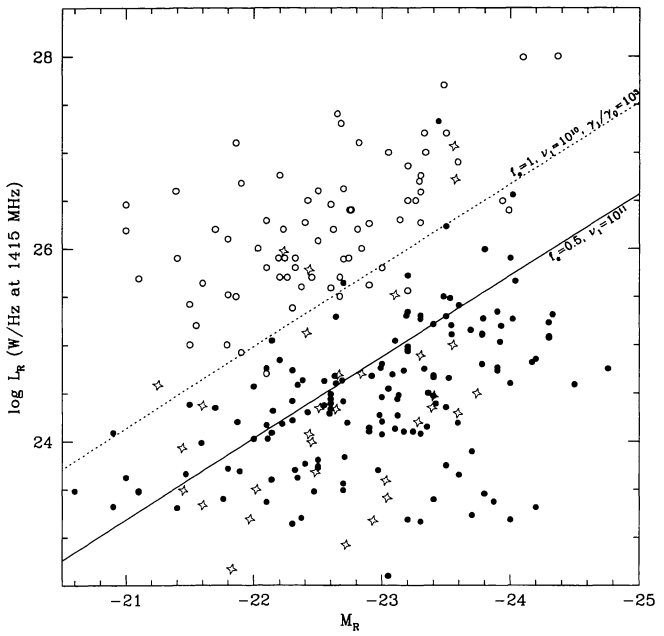


FIG. 16.—The host galaxy absolute magnitudes vs. absolute radio power levels for FR 1's (*filled circles*) and FR 2's (*open circles*) from Ledlow & Owen (1995) and for BL Lac objects (*stars*). For this plot only, these values have been converted to $H_0 = 75$ km s$^{-1}$ Mpc$^{-1}$ and $q_0 = 0$ to match the data of Ledlow & Owen. The dotted and solid lines are two models for the FR 1/FR 2 dividing line which span the assumed parameter space in the work of Bicknell (1994, 1995). Note the absence of BL Lac objects compared to FR 1's at the right-hand edge of the diagram and at the lower right-hand corner of this plot.

lative distribution comparisons described above plus other FR 1's and so it is a substantially larger but more heterogeneous sample. Note that the absolute host galaxy magnitudes for FR 1's and 2's largely overlap, with the difference being that some FR 1's are found in more luminous host galaxies than any FR 2's. The BL Lacertae points are a large subset ($\frac{2}{3}$) of the CFHT sample, containing only those which are resolved by both radio and optical imaging. The remaining galaxies in our sample are absent from Figure 16 because they lack high dynamic range $L$-band maps. So we believe that the BL Lac objects shown in Figure 16 are a fair sample of the whole CFHT sample. Only the extended radio power levels were used for the BL Lac objects since the core is Doppler-boosted, which would inflate the radio power levels significantly compared to the FR 1's and FR 2's. But because the core sources are such a small fraction of the total radio power levels in FR 1s, the isotropic radio luminosities of the BL Lac objects are only slightly underestimated by excluding the core power. The optical magnitudes for the BL Lac objects have been corrected to the Kron-Cousins $R$-band $M_{24.5}$ magnitude scale ($H_0 = 75$ km s$^{-1}$ Mpc$^{-1}$; $q_0 = 0$) of Ledlow & Owen (1995) to match the optical data for the FR 1's and FR 2's.

The diagonal lines are from a family of models for the dividing line between FR 1's and FR 2's based upon the recent theoretical models of Bicknell (1994, 1995), who suggested that FR 1 jets are strongly decelerated by the hot, diffuse X-ray–emitting gas found in all elliptical galaxies (see Fabbiano 1989), while FR 2 jets are too powerful to be decelerated significantly by the hot gas. Because more luminous elliptical galaxies possess denser hot gas in their cores, FR 2 host galaxies tend to be somewhat less luminous than FR 1 hosts, leading to the diagonal dividing line in Figure 16. Clearly, the large majority of BL Lac objects are consistent with being FR 1's, since they fall near or below the diagonal line. The five BL Lac objects which are above the FR 1/2 dividing line are 3C 66A, 1538+149, 1400+162, 0521−365, and OJ 287 in order of decreasing radio power level. Of these five, only 1400+162 possesses a possible FR 2 morphology, although it is much more likely a WAT given its noncolinear outer structure and luminous twin jets (Antonucci & Ulvestad 1985; Perlman & Stocke 1983). 3C 66A and PKS 0521−365 are clearly WATs, and 0521−365 is not considered a BL Lac object, but rather an FR 1 radio galaxy, by some authors (e.g., Stickel et al. 1993a). The BL Lac object 1538+149 is a possible FR 1 galaxy (Murphy, Browne, & Perley 1993), but it is not well resolved at $z = 0.6$, and OJ 287 is a NAT (Perlman & Stocke 1993). While Figure 16 suggests that all but a handful of BL Lac objects are consistent with being beamed FR 1's, we remind the reader that the CFHT BL Lacertae survey was restricted to objects with $z < 0.65$ and so does not contain several BL Lac objects like AO 0235+164 and PKS 0215+015, whose extended radio power levels would place them far above the diagonal line for any plausible host galaxy magnitude. Note particularly that Figure 16 shows the same intriguing difference between the BL Lac objects and FR 1's as does Figure 14. Specifically, there appears to be a dearth of BL Lacertae points at very bright host galaxy magnitudes and also a dearth of BL Lac objects in the lower right-hand corner of Figure 16.

### 4.5. *The BL Lacertae Parent Population: A Subset of FR 1 Galaxies*

For several years, the primary difficulty in the identification of FR 1 radio galaxies as the parent population of BL Lac objects has been the absence of BL Lac objects in rich clusters (Prestage & Peacock 1988). Recent work (Smith et al. 1995; Paper II) has now confirmed the earlier Prestage & Peacock (1988) result that BL Lac objects avoid the richest clusters at low redshift.

And yet FR 1 radio galaxies have been found primarily in rich clusters at low redshifts (e.g., Burns & Owen 1980; O'Dea & Owen 1986; O'Donoghue, Owen, & Eilek 1990; but see Stocke & Burns 1978), and theories for the distortions in their extended radio structure rely upon interactions with a dense intracluster medium found in such clusters (e.g., Begelman, Blandford, & Rees 1984; Eilek et al. 1980; Burns, Norman, & Clarke 1991). Thus, at least some BL Lac objects would be expected to be found in rich clusters. But an extensive, optical search for low-luminosity BL Lac objects among rich cluster FR 1's has discovered an order of magnitude fewer candidates than expected if BL Lac objects are beamed FR 1's (Owen, Ledlow, & Keel 1996).

However, FR 1 sources also are found in poorer clusters (e.g., Ekers et al. 1978; Stocke & Burns 1978; Burns et al. 1987; Fanti et al. 1987; Venkatesan et al. 1994), with radio morphologies similar to rich cluster FR 1's. A recent appraisal of poor cluster FR 1's compared to rich cluster FR 1's by Venkatesan

et al. (1994) finds that their detailed morphologies are very similar, except perhaps that the jet opening angle may be a factor of 2 larger for the poor cluster FR 1's (but the sample size is small and the measurement errors on this quantity are large; see also Stocke & Burns 1978).

The results of the CFHT BL Lacertae imaging study now allow us to modify the suggested parent population of BL Lac objects to exclude the BCGs in rich clusters and perhaps all radio galaxies in rich clusters as well. This modification is based upon both the absence of the most luminous host galaxies among BL Lac objects and also on the absence of BL Lac objects in the richest clusters (at low $z$ at least; see Paper II).

It may be possible to explain the absence of BL Lac objects at very bright optical magnitudes and/or very low radio power levels in Figure 16 using the Bicknell (1994, 1995) models. In those models, the difference between FR 1 and FR 2 morphology is determined by whether the radio jets are significantly decelerated by the hot, interstellar medium of the host galaxy. And by that model, the further below the diagonal line a radio galaxy lies, the more deceleration occurs in the radio jet; i.e., the FR 1's in the lower right-hand corner of Figure 16 are the most decelerated by this model. It is possible that in these "extreme" FR 1 sources the radio jet is so severely decelerated by the hot gas in the host galaxy that the Doppler-boosting of the core is greatly diminished and such objects are not seen as BL Lac objects at all. This would be extraordinary if correct, since this interpretation requires the jet to be decelerated to nonrelativistic velocities within 1 – 10 pc of the core, since the Doppler-boosted X-ray and optical emission must arise on very small scales given their short variability timescales (Moore et al. 1982; Doxsey et al. 1983).

The deceleration of the jet might also explain why so few BL Lac objects are found in rich clusters of galaxies. Not only are the rich clusters where the most luminous galaxies (the BCGs) are found, but also the dense intracluster medium (ICM) found in such clusters could supply an additional pressure (both static and dynamic) within the central regions of the host galaxy that could increase the hot gas density and pressure in the core of rich cluster galaxies. Estimates based upon observed mean properties of X-ray emission from individual galaxies (Fabbiano 1989) and from rich clusters (Sarazin 1988) suggest that the rich cluster ICM could increase the pressure in the central regions of a cluster elliptical by >10%; an even larger effect would be expected in clusters with cooling cores. This larger ambient pressure would more strongly decelerate the jets in cluster radio galaxies, since FR 1's in rich and poor clusters seem to have comparable internal jet pressures (Venkatesan et al. 1994). Effects related to cooling cores (e.g., formation of massive central star clusters, whose stellar winds could create very dense gaseous environments into which the nuclear jet is propagating) should be explored to determine if such effects would be sufficient to decelerate jets as rapidly as required to prevent the formation of the physical conditions necessary to create BL Lac objects.

The same host galaxy gas which decelerates the jets could also confine the outwardly moving jets in lateral directions, which would make them narrower than the FR 1 jets in poorer clusters. This has been marginally observed (Venkatesan et al. 1994; Stocke & Burns 1978) at the factor of 2 level. If the jet opening angles in rich cluster FR 1 galaxies are half as large, it would be 4 times less likely for an observer to be within the beaming cone; and if the jets are more decelerated and so less relativistic, the Doppler-boosting factor will be significantly lower, also decreasing the probability that such a source would be seen as a BL Lac object. Both these effects would bias cluster radio galaxies against being BL Lac objects and would explain both the statistical absence of BL Lac objects from rich clusters (Prestage & Peacock 1988; Paper II) and the failure to find significant numbers of low-luminosity BL Lac objects among cluster radio galaxies (Owen et al. 1996). The amorphous, steep-spectrum radio sources found in the central galaxies in cooling flow clusters are an extreme example of this phenomenon, in which the jets are decelerated and disrupted before they become observable at arcsec resolution (Ball et al. 1993; Zhao et al. 1992). Since these relatively low-luminosity radio sources occur in some of the most luminous BCGs, they would be found in the lower right-hand corner of Figure 16, as expected in the Bicknell models. The absence of radio jets in such sources supports the interpretation given in this section, since if a radio source lacks a jet, it cannot be a BL Lac object at any viewing angle.

Therefore, we conclude that not all FR 1's produce BL Lac objects given the correct orientation of their jet axes. Specifically, the FR 1's associated with BCGs in rich clusters and possibly other rich cluster FR 1's as well do not produce BL Lac objects. This modification of the beamed FR 1 hypothesis for BL Lac objects now means that all the "unbeamed" properties of BL Lac objects (host galaxies, extended radio powers, clustering environments, and space densities) are consistent with a parent population which is a large subset of FR 1's. This subset excludes the BCGs in rich clusters and probably all FR 1's in rich clusters as well. Because this result is consistent with the Bicknell (1994, 1995) theoretical models for the difference between FR 1's and 2's, these models should be expanded to include the effects of the ICM pressure of a rich cluster, with or without a cooling flow present. Numerical models (e.g., Norman, Burns, & Sulkanen 1988; Zhao et al. 1992) of decelerating/disrupting jets can also be used to determine whether the hot gas in a radio galaxy augmented by the hot, dense ICM of a surrounding cluster can decelerate an FR 1 jet quickly enough to avoid making a BL Lac object.

These results also suggest that the occurrence of a relativistic jet embedded in a rich cluster ICM is rare. Sarazin & Wise (1993) have suggested that it might be possible to observe Doppler-boosted jet radiation scattered off the rich cluster ICM that surrounds it. If our inferences above are correct, the combination of circumstances required for observing this phenomenon might be exceptionally rare.

## 5. CONCLUSIONS

This paper has presented the first portion of the results from the CFHT BL Lacertae imaging survey, those results pertinent to the nature of the BL Lacertae host galaxy. A companion paper (Paper II) will report on the clustering environment of BL Lac objects. The host galaxy results are based upon deep, primarily sub-arcsecond images of 50 X-ray and radio-selected BL Lac objects with observed $z < 0.65$. While BL Lac objects with diverse properties are included in this sample, we have specifically excluded high-$z$ and spectroscopically featureless

BL Lac objects whose distances are unknown. The redshift cutoff was motivated by the observational constraints of CFHT, not any property inherent to the BL Lacertae samples themselves. This restriction was made to maximize the likelihood of detecting the underlying host galaxy, and featureless objects were not included, so that any host galaxy detection could be interpreted with a minimum of uncertainty. But this also means that we cannot claim to have sampled the entire BL Lacertae population unless the high-$z$, low-$z$, and featureless objects are all very similar. Excepting a small increase in host galaxy luminosity with $z$, there is no evidence for a distinct change in BL Lacertae host galaxy properties as a function of redshift within our sample that would suggest that $z > 0.65$ BL Lac objects are a distinct population of objects.

The primary results of the CFHT BL Lac host galaxy results are as follows.

1. All but four BL Lac objects were resolved by these observations; 36 host galaxies are well enough detected that a morphological type can be assigned on the basis of the shape of their extended surface brightness profiles. Twenty of these 36 are unambiguous ellipticals, 10 are likely ellipticals, three are possible spirals (but with problems associated with the extraction of their surface brightness profiles), and three are unambiguous spirals. Of the marginally resolved objects, all are consistent with being elliptical galaxies, although that cannot be proven using the current observations. The three BL Lac objects with spiral host galaxies are MS 0205+351, PKS 1413+135, and OQ 530 (1418+546). MS 0205+351 also possesses the lowest luminosity "host galaxy" in the sample at $M_r = -21.7$ and has a core which is off-center in its surrounding "host" (see Stocke, Wurtz, & Perlman 1995 for further information on this unusual object). PKS 1413+135 is one of the most unusual BL Lac objects in the sky, and there have been suggestions that it is not a BL Lac object at all. We refer the reader to Perlman et al. (1994), Stocke et al. (1992), Carilli et al. (1992), McHardy et al. (1991, 1994), and Bregman et al. (1981) for detailed information on this very unusual BL Lac object, which Stocke et al. (1992) claim is a distant quasar viewed through a foreground spiral galaxy.

2. Only one BL Lac object possesses a host galaxy which is definitely offset (>0".1) relative to its core source (MS 0205+351). As this is a hallmark of a BL Lac object which may be gravitationally lensed (Merrifield 1992), we conclude that most BL Lac objects at $z < 0.65$ are *not* gravitationally lensed objects whose observed characteristics are modified by foreground micro- and macrolensing (Ostriker & Vietri 1985; Ostriker 1989; but see Merrifield 1992 and Abraham et al. 1993).

The consistency between BL Lacertae and FR 1 host galaxies (see below) for all but three cases also suggests that gravitationally lensed BL Lac objects are rare. Further, based upon the relative brightness of the BL Lacertae point source and the host galaxy seen in our images, the typical emission-line strengths found in normal quasar spectra cannot be diminished enough by the BL Lacertae continuum to hide" these lines in ≥80% of our sample. Thus, a background AGN in a gravitationally lensed BL Lacertae scenario must possess intrinsically weak emission lines, as pointed out by Ostriker (1989), if it is to be classified as a BL Lac object.

But a minority population of gravitationally lensed BL Lac objects cannot be excluded, particularly among the radio-selected BL Lac objects. Many of the more interesting cases for gravitational lensing (e.g., AO 0235+164, PKS 0215+015, PKS 0537−44, and W1 0846+51; Narayan & Schneider 1990, Abraham et al. 1993) were systematically excluded from study here because they are either at high $z$ (>0.65) or are optically featureless so that their true distances remain unknown. The three spiral host galaxy BL Lac objects, the one decentered BL Lac object, and high-$z$ and featureless 1 Jy BL Lac objects should be imaged at higher resolution so that the full extent of this minority population can be determined.

3. The four BL Lac objects unresolved by our images (MS 0950+494, MS 1402+042, 4U 1722+119, and PKS 2155−304) have upper limits on their host galaxy luminosities which are not inconsistent with being drawn from the observed distribution of well-resolved BL Lacertae host galaxy luminosities. Since three of these four have well-resolved radio structures, we find no evidence from the current work that they are in any way different from other BL Lac objects excepting their large optical core dominance values. The fourth of these, MS 0950+494, is unresolved in both the radio and optical and is optically featureless, suggesting it has a high redshift ($z > 0.5$).

4. Using comparisons internal to our uniformly observed and analyzed sample, we find no strong evidence that any subset of BL Lac objects with varying point-source properties (e.g., X-ray vs. radio-loud objects; high vs. low polarization; presence of weak emission lines; preferred position angle of optical polarization) possesses unusual host galaxy properties. This is particularly important for the X-ray versus radio-loud comparison for which the host galaxy luminosity distributions are consistent with being drawn from the same parent population at the 64% level. Since Paper II finds no difference in the clustering environment of these two types of BL Lac objects, there is no evidence from "unbeamed" optical properties that X-ray and radio-selected BL Lac objects are different types of objects.

5. While the observed core-to-host galaxy flux ratios for almost all (43 of 50) of the BL Lac objects observed in this program are insufficient to hide luminous emission lines typical of those found in quasars, the bright continua in the CFHT sample BL Lac objects is sufficient to diminish the weak emission lines typical of FR 1 galaxies to an equivalent width at or below the levels required to be classified as BL Lac objects (e.g., $W_\lambda \leq 5$ Å; Stocke et al. 1989, Stickel et al. 1991). We conclude that physical models for BL Lac objects cannot rely upon Doppler-boosting to hide luminous broad emission-line regions and that other mechanisms must be required to either occult (e.g., Falcke et al. 1995) such regions or suppress broad-line cloud formation and/or stability (e.g., Guilbert et al. 1983; Perlman et al. 1996b).

6. The CFHT BL Lacertae survey allows us to compare the host galaxy properties of BL Lac objects with other radio galaxy populations for the first time using a sample of BL Lac objects which is large enough to effect a detailed comparison. Using full sample comparisons between BL Lac objects, brightest rich cluster galaxies (BCGs), FR 1's and FR 2's, we have found, surprisingly, that the distribution of host galaxy luminosities of BL Lac objects is most similar to that of FR 2 radio galaxies. Paper II shows that the clustering environment and the cosmological evolution in environment is also more consistent with FR 2's than with FR 1's. This is contrary to the conclusions reached using the extended "unbeamed" radio

power levels and morphologies and BL Lacertae, FR 1, and FR 2 emission-line properties.

However, the host galaxy luminosity distributions of FR 1's and 2's largely overlap and do not offer as definitive a discriminant as the radio power levels of these sources, which are considerably more disjoint from one another (e.g., Owen & Laing 1989; Owen & Ledlow 1994; Ledlow & Owen 1995). Further, a consistent picture can be reached if the parent population of BL Lac objects is a subset of FR 1's. This subset excludes the BCGs in rich galaxy clusters and probably all radio galaxies in rich clusters as well.

By making this slight modification to the previously proposed parent population of BL Lac objects, this survey now finds consistent evidence that BL Lac objects are beamed, non-rich cluster FR 1's from all their unbeamed properties: optical host galaxy luminosity distribution (this paper), host galaxy morphologies (this paper), clustering environment (Prestage & Peacock 1988; Smith et al. 1995; Paper II), extended radio powers and morphologies (e.g. Perlman & Stocke 1993, and references therein), and luminosity functions and space densities (Padovani & Urry 1990, 1991; Urry, Padovani, & Stickel 1991; Morris et al. 1991).

Multiwavelength studies of BL Lac objects at the University of Colorado are supported by NASA grant NAGW-2645. J. T. S. and R. W. also acknowledge partial support of this work from NSF grant AST-9020008. H. K. C. Y. wishes to thank NSERC of Canada for support through an operating grant. Bob Abraham is thanked for many useful discussions and invaluable suggestions on host galaxy extraction and profile fitting. Geoff Bicknell and Michael Ledlow are thanked for helpful discussions and the use of Figure 16, which is a modification of a plot that will appear both in Bicknell (1995) and Ledlow & Owen (1995). Simon Morris is thanked for his work on an abortive first attempt at this research which used the Palomar 60 inch telescope and which provided calibration for some of the significantly deeper images of BL Lac objects obtained at the CFHT. Mitch Begelman is thanked for helpful discussions. And finally, the CTAC is thanked for support of BL Lacertae imaging and the CFHT staff for maintaining the exquisite image quality that made this work possible. This work is a portion of the Ph.D. thesis of Ron Wurtz, submitted to the University of Colorado.

## REFERENCES


Abraham, R. G. 1994, private communication
Abraham, R. G., Crawford, C. S., & McHardy, I. M. 1992, ApJ, 401, 478
Abraham, R. G., Crawford, C. S., Merrifield, M., & Hutchings, J. B. 1993, ApJ, 415, 101
Abraham, R. G., McHardy, I. M., & Crawford, C. S. 1991, MNRAS, 252, 482 (AMC)
Antonucci, R., & Ulvestad, J. 1985, ApJ, 294, 158
Bahcall, J. N., Kirhakos, S., & Schneider, D. P. 1994, ApJ, 435, L11
———. 1995, ApJ, 447, L1
Ball, R., Burns, J. O., & Loken, C. 1993, AJ, 105, 53
Begelman, M. C., Blandford, R. D., & Rees, M. J. 1984 Rev. Mod. Phys., 26, 255
Bicknell, G. V. 1994, ApJ, 422, 542
———. 1995, ApJS, 101, 29
Blandford, R. D., & Rees, M. J. 1978, in Pittsburgh Conf. on BL Lacs, ed. A. M. Wolfe (Pittsburgh, Univ. Pittsburgh), 328
Bregman, J. N., Lebofsky, M. J., Aller, M. F., Rieke, G. H., Aller, H. D., Hodge, P. E., Glassgold, A. E., & Huggins, P. J. 1981, Nature, 293, 714
Browne, I. 1989, in BL Lac Objects, ed. L. Maraschi, T. Maccacaro, & M.-H. Ulrich (Springer:Heidelberg), 401
Browne, I. W. A., & Marcha, M. J. M. 1993, MNRAS, 261, 795
Burbidge, G., & Hewitt, A. 1987, AJ, 93, 1
Burns, J. O., Hanisch, R. J., White, R. A., Nelson, E. R., Morrisette, K. A., & Moody, J. W. 1987, AJ, 94, 587
Burns, J. O., Norman, M. L., & Clarke, D. A. 1991, Science, 253, 522
Burns, J. O., & Owen, F. N. 1980, AJ, 85, 204
Burstein, D., & Heiles, C. 1978, ApJ, 225, 40
Carilli, C. L., Perlman, E. S., & Stocke, J. T. 1992, ApJ, 400, L13
Cayette, V., & Sol, H. 1987, A&A, 171, 25
Ciliegi, P., Bassani, L., & Caroli, G. 1995, ApJ, 439, 80
Coleman, G. D., Wu, C. C., & Weedman, D. W. 1980, ApJS, 43, 393
Colla, G., Fanti, C., Fanti, R., Gioia, I., Lari, C., Lequeux, J., Lucas, R., & Ulrich, M. H. 1975a, A&A, 38, 209
———. 1975b, A&AS, 20, 1
DeRobertis, M. M., & Yee, H. K. C. 1990, AJ, 100, 84
de Vaucouleurs, G., & Capaccioli, M. 1979, ApJS, 40, 699
de Vaucouleurs, G., de Vaucouleurs, A., & Corwin, H. G. 1976, Second Reference Catalogue of Bright Galaxies (Austin: U. of Texas)
Doxsey, R., Bradt, H., McClintock, J., Petro, L., Remillard, R., Ricker, G., Schwartz, D., & Wood, K. 1983 ApJ, 264, L43
Eilek, J., Burns, J. O., O'Dea, C. D., & Owen, F. N. 1984, ApJ, 278, 37
Ekers, R., Fanti, R., Lari, C., & Ulrich, M-H. 1978, A&A, 69, 253
Ellingson, E., Yee, H. K. C., & Green, R. F. 1991, ApJ, 371, 49
Elston, R., Jannuzi, B. T., & Smith, P. S. 1989, in BL Lac Objects, ed. L. Maraschi, T. Maccacaro, & M.-H. Ulrich (Springer: Heidelberg), 253
Fabbiano, G. 1989, ARA & A, 27, 87
Falcke, H., Gopal-Krishna, & Biermann, P. L. 1995, A&A, 298, 395
Falomo, R., Pesce, J. E., & Treves, A. 1993a, AJ, 105, 2031
———. 1993b, ApJ, 411, 63
Falomo, R., & Tanzi, E. G. 1991, AJ, 102, 1294
Fanaroff, B. L., & Riley, J. M. 1974, MNRAS, 167, 31
Fanti, C., Fanti, R., de Ruiter, H. R., & Parma, P. 1987, A&AS, 69, 57
Fried, J. W., Stickel, M., & Kuhr, H. 1993, A&A, 268, 53
Gioia, I. M., Maccacaro, T., Schild, R. E., Wolter, A., Stocke, J. T., Morris, S. L., & Henry, J. P. 1990, ApJS, 72, 567
Giommi, P., & Padovani, P. 1994, MNRAS, 268, L51
Giommi, P., et al. 1991, ApJ, 378, 77
Griffiths, R. E., Wilson, A. S., Ward, M. J., Tapia, S., & Ulvestad, J. S. 1989, MNRAS, 240, 33
Guilbert, P. W., Fabian, A. C., & McCray, R. 1983, ApJ, 266, 466
Gunn, J. E., & Oke, J. B. 1975, ApJ, 195, 255
Halpern, J. B., Impey, C. D., Bothun, G. D., Tapia, S., Skillman, E. D., Wilson, A. S., & Meurs, E. J. A. 1986, ApJ, 302, 711
Hoessel, J. G., Gunn, J. E., & Thuan, T. X. 1980, ApJ, 241, 486
Hutchings, J. B. 1987, ApJ, 320, 12
Impey, C. D. 1989, in BL Lac Objects, ed. L. Maraschi, T. Maccacaro, & M.-H. Ulrich (Springer: Heidelberg), 149
Jannuzi, B. T., Smith, P. S., & Elston, R. 1993, ApJS, 85, 265
———. 1994, ApJ, 428, 130
Jedrzejewski, R. I. 1987, MNRAS, 226, 747 (J87)
Kent, S. M. 1985, PASP, 97, 165
Kollgaard, R. I., Wardle, J. F. C., Roberts, D. H., & Gabuzda, D. C. 1992, AJ, 104, 1687
Kuhr, H., & Schmidt, G. D. 1990, AJ, 99, 1
Lanzetta, K. M., Turnshek, D. A., & Sandoval, J. 1993, ApJS, 84, 109
Lauer, T. R. 1985, ApJ, 292, 104
Laurent-Muehleisen, S. A., Kollgaard, R. I., Moellenbrock, G. A., & Feigelson, E. D. 1993, AJ, 106, 876
Lawrence, A. 1987, PASP, 99, 309
Ledden, E., & O'Dell, S. L. 1985, ApJ, 298, 630
Ledlow, M. J., & Owen, F. N. 1995, AJ, 110, 1959
Longair, M. S., & Seldner, M. 1979, MNRAS, 189, 433
Maccacaro, T., Gioia, I. M., Maccagni, D., & Stocke, J. T. 1984, ApJ, 284, L23
Maccacaro, T., Wolter, A., McClean, B., Gioia, I. M., Stocke, J. T., Della

Ceca, R., Burg, R. & Faccini, R. 1994, Astrophys. Lett. Commun., 29, 267
Macchetto, F., et al. 1991, ApJ, 369, 55
McHardy, I. M., Abraham, R. G., Crawford, C. S., Ulrich, M.-H., Mock, P. C., & Vanderspeck, R. K. 1991, MNRAS, 249, 742
McHardy, I. M., Luppino, G. A., George, I. M., Abraham, R. G., & Cooke, B. A. 1992, MNRAS, 256, 655
McHardy, I. M., Merrifield, M. R., Abraham, R. G., & Crawford, C. S. 1994, MNRAS, 268, 681
Merrifield, M. R. 1992, AJ, 104, 1306
Miller, J. S., French, H. B., & Hawley, S. A. 1978, in Pittsburgh Conference on BL Lac Objects, ed. A. M. Wolfe (Pittsburgh: Univ. Pittsburgh), 176
Moore, R. L., et al. 1982, ApJ, 260, 415
Morgan, W. W., Kayser, S., & White, R. A. 1975, ApJ, 199, 545
Morris, S. L., & Stocke, J. T. 1991, BAAS, 23, 1429
Morris, S. L., Stocke, J. T., Gioia, I. M., Schild, R. E., Wolter, A., Maccacaro, T., & Della Ceca, R. 1991, ApJ, 380, 49
Murphy, D. W., Browne, I. W. A., & Perley, R. A. 1993, MNRAS, 264, 298
Narayan, R., & Schneider, P. 1990, MNRAS, 243, 192
Norman, M. L., Burns, J. O., & Sulkanen, M. 1988, Nature, 335, 146
O'Dea, C., & Owen, F. N. 1986, ApJ, 301, 814
O'Donaghue, A. A., Owen, F. N., & Eilek, J. A. 1990, ApJS, 72, 75
Ostriker, J. P. 1989, in BL Lac Objects, ed. L. Maraschi, T. Maccacaro, & M.-H. Ulrich (Springer: Heidelberg), 420
Ostriker, J. P., & Hausman, M. A. 1977, ApJ, 217, L125
Ostriker, J. P., & Tremaine, S. D. 1975, ApJ, 202, L113
Ostriker, J. P., & Vietri, M. 1985, Nature, 318, 446
Owen, F. N., & Laing, R. A. 1989, MNRAS, 238, 357
Owen, F. N., & Ledlow, M. J. 1994, in The Physics of Active Galaxies, ed. G. V. Bicknell, M. A. Dopita, & P. J. Quinn (San Francisco: ASP), 319
Owen, F. N., Ledlow, M. J., & Keel, W. C. 1996, AJ, in press
Padovani, P., & Giommi, P. 1995, ApJ, 444, 567
Padovani, P., & Urry, C. M. 1990, ApJ, 356, 75
———. 1991, ApJ, 368, 373
Perlman, E. S. 1994, private communication
Perlman, E. S., & Stocke, J. T. 1993, ApJ, 406, 430
Perlman, E. S., Stocke, J. T., & Elston, R. 1996c, in preparation
Perlman, E. S., Stocke, J. T., Schachter, J., Elvis, M., Urry, C. M., Impey, C. D., & Smith, P. S. 1996, ApJS, submitted
Perlman, E. S., Stocke, J. T., Shaffer, D. B., Carilli, C. L., & Ma, C. 1994, ApJ, 424, L69
Perlman, E. S., Stocke, J. T., Wang, Q. D., Morris, S. L. 1996b, ApJ, 456, 000
Pesce, J. E., Falomo, R., & Treves, A. 1994, AJ, 107, 494
———. 1995 AJ, 110, 1554
Piccinotti, G., Mushotzky, R. F., Boldt, E. A., Holt, S. S., Marshall, F. E., Serlemitsos, P. J., & Shafer, R. A. 1982, ApJ, 253, 485
Press, W. H., Teukolsky, S. A., Vetterling, W. T., & Flannery, B. P. 1992, Numerical Recipes, The Art of Scientific Computing (2d ed.; Cambridge: Cambridge Univ. Press)
Prestage, R. M., & Peacock, J. A. 1988, MNRAS, 230, 131
Romanishin, W. 1992, ApJ, 401, L65
Sarazin, C. 1988, X-Ray Emissions from Clusters of Galaxies (Cambridge: Cambridge Univ. Press)
Sarazin, C., & Wise, M. W. 1993, ApJ, 411, 55
Schachter, J. F., et al. 1993, ApJ, 412, 541
Schwartz, D., & Ku, W. 1983, ApJ, 266, 459
Schweitzer, F. 1979, ApJ, 233, 23
Sebok, W. L. 1986, ApJS, 62, 301
Smith, E. P., Heckman, T. M., Bothun, G. D., Romanishin, W., & Balick, B. 1986, ApJ, 306, 64
Smith, E. P., O'Dea, C. D., & Baum, S. 1995, ApJ, 441, 113
Smith, P. S., Hall, P. B., Allen, R. G., & Sitko, M. L. 1992, ApJ, 400, 115
Smith, P. S., Jannuzi, B. T., & Elston, R. 1991, ApJS, 76, 67
Stark, A. A., Gammie, C. F., Wilson, R. F., Bally, J., Linke, R. A., Heiles, C., & Hurwitz, M. 1992, ApJS, 79, 77
Stetson, P. B. 1990, PASP, 102, 932
Stickel, M., Fried, J. W., & Kuhr, H. 1988a, A&A, 198, L13
———. 1988b, A&A, 206, L30
———. 1993a, A&AS, 97, 483
———. 1993b, A&AS, 98, 393
Stickel, M., Padovani, P., Urry, C. M., & Fried, J. W. 1991, ApJ, 374, 431
Stocke, J. T., & Burns, J. O. 1978, ApJ, 319, 671
Stocke, J. T., Liebert, J., Schmidt, G., Gioia, I. M., Maccacaro, T., Schild, R. E., Maccagni, D., & Arp, H. C. 1985, ApJ, 298, 619
Stocke, J. T., Morris, S. L., Gioia, I. M., Maccacaro, T., Schild, R. E., & Wolter, A. 1989, in BL Lac Objects, ed. L. Maraschi, T. Maccacaro, & M.-H. Ulrich (Springer: Heidelberg), 242
Stocke, J. T., Morris, S. L., Gioia, I. M., Maccacaro, T., Schild, R., Wolter, A., Fleming, T. A., & Henry, J. P. 1991, ApJS, 76, 813
Stocke, J. T., & Perrenod, S. C. 1981, ApJ, 245, 375
Stocke, J. T., Rector, T., Perlman, E. S., Morris, S. L., & Ellingson, E. 1996, in preparation
Stocke, J. T., Wurtz, R., & Perlman, E. S. 1995, ApJ, 454, 55
Stocke, J. T., Wurtz, R. E., Wang, Q. D., Elston, R., & Jannuzi, B. T. 1992, ApJ, 400, L17
Thuan, T. X., & Gunn, J. E. 1976, PASP, 88, 543
Thuan, T. X., & Romanishin, W. 1981, ApJ, 248, 439
Ulrich, M.-H. 1989, in BL Lac Objects, ed. L. Maraschi, T. Maccacaro, & M.-H. Ulrich (Springer: Heidelberg), 45
Ulrich, M.-H., Hackney, K. R. H., Hackney, R. L., & Kondo, Y. 1984, ApJ, 276, 466
Urry, C. M., Padovani, P., & Stickel, M. 1991, ApJ, 382, 501
Venkatesan, T. C. A., Batuski, D. J., Hanish, R. J., & Burns, J. O. 1994, ApJ, 436, 67
Wardle, J. F. C., Moore, R. G., & Angel, J. R. P. 1984, ApJ, 279, 93
Weistrop, D., Shaffer, D. B., Mushotzky, R. F., Reitsma, H. J., & Smith, B. A. 1981, ApJ, 249, 3
Wiklind, T., & Combes, F. 1995, in QSO Absorption Lines, ed. G. Meylen (Heidelberg: Springer), 175
Wills, D., & Wills, B. J. 1976, ApJS, 31, 143
———. 1981, Nature, 384, 289
Wurtz, R. 1994, Ph.D. dissertation, Univ. Colorado (W94)
Wurtz, R., Ellingson, E., Stocke, J. T., & Yee, H. K. C. 1993, AJ, 106, 869
Wurtz, R., Stocke, J. T., Ellingson, E. E., & Yee, H. K. C. 1996, in preparation (Paper II)
Yanny, B., York, D. G., & Gallagher, J. S. 1989, ApJ, 338, 735
Zhao, J. H., Burns, J. O., Norman, M. L., & Sulkanen, M. E. 1992, ApJ, 386, 69